A zebrafish larval model for drug-induced hepatic Injury due to first-line antituberculosis drugs and possible prevention/treatment with N-acetyl-cysteine

Khethiwe Joice Motha

Thesis presented for the degree of Master of Science (Pharmacology) in the Faculty of Medicine and Health Sciences at Stellenbosch University

Supervisors:

Dr Tracy Kellermann

Department of Medicine (Division of Clinical Pharmacology)

Stellenbosch University

Prof Carine Smith

Department of Medicine (Division of Clinical Pharmacology)

Stellenbosch University

Declaration

I, the undersigned, declare that the work obtained in this thesis, is my original work and that I have not previously submitted it for the award of any other degree at any other University/ Institute.

Signature: .....

Date: .....December 2022.....

Abstract

Background

Tuberculosis (TB) is ranked as the second most deadly infectious disease worldwide. First-line TB medication is associated with the development of drug-induced liver injury (DILI). The hepatotoxicity from this combination therapy is mostly due to pyrazinamide (PZA), isoniazid (INH) and rifampicin (RIF), however, no information has been reported on the hepatotoxicity potential of ethambutol (EMB). DILI typically occurs within the initial few weeks of the intensive phase of therapy. The only way to treat DILI is by stopping the medication and considering a liver transplant in the case of liver failure. Halting treatment can lead to the development of multi-drug resistant TB (MDR-TB). Therefore, close monitoring during therapy is required. Moreover, a preventative intervention needs to be put in place in order to prevent TB-DILI from developing in the first place. Acetaminophen (APAP) has been shown to cause DILI due to the accumulation of the drug's toxic metabolites in the liver following overdose of the drug. N-acetylcysteine (NAC) is an effective treatment and works by replenishing cellular glutathione in hepatocytes, thereby preventing liver injury from progressing to liver failure. It is therefore hypothesized that NAC may be able to reverse liver injury due to first line TB medication since it has been shown to be highly effective in the treatment of DILI associated with APAP, and has in fact become the standard of care. Previous studies have reported the potential of NAC in treating TB-dug associated DILI. However, this needs to be confirmed through further studies. Therefore, new models are needed for predicting which therapeutic compounds couldcause DILI in humans, and new markers and mediators of DILI need to be identified. The physiological and metabolic processes in zebrafish (*Danio rerio*) are similar to that of humans and the transparency of the zebrafish larvae makes this vertebrate a suitable model for studying TB-DILI mechanism and treatment. This study therefore aims to develop a zebrafish larval model (<5dpf) for DILI due to TB drugs, using APAP as a positive control that is known to cause DILI and to investigate the potential of NAC in preventing liver injury.

Methods

High-performance liquid chromatography (HPLC) analysis of INH, PZA and RIF was performed using previously developed methods, while liquid chromatography tandem mass spectrometry (LC-MS/MS) using a previously developed method was used for the evaluation of EMB. An HPLC method for the quantitation of APAP was developed and partially validated. The method used a Shimadzu HPLC system coupled with a PDA detector. Successful separation was achieved by isocratic elution on a reverse-phase Venusil XBP C18 (4.6 X 100 mm, 5 µm) column using a mobile phase consisting of 0.1% formic acid in water and acetonitrile (82:18; A:B, v:v) at 0.650 ml/min flow rate, detection wavelength of 247 nm, column oven temperature

of 28°C and injection volume of 10 µl. The chromatographic retention time was consistent at 3.26 min. The calibration curve covered a range of 3.13 to 200 µg/ml with a quadratic regression weighted 1/c (c: concentration). These analytical methods were used to determine the solubility and stability of these drugs in E3 medium at 28°C for 3 days. Thereafter, dose response experiments were performed for all drugs to obtain the dose (s) that resulted in liver steatosis as an indicator of DILI using Oil red O positive liver stains and EthoVision movement tracking software (for NAC) as endpoints. Optimisation of the doses and the evaluation of the ability of NAC to prevent or reverse TB drug-associated DILI was attempted in zebrafish larvae. For NAC, APAP, INH and PZA, previously reported zebrafish larval doses for each drug were used a as reference for the study. However, for rifampicin (RIF) and EMB, the doses were adjusted according to the human dose.

Results

Solubility and stability data showed that APAP, INH, PZA and EMB were soluble in E3 embryo water and stable at 28˚C for 3 days. However, RIF remained insoluble and unstable in E3 medium at 28°C after 24 hours, even with the addition of ascorbic acid at 20 µg/ml. Doses of 1 mM, 7 mM, 10 µM, 1.2 mM and 0.5 mM were selected as the doses associated with DILI for INH, PZA, RIF, EMB and APAP, respectively. EthoVision data showed that 12 µM and 16 µM NAC resulted in irritation and toxicity, respectively. However, 8 µM NAC was shown to be consistent with the negative control and was therefore selected as the safe dose for NAC. Due to time constraints and difficulties in breeding, NAC was not evaluated for its ability to prevent or reverse DILI due to first-line TB drugs and this will be elucidated in future.

Conclusion

A time efficient, economical zebrafish larval model for DILI was successfully developed. Current data illustrates that this model is able to accurately simulate known toxicity effects of first-line antituberculosis drugs on the liver. Furthermore, this model can be used to evaluate potential treatment interventions and prophylaxis for the reversal and/or prevention of DILI.

Abstrak

Agtergrond

Tuberkulose (TB) word as die tweede dodelikste infeksiesiekte ter wêreld beskou. Eerstelinie-TB-medisyne word met die ontwikkeling van middelgeïnduseerde lewerskade (DILI) verbind. Die hepatotoksisiteit van hierdie kombinasiebehandeling is hoofsaaklik te wyte aan pirasinamied (PZA), isoniasied (INH) en rifampisien (RIF), hoewel geen inligting nog oor die hepatotoksisiteitspotensiaal van etambutol (EMB) aangemeld is nie. DILI kom gewoonlik binne die eerste paar weke van die intensiewe behandelingsfase voor. Die enigste manier om DILI te behandel is om die medisyne te staak en, in geval van lewerversaking, 'n leweroorplanting te oorweeg. Die staking van behandeling kan multimiddelweerstandige TB (MDR-TB) tot gevolg hê. Daarom word sorgvuldige monitering gedurende behandeling vereis. Boonop moet voorkomingsmaatreëls getref word om te probeer keer dat TB-DILI in die eerste instansie ontwikkel. Asetaminofeen (APAP) is bekend daarvoor dat dit DILI veroorsaak weens die opeenhoping van die toksiese metaboliete van dié middel in die lewer ná 'n oordosis. N-asetielsisteïen (NAC) is 'n doeltreffende behandeling wat sellulêre glutatioon in hepatosiete vervang en sodoende keer dat lewerskade in lewerversaking omsit. Daarom is die hipotese dat NAC dalk lewerskade as gevolg van eerstelinie-TB-medisyne kan omkeer omdat dit hoogs doeltreffend is in die behandeling van APAP-verwante DILI, en trouens die standaardbehandeling daarvoor geword het. Vorige studies het aangedui dat NAC potensiaal toon vir die behandeling van TB-middelverwante DILI. Nietemin moet dít deur verdere navorsing bevestig word. Daarom word nuwe modelle vereis om te voorspel watter terapeutiese verbindings DILI by mense kan veroorsaak, en moet nuwe DILI-merkers en -mediators geïdentifiseer word. Die fisiologiese en metaboliese prosesse by die visspesie bontrok (*Danio rerio*, of "zebra fish") is soortgelyk aan dié by mense, en die deursigtigheid van die bontroklarwes maak dié werweldier 'n geskikte model vir die studie van die TB-DILI-meganisme en -behandeling. Die doel van hierdie studie was dus om 'n bontroklarwemodel (<5 dpf) te ontwikkel vir TB-middelverwante DILI, met APAP as 'n positiewe kontrole wat bekend is daarvoor dat dit DILI veroorsaak, en om die potensiaal van NAC vir die voorkoming van lewerskade te evalueer.

Metodes

Hoëprestasievloeistofchromatografie (HPLC) met behulp van voorheen ontwikkelde metodes en APAP is gebruik om eerstelinie-TB-middels te ontleed [EMB is met behulp van vloeistofchromatografie-massaspektrometrie (LC-MS) ontleed] ten einde oplosbaarheid en stabiliteit in E3-medium by 28 °C oor drie dae te bepaal. APAP is op 'n Shimadzu HPLC-stelsel

in samehang met 'n PDA-opspoorder ontleed. Suksesvolle skeiding is verkry met behulp van isokratiese eluering op 'n omgekeerdefase- Venusil XBP C18- (4.6 X 100 mm, 5 µm) kolom, met 'n mobiele fase wat uit 0.1% mieresuur in water en asetonitriel bestaan (82:18; A:B, v:v), met 'n vloeitempo van 0.650 ml/min, 'n opsporingsgolflengte van 247 nm, 'n kolom-oondtemperatuur van 28 °C en 'n inspuitingsvolume van 10 µl. Die chromatografiese retensietyd was deurgaans 3.26 min. Die kalibreerkromme het oor 'n bestek van 3.13 tot 200 µg/ml gestrek, met 'n lineêre regressie met 'n gewigstoekenning van 1/c (c: konsentrasie). Daarna is dosisreaksieproewe met alle middels uitgevoer om te bepaal watter dosis(se) tot lewersteatose, as 'n aanwyser van DILI, lei. Hiervoor is ORO- ("oil red O"-)positiewe lewerkleuring en EthoVision-nasporingsagteware (vir NAC) as eindpunte gebruik. Bontroklarwes is gebruik vir dosisoptimalisering en die evaluering van die vermoë van NAC om TB-middelverwante DILI te voorkom of om te keer. Vir NAC, APAP, INH en PZA is voorheen aangemelde bontroklarwedosisse van elke middel as verwysingspunt vir die studie gebruik. Vir rifampisien (RIF) en EMB is die dosisse egter na gelang van die menslike dosis aangepas.

Resultate

Oplosbaarheid- en stabiliteitsdata toon dat APAP, INH, PZA en EMB oplosbaar en stabiel is in E3-embriowater by 28 ˚C oor drie dae. Nietemin bly RIF onoplosbaar en onstabiel in E3-embriowater by 28 °C na 24 uur, selfs al word askorbiensuur in 'n konsentrasie van 20 µg/mL bygevoeg. Deur ORO-positiewe kleuring van die lewer van bontroklarwes is dosisse van onderskeidelik 1 mM, 7 mM, 10 µM, 1.2 mM en 0.5 mM gekies as die dosisse INH, PZA, RIF, EMB en APAP wat met DILI verband hou. EthoVision-data toon dat onderskeidelik 12 µM en 16 µM NAC tot irritasie en toksisiteit lei. Die 8 µM NAC-dosis het egter met die negatiewe kontrole ooreengestem. Daarom is 8 µM NAC gekies as die veilige dosis om te evalueer in watter mate NAC TB-middelverwante lewerskade by bontroklarwes kan voorkom/omkeer. Weens beperkte tyd en uitdagings met teling is die vermoë van NAC om eerstelinie-TB-middelverwante DILI te voorkom of om te keer, nié geëvalueer nie. Dít sal in toekomstige navorsing bestudeer word.

Gevolgtrekking

'n Tyddoeltreffende, ekonomiese bontroklarwemodel vir DILI is suksesvol ontwikkel. Huidige data toon dat die model bekende toksisiteitsuitwerkings van eerstelinie-TB-middels op die lewer akkuraat simuleer. Boonop kan die model gebruik word om moontlike behandelingsintervensies en profilakses vir die omkering en/of voorkoming van DILI te evalueer.

Acknowledgements

I would like to thank Dr Tracy Kellermann for supervising this MSc and Professor Carine Smith for co-supervising this MSc. Thank you for your patience, support and guidance throughout my MSc. This would not have been possible without you.

To my family, thank you for your support and always encouraging me to do great.

Cassius Phogole, thank you for allowing me to use your previously developed and validated HPLC methods.

Lesha Pretoris and Tracy Ollewagen, thank you for your patience and for assisting me in the lab.

To the Division of Clinical Pharmacology at large, thank you for the constant encouragement and support throughout my MSc. I will forever be grateful

The National Research Foundation (NRF) and the Harry Crossley Foundation, thank you for your financial support, which greatly assisted me throughout my MSc.

List of tables

List of figures

List of abbreviations and symbols

5-OH-PA	5-hydroxypyrazinoicacid
5-OH-PZA	5-hydroxypyrazinoicacid
ABC	ATP-binding cassette
ACP	Acyl-carrier-protein
ALP	Akaline phosphatase
ALT	aAanine transaminase
AM404	N-arachidonoylaminopheno
ANOVA	Analysis of variance
APAP	Acetaminophen
APCI	Atmospheric Pressure Chemical Ionization
API	Atmospheric Ion Source
AST	Aspartate aminotransferase
ATP	Adenosine triphosphate
BDQ	Bedaquiline
CaCl2	Calcium chloride
KatG	Catalase-peroxidase
CB1	Cannabinoid type 1 receptor
CFZ	Clofazimine
CO2	Carbon dioxide
CV	Coefficient of variation
CYP2D6	Cytochrome P450 2D6 enzyme
CYP2E1	Cytochrome P450 2E1 enzyme
CYP3A4	Cytochrome P450 3A4 enzyme
CYP450	Cytochrome P450 enzyme
DAMP	Danger-Associated Molecular Patterns
DILI	Drug-induced liver injury
DMSO	Dimethyl sulfoxide

DNA	Deoxyribonucleic acid
DOTS	Directly Observed Therapy Short course
dpf	Days post fertilisation
EMB	Ethambutol
ER	Endoplasmic reticulum
ESI	Electrospray Ionization
ETA	Ethionamide
ETC	Electron transport chain
FAAH	Fatty acid amide hydrolase
FDA	Food and Drug Administration
GGT	Gamma-glutamyl transferase
GSH	Glutathione
GST	Glutathione S-transferase
H2O2	Hydrogen peroxide
HIV	Human immunodeficiency virus
hpe	Hours post exposure
HPLC	High-performance liquid chromatography
ICH	International Council for Harmonisation
INH	Isoniazid
JNK	c-Jun N-terminal kinase
KCl	Potassium chloride
LC-MS	Liquid chromatography-mass spectrometry (LC-MS
LLOQ	Lower limit of quantitation
M. tb	*Mycobacterium Tuberculosis*
m/z	Mass to charge
MDR-TB	Multi-drug resistant TB
MgSO4	Magnesium sulphate
MIC	Minimal inhibitory concentration
MPT	Mitochondrial permeability transition

Na_2CO_2	Sodium carbonate
NAC	N-acetylcysteine
NaCl	Sodium chloride
NAD+	Nicotinamide adenine dinucleotide
NADH	Nicotinamide adenine dinucleotide (NAD) + hydrogen
NADPH	Reduced nicotinamide adenine dinucleotide phosphate
NAPQI	N-acetyl-p-benzoquinone imine
NAT2	N-acetyltransferase 2
NH_2	Amino group
NO_2	Nitrogen Dioxide
NO(X)	(Nitrogen oxides)
NP-HPLC	Normal phase HPLC
NQO1	NADPH quinone oxidoreductase 1
ORO	Oil red O
PA	Pyrazinoic acid
PAS	Para-aminosalicylic acid
PBS	Phosphate-buffered saline
1XPBST	1 X Phosphate Buffered Saline with Tween
RT-PCR	Real Time polymerase chain reaction
PDA	Photodiode-Array
PFA	Paraformaldehyde
PZA	Pyrazinamide
PZase	A *pncA* encoded pyrazinamidase
QC	Quality control
QCH	High quality control
QCL	Low quality control
QCM	Medium quality control
RIF	Rifampicin
RNA	Ribonucleic acid

RNAP	RNA polymerase
ROS	Reactive oxygen species
RP-HPLC	Reversed phase HPLC
RUCAM	Rouseel-Uclaf Casuality Assessment Method
SD	Standard deviation
SEM	Standard error of the mean
SLC	Solute carrier
SM	Streptomycin
SOD	Superoxide dismutase
SS	Reference standard
STD	Standard
TB	Tuberculosis
TST	Tuberculin skin test
UDCA	Ursodeoxycholic acid
UGT	Uridinediphosphateglucuronosyltransferase
UV	Ultraviolet
WHO	World Health Organization
WS	Working solution
WSQ	Working solution of quality control
XDR-TB	Extensively drug-resistant TB

Table of contents

Chapter 1

Introduction and literature review

1.1 Tuberculosis: the world's epidemic

Tuberculosis (TB) is an infectious disease that is caused by the water, soil, and dust-inhabiting bacillus *Mycobacterium Tuberculosis* (*M. tb*) that belongs to the *Mycobacterium* genus that is believed to have emerged approximately 150 million years back (Barberis *et al*., 2017). Discovered by Robert Koch in 1882, the human tubercle bacillus originated in east Africa as the ancestor to *M. tb* and is estimated to have evolved about 3 million years ago (Bhandari, 2021). As years passed by, people started to migrate from Africa and that led to the wide spread of the TB strains mainland (Bhandari, 2021). Physicians use the tuberculin skin test (TST) as an indicator of exposure to the (*M. tb*) bacillus by injecting patients with tuberculin (*M. tb* isolate) (Dal, 2018). This disease has become a major problem globally and poses a serious threat to society (Cao *et al*., 2018; Agathis *et al*., 2021; Su, *et al*., 2021). As reported by the World Health Organization (WHO), the COVID-19 pandemic has interrupted the processof diagnosing and treating TB in newly infected individuals, leading to an increase in the number of TB death cases in 2021 compared to 2019 (figure 1). The global incidence rate increased in 2021 compared to 2020 (WHO, 2021). In 2019 and 2020, 1.7 million and 5.8 million people were diagnosed with TB, respectively, suggesting a global 4.1% drop in newly diagnosed TB cases from 2019 to 2020. This was due to the COID-19 interruptions. This had therefore increased the number of TB death cases in 2020 compared to 2019.. It is evident that following the deadly COVID-19 virus, TB results in the second highest mortality rate worldwide, originating from a single *M. tb* pathogen (WHO, 2021).

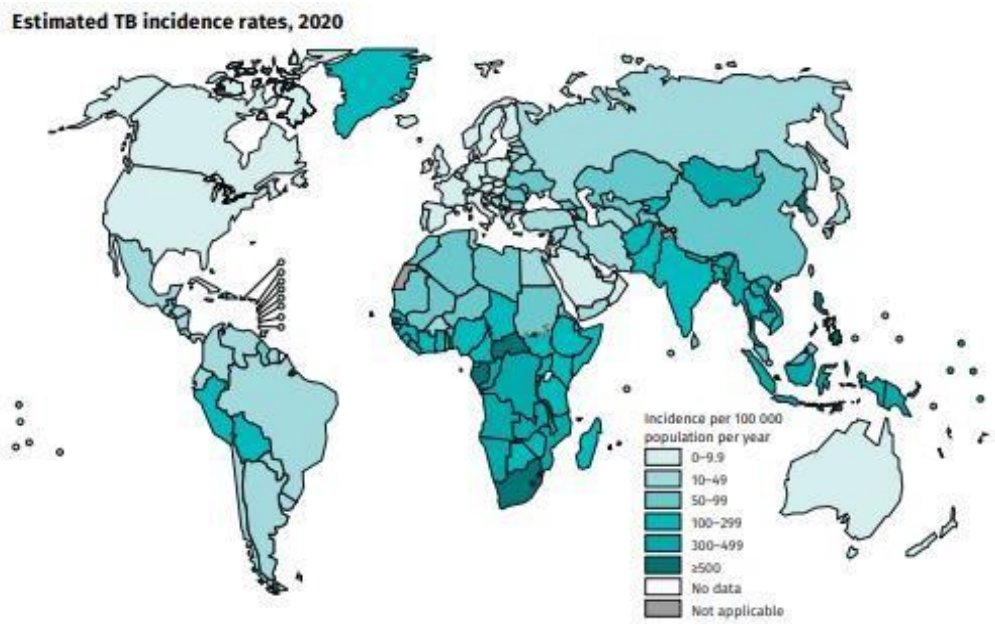

Figure 1: Overview of the 2020 global TB incidence rates. TB incidence rates were estimated as the number of active TB cases per 100,000 population in a given year (WHO, 2021)

Although TB is mostly known as a disease associated with the lungs, TB can also affect the bladder, bones, kidneys, and various parts of the human body (Visovsky *et al*., 2021). TB is spread in the air from one infected person or animal to another and multiplies in the host. TB transmission mostly occurs between humans and less commonly from animals to humans. When an infected individual coughs or sneezes, the droplets travel into the other individual and are inhaled into the lungs (see figure 2 below).

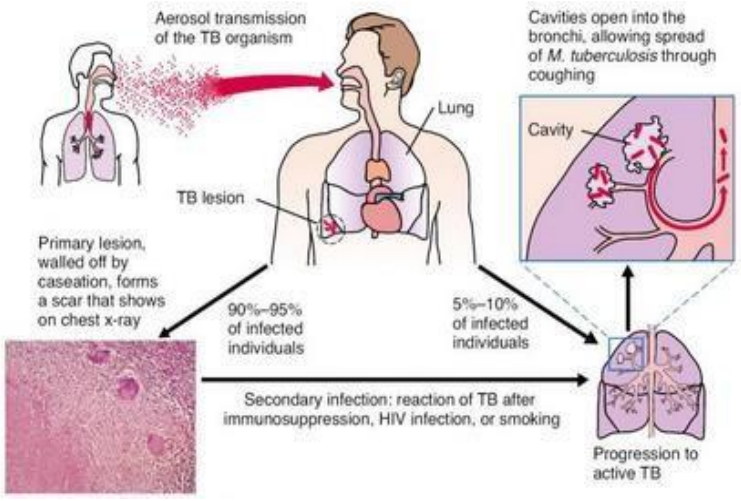

Figure 2: The progression of latent TB to active TB (Visovsky *et al*., 2021)

Once in the lungs, the bacteria then multiply. If the patient's immune system is strong, the bacteria can be engulfed by macrophages and the person will not get active TB but will have inactive or latent TB (figure 2) (Kim *et al*., 2021; Visovsky *et al*., 2021; Parmer, *et al*., 2021). People with latent TB stay healthy with the bacteria for many years without showing any symptoms (Bhandari, 2021). However, if the immune system gets vulnerable due to other infections, the patient will develop active TB and as a result, will then require therapy (Visovsky *et al*., 2021; Talwar and Langer, 2021). Moreover, HIV (Human Immunodeficiency Virus) positive people are at a higher risk of developing active TB faster than HIV negative individuals (Karumbi and Garner, 2015).

1.2 Drug resistant tuberculosis

Strains that are resistant to TB medication develop during therapy and this poses a great threat all over the world (Tiberi *et al*., 2019). Multi-drug resistant TB (MDR-TB) occurs as a result of an infection caused by a strain that is resistant to TB medication, usually isoniazid (INH) and rifampicin (RIF) (Mirzayev *et al*., 2021; Sotgiu *et al*., 2012; Caminero, and Scardigli, 2015), or treatment that is not enough to overcome the activity of the bacteria (Manjelievskaia *et al*., 2016). Other contributing factors include the long-term nature of treatment - patients may feel

better and stop taking the medication as prescribed (Su *et al*., 2021) or the quality of the drug may be poor (Stosic *et al*., 2018; Tiberi *et al*., 2019). This requires an increase in dosage of the medication to reach higher concentrations of the drugs *in vivo* to reach the minimal inhibitory concentrations (MICs) that are required to kill the mycobacterium that is resistant to the medication. This then leads to adverse drug reactions (Sotgiu *et al*., 2012) which lead to drug-induced liver injury (DILI) (Imam *et al*., 2020). To reduce the incidence of TB drug resistance and to improve patient outcomes, the WHO has introduced a Directly Observed Therapy Sort course (DOTS) strategy that focuses on the strict monitoring of the patient by anobserver (family or community member or health care worker), recording every dosage thereby making certain that the patients takes their medication correctly (Karumbi and Garner, 2015). Untreated MDR-TB leads to extensively drug-resistant TB (XDR-TB) which is multidrug resistant and rifampicin resistant TB (MDR/RR-TB) that is resistant to at least a fluoroquinolone (levofloxacin) and one of the Group A drugs such as bedaquiline (BDQ) (Karumbi and Garner,2015).

1.3 Antituberculosis therapy

In 1932, a scientist by the name of Gerhard Domadk and his colleagues conducted an experiment in mice and discovered that sulfonamides analogues can be used against *M. tb* (Vilchèze, 2020; Vilchèze and Jacobs, 2014). Schatz and Waksman also made a discovery on the use of streptomycin (SM) in the treatment of *M. tb*. The efficacy of streptomycin in treating TB was confirmed on a woman aged 21 who had severe TB of the lungs (Schatz and Waksman, 1944; Vilchèze, 2020). Thereafter, other drugs like para-aminosalicylic acid (PAS) and INH were also discovered and were found to be active against *M. tb*, however, strains thatwere resistant to treatment soon developed (Lehmann, 1946). To counteract this, combination therapy using INH, PAS and SM was then initiated in TB patients. This was effective and was used for quite some time. However, patients started to discontinue treatment due to the long period and costs related to the treatment (Crofton, 1959). As part of a solution, a drug regimen comprised of RIF, INH, ethambutol (EMB) and pyrazinamide (PZA) for the first two months and RIF and INH for the next four months was used instead (Crofton, 1959), which is the current combination therapy used during antituberculosis therapy (Combrink and du Preez, 2020). This showed high efficacy and the patients responded well to treatment. However, again, strains that were resistant to INH and RIF developed during treatment leading to MDR-TB (Vilchèze and Jacobs, 2014) and then second-line TB drugs such as ethionamide (ETA), BDQ and clofazimine (CFZ) were then introduced to be used as treatment for MDR-TB (Drew and Sterling, 2017). Moreover, second generation antituberculosis drug, linezolid, has been shown to be highly effective at treating MDR-TB (Sotgiu *et al*., 2012).

1.3.1 Isoniazid

i. Pharmacology

INH (figure 3) is available in different formulations. These include intramuscular or intravenous injection, tablet or syrup. (O'Connor and Brady, 2020). INH is taken at a dose of 15 mg/kg per day (Jung *et al*., 2015). The absorption of INH occurs mostly in the intestine. The rate of absorption of this drug becomes low when taken together with food or food high in sugar content. INH undergoes hepatic metabolism leading to 80% of its metabolites being excreted in urine with less than 10% being excreted through faeces. INH is distributed entirely in body tissues and body fluids with a volume of distribution of 0.6 l/kg (Klein *et al*., 2016).

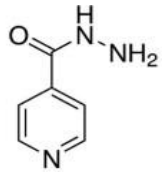

Figure 3: The chemical structure of INH (Babu *et al*., 2019)

ii. Mechanism of action

The anti-microbial activity of INH is as a result of the peroxidation of INH into a highly reactive isonicotinoyl aryl radical (INH+) by a catalase-peroxidase enzyme that is encoded by a catalase-peroxidase from *M.tb* (KatG) gene (figure 4) in the presence of hydrogen peroxide (H_2O_2). Hence, INH is a prodrug that needs to be activated before exerting its antimicrobial action. Nicotinamide adenine dinucleotide (NAD+) undergoes oxidation and reacts with INH+ to produce an INH- nicotinamide adenine dinucleotide (INH-NAD+) adduct. INH-NAD+ further blocks an Inh A enzyme that converts trans-2-enoyl acyl-carrier-protein (ACP) into acyl-ACP intermediate in the cell. This then inhibit the synthesis of acyl-ACP which promotes the biosynthesis of long fatty acid chains of mycolic acid, which are responsible for cell wall synthesis. Hence, its inhibition leads to the inhibition of the cell wall of *M.tb*. However, the mechanism of INH is still not completely understood and therefore requires further research (Babu *et al*., 2019).

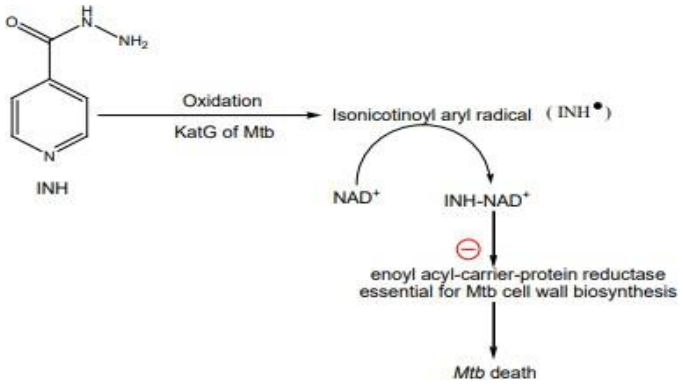

Figure 4: The mechanism of action of INH (Khan and Saifur, 2017)

iii. Metabolism

The liver serves as the site for the metabolism and clearance of INH (Klein *et al*., 2016). The metabolic pathway is facilitated by the N-acetyltransferase 2 (NAT2) and microsomal cytochrome P4502E1 (CYP2E1) enzymes, which in turn direct the hepatotoxicity potential of INH. INH is metabolised into N-acetyl-INH, which undergoes further hydrolysation into acetyl hydrazine (figure 5). Acetyl hydrazine can either be the metabolite that is responsible for INH hepatotoxicity or can be broken down into the acetyl radical, ketene or reactive acetyl onium ion ketene, which then forms covalent bonds with macromolecules in the liver leading to injury of the liver (Ramappa and Aithal, 2013).

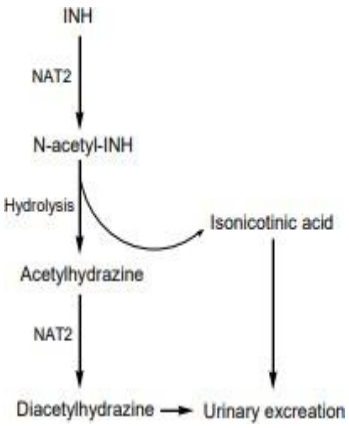

Figure 5: The metabolic pathway of INH (Khan and Saifur, 2017)

iv. Side effects and contraindications

The most common adverse effects include those of the gastrointestinal tract and rash while the less common include peripheral neuropathy and hepatotoxicity. Breastfeeding or pregnant women and patients living with HIV and diabetes are at higher risk of experiencing these adverse effects from taking INH (O'Connor and Brady, 2020). Some patients experience

cognitive impairment, headache, sleep disturbances, blurred vision and psychosis (Denholm *et al*., 2014).

1.3.2 Pyrazinamide

i. Pharmacology

The typical adult dosage of PZA (figure 6) is 25 mg/kg per day administered orally (Katzung, 2012). The absorption of PZA occurs mostly in the gastrointestinal tract. The distribution of PZA occurs in all tissues of the body, even on the membranes of the body that experience inflammation. Following absorption, PZA has a half-life of eight to eleven hours (Katzung, 2012).

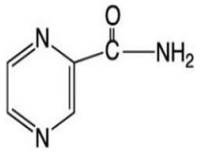

Figure 6: The chemical structure of PZA (Zhang *et al*., 2014)

ii. Mechanism of action

PZA (pyrazine-2-carboxamide) is a prodrug that becomes active once it gets inside the bacterial cell. A *pncA* encoded pyrazinamidase (*PZase*) enzyme from the cytoplasm converts PZA into active pyrazinoic acid (PA) after the entry of PZA into the cell, facilitated by passive diffusion. PA then inhibits the synthesis of mycolic acid by fatty acid synthase type 1 thereby inhibiting the bacterial cell wall synthesis. At acidic pH, PA moves out of the cell (figure 7) and combines with hydrogen ions, then diffuses back into the cell and accumulates. This then leads to disruption of membrane potential and interferes with energy production, which is necessary for the survival of the *M. tb* (Zhang *et al*., 2014). A mutation in the *pncA* can results in the resistance of the *M. tb* towards PZA medication.

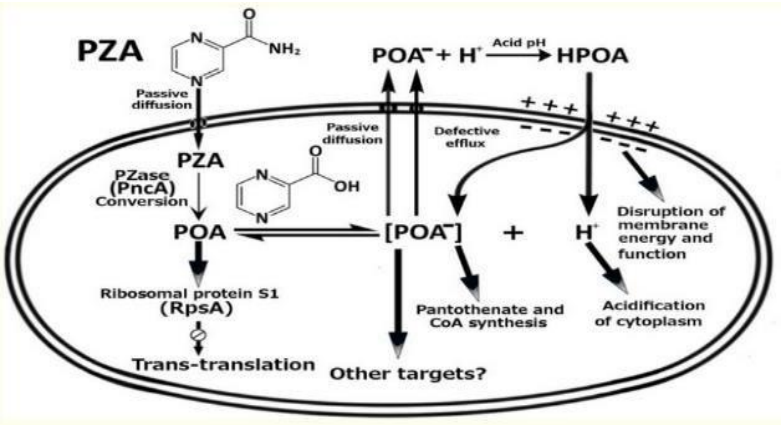

Figure 7: The mechanism of action of PZA (Zhang *et al*., 2014)

iii. Metabolism

The metabolism of PZA occurs in the liver through a process facilitated by the amidase and xanthine oxidase enzymes (figure 8) in the liver. The amidase enzyme produces PA, which is the first metabolite. 5-hydroxypyrazinoicacid (5-OH-PA) is produced in a hydroxylation reaction of PA catalysed by the xanthine oxidase enzyme. The 5-hydroxypyrazinoicacid (5-OH-PA) metabolite can also be produced from the amidase catalysed reaction of the hydrolysis of 5 - hydroxypyrazinoicacid (5-OH-PZA) that is formed from the oxidation of PZA. The excretion of these metabolites is through urine (Shih *et al*., 2013).

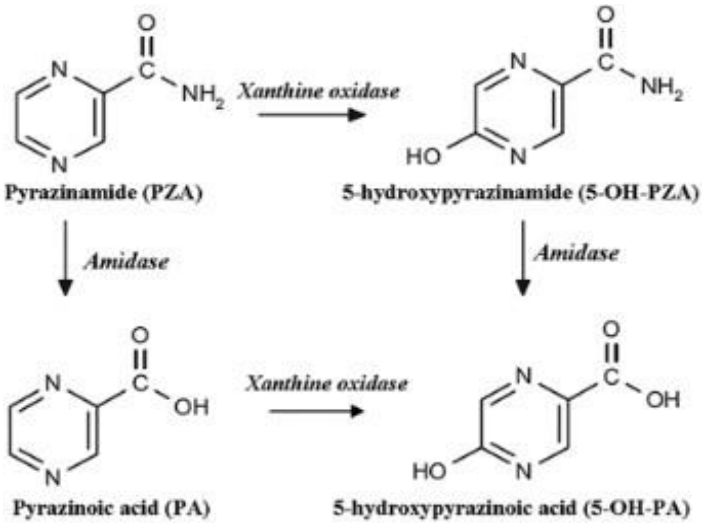

Figure 8: The metabolic pathway of PZA (Shih *et al*., 2013)

iv. Side effects and contraindications

Since pyrazinamide is an inhibiter of uric acid excretion, this means that there will be higher concentrations of uric acid in the urine, which potentially lead to gout, urate nephropathy and urolithiasis. Other adverse reactions associated with PZA include fever, nausea and vomiting (Katzung, 2012).

1.3.3 Rifampicin

i. Pharmacology

The high lipid-solubility nature of RIF (figure 9) allows it to be taken orally or intravenously. RIF is taken at a maximum dosage of 10 mg/kg per day (Satoskar and Bhandarkar, 2020). RIF is 70-80% protein bound. The rate of RIF absorption decreases when the drug is taken with food. The half-life of RIF is 2-5 hours depending on the dosage. The metabolites of RIF, together with RIF are excreted through faeces. However, 17% of RIF is also excreted unchanged in urine (Abulfathi *et al*., 2019).

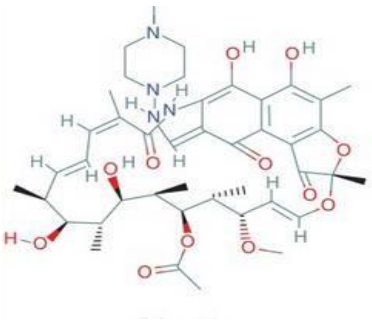

Figure 9: The chemical structure of RIF (Rothstein, 2016).

ii. Mechanism of action

RIF exhibits its bactericidal activity by binding to the β-subunit of DNA dependant RNA polymerase (RNAP) thereby restricting elongation at the 5' end (figure 10). The binding of RIF to RNAP also reduces the bond between RNAP and short RNA segments transcribed from DNA molecules thereby inhibiting RNA polymerase (RNAP) that transcribe RNA from DNA (Campbell *et al*., 2001). Therefore, RNA cannot be transcribed from DNA in the cell. RIF only acts on the RNAP of the microorganism and not on the enzymes in the organism's internal environment thereby reducing the risks of adverse effects (Suresh and Wadhwa, 2020).

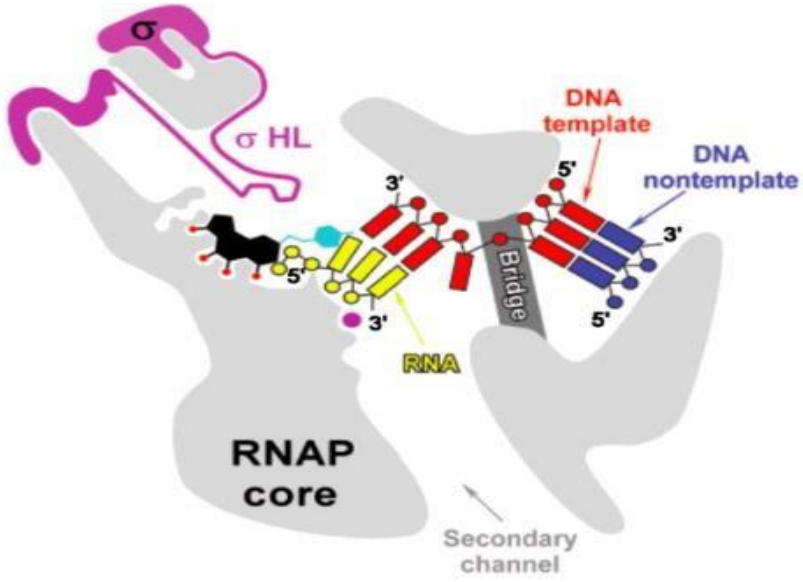

Figure 10: The mechanism of action of RIF (Aristoff *et al*., 2010)

iii. Metabolism

The liver is the primary site for the metabolism of RIF. Desacetylation and hydrolysis occurs in the liver during RIF metabolism to produce 25-desacetyl RIF and 3-formyl RIF, respectively

(figure 11). The metabolites of RIF are found to be non-toxic. The polarity of 3-formyl RIF is higher compared to RIF and has more bactericidal activity towards the microorganism (Ramappa and Aithal, 2013).

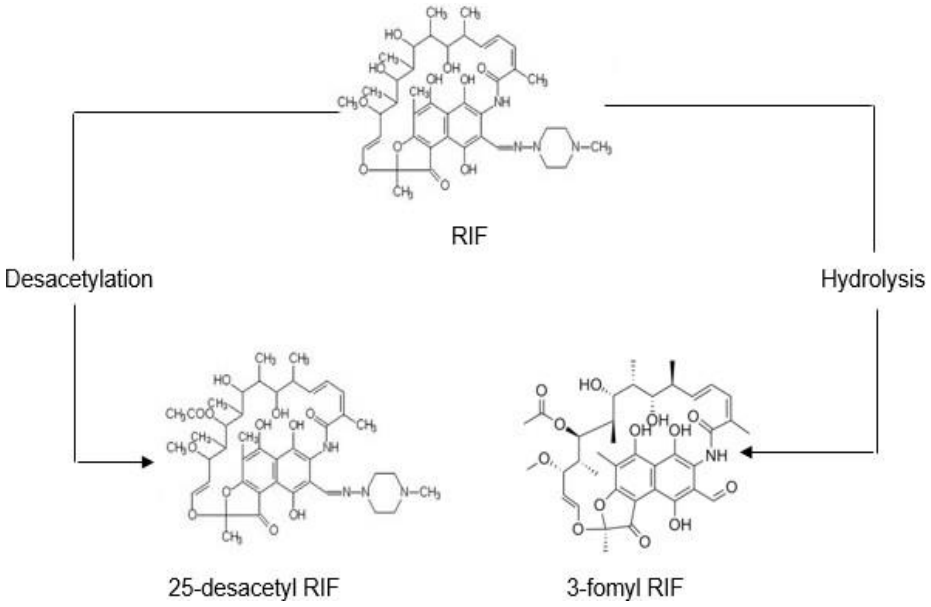

Figure 11: The metabolic pathway of RIF (modified from Kumar *et al*., 2015)

iv. Side effects and contraindications

RIF administration causes body fluids, like sweat, urine, saliva, tears and also faeces, to turn orange and these form part of the dose-dependent side effects. Gastrointestinal symptoms include diarrhoea, anorexia and nausea. Symptoms like renal failure, thrombocytopenia, hemolysis and urticaria form part of the effects that are independent on the amount of dosage. These develop when RIF has been used for a longer time and cease upon discontinuation of RIF. Patients with a dysfunctional liver tend to develop hypersensitivity (Suresh and Wadhwa, 2020). Rifampicin undergoes drug-drug interactions with other drugs and induces the activation of a pregnane X receptor that further induces the cytochrome P450 enzymes and p-glycoprotein, and this leads to the alteration of both the metabolism and transportation of the drugs (Chen and Raymond, 2006).

1.3.4 Ethambutol

i. Pharmacology

EMB (figure 12) is administered daily at a dose of 25 mg/kg orally (Lee and Nguyen, 2020). EMB has a bioavailability of about 70-80%, at 1-2 hours following oral administration. EMB is 20-30% protein bound with a volume of distribution of 76.2 l is eliminated via the kidneys and is excreted unchanged in urine and as metabolites that account for 12-19% of the ethambutol (Sundell *et al*., 2020).

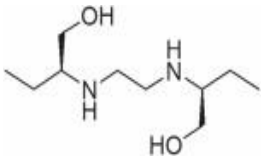

Figure 12: The chemical structure of EMB (Ahn and Park, 2017)

ii. Mechanism of action

EMB inhibits the synthesis of the cell wall of the mycobacteria by inhibiting the synthesis of arabonogalacton which is responsible for linking mycolic acid chains that form the cell wall of the bacteria (Sarkar *et al*., 2016). The embC, embA and embB genes in *M. tb* code for specific EmbCAB proteins that are responsible for the transfer of arabinosyl, which is responsible for synthesising arabonogalacton. Ethambutol works by inhibiting these EmbCAB proteins (figure 13) and thereby causes the bacterial cell wall to be more permeable, leading to the death of the bacteria (Kumar *et al*., 2015).

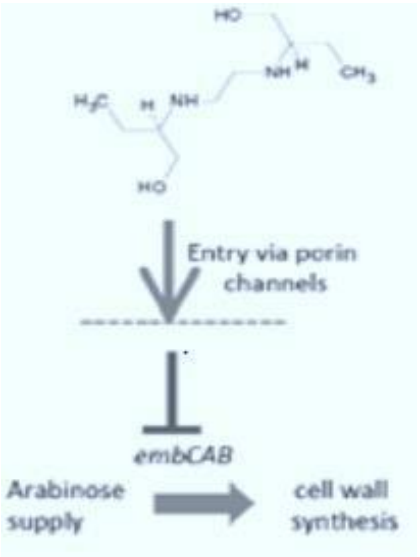

Figure 13: The mechanism of action of EMB (Kumar *et al*., 2015)

iii. Metabolism

EMB undergoes oxidation to ethambutol-aldehyde, facilitated by alcohol dehydrogenase. Ethambutol-aldehyde is further oxidised by alcohol dehydrogenase into 2, 2'-(Ehylenediimino) di-butyric acid (figure 14) as the metabolite that is excreted in urine (Sarkar *et al*., 2016).

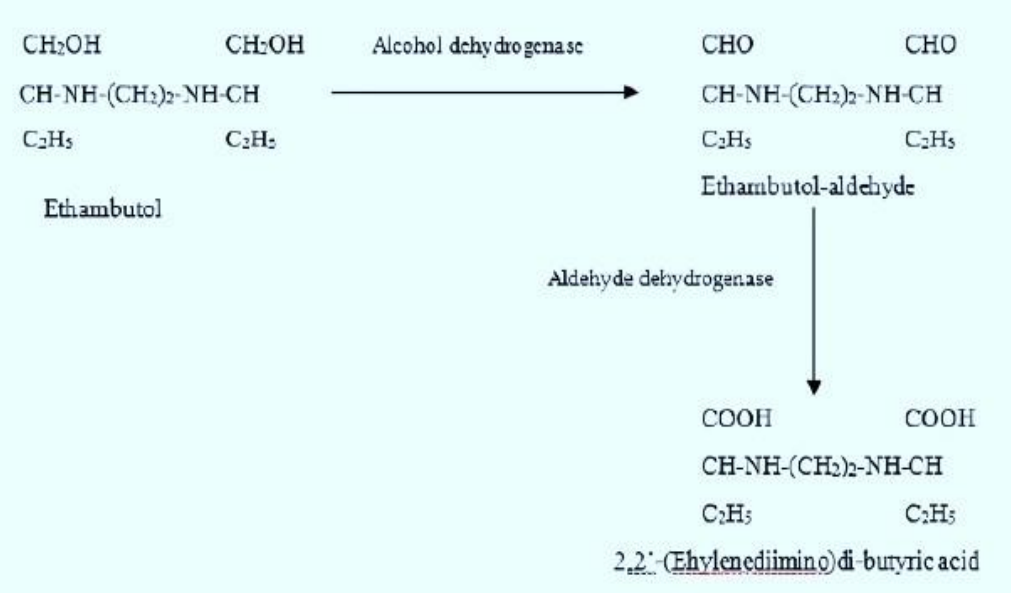

Figure 14: The metabolic pathway of EMB (Sarkar *et al*., 2016)

iv. Side effects and contraindications

Side effects associated with the use of ethambutol are dose and duration related and include retrobulbar neuritis. This commonly affects patients suffering from kidney dysfunction since EMB undergoes hapatic excretion. Hypertension, tobacco smoking and heavy alcohol consumption may worsen the effects (Makunyane and Mathebula, 2016).

1.4 Drug metabolism in the liver

The metabolism of drugs in the liver occurs in three phases to detoxify the drugs and remove those drugs through excretion (as shown in figure 15).

i. Phase 1: Modification

The reactions in this phase of drug metabolism may include reduction, oxidation or hydrolysis that are catalysed by cytochrome P450 and involve Reduced nicotinamide adenine dinucleotide phosphate (NADPH) and oxygen. Reactive and polar groups are introduced into the parent drug to increase the hydrophilicity of the drug. The products of this phase are activated metabolites that can be excreted if they are more polar (Lokhande, 2017).

ii. Phase 2: Conjugation

Charged species such as glutathione (GSH), sulphate, glycine, or glucuronic acid are added in either the carboxy (-COOH), hydroxy (-OH), amino (NH_2), or thiol (-SH) groups of the active metabolites from phase 1 metabolism to make these metabolites less active. This reaction is

catalysed by uridinediphosphateglucuronosyltransferase (UGT), N-acetyltransferase 2 (NAT2), and most commonly, by the glutathione S-transferase (GST) enzyme (Corrine and Bortolini, 2013; van Wijk *et al*., 2016).

iii. Phase 3: Transportation

The products of conjugation from phase 2 reactions may be further metabolised and then be transported to the outside of the cell and be excreted. The proteins that are involved in this phase belong to the ATP-binding cassette (ABC) and solute carrier (SLC) transporters superfamilies (Lokhande, 2017).

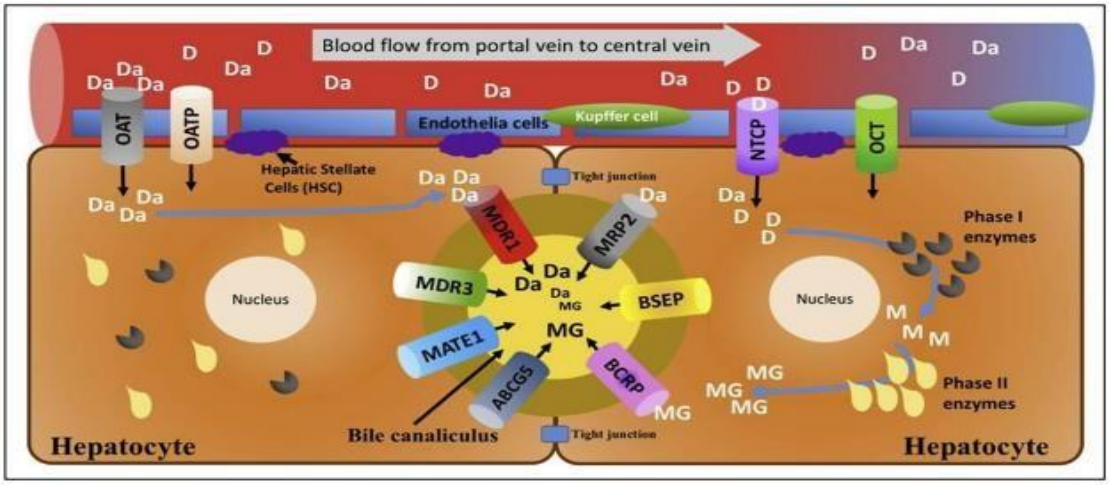

Figure 15: Metabolism of drugs in the liver during phase 1 and phase 2 metabolism (Lokhande, 2017)

1.5 Drug Induced Liver Injury

Even though DILI is most commonly associated with APAP, other drugs like anti-cancer drugs, antiretrovirals, some antibiotics, cardiac drugs and traditional herbal supplements are associated with DILI (David, and Hamilton, 2010). Patients with DILI present with symptoms including abdominal pain, jaundice, nausea and vomiting (Abbara *et al*., 2017). Other reported risk factors associated with DILI include age, gender, malnutrition, infections and alcohol consumption (Devarbhavi *et al*., 2011; Warmelink *et al*., 2010; Sandmann *et al*., 2019; Baniasadi *et al.*, 2010). Discontinuation of treatment serves as the best option to immediately manage DILI (Chughlay *et al*., 2016). Therefore, patients on anti-TB therapy should be made aware of the various factors associated with the development of DILI and should stop treatment immediately on the onset of signs of hepatotoxicity to prevent progression of DILI. Other interventions for DILI include the use of corticosteroids in combination with ursodeoxycholic acid (UDCA) and this leads to the rapid recovery of liver function (Hu and Xie, 2019; Garcia-Cortes *et al*., 2020). Inhibition of hepatic gap junctions have also been associated with the prevention of the development of DILI in mice (Patel *et al*., 2012). Acute liver failure from DILI

can only be managed through liver transplantation. In addition, DILI can be prevented or managed by alerting authorities about the offending drug so that the drug can be evaluated and possibly taken out of the market (Francis and Navarro, 2021).

1.5.1 Types of DILI

DILI can either be direct, indirect or idiosyncratic, depending on different characteristics of the DILI (David and Hamilton, 2010). Table 1 below summarizes the differences between the three types of DILI.

Table 1: Differences between the three types of DILI (Garcia-Cortes *et al*., 2020; Hoofnagle and Björnsson, 2019).

Characteristic	Direct	Idiosyncratic	Indirect
Prevalence	Common	Uncommon	Intermediate
Dose related	Yes	No	No
Foreseeable	Yes	No	Partly
Occurrence rate	High	No	Average
Response time	Short	Irregular	Long

1.5.2 Mechanism of DILI

DILI occurs in three subsequent main steps that can be divided into upstream events (initial mechanisms) and downstream events (involving the innate immune system) (Russmann *et al*., 2009). Below are the steps involved in the development of DILI.

i. Initial mechanisms of toxicity: direct cell stress, direct mitochondrial impairment, and specific immune reactions

Drug metabolites induce immune responses, cell stress and inhibition of mitochondria that cause cell injury. These metabolites induce cell stress by binding to cell structures and causing reduction of GSH (Russmann *et al*., 2009; Yuan and Kaplowitz, 2013). During mitochondrial impairment, both metabolites and parent drugs work by inhibiting the respiratory chain of the mitochondria, leading to ATP reduction, reactive oxygen species (ROS) overproduction and beta oxidation inhibition. Mitochondrial impairment can also result through the opening of a protein called the mitochondrial permeability transition (MPT) pore that can lead to the entrance of toxic molecules into the mitochondria leading to hepatotoxicity though hepatocytedamage (Russmann *et al*., 2010; Yuan and Kaplowitz, 2013; Garcia-Cortes *et al*., 2020). During specific immune responses, metabolites can react with proteins (figure 16) and form covalent bonds and thereby end up being perceived as neo-antigens. This then leads to the

formation of specific immune responses that cause cytotoxic T-cells to release cytokines that lead to inflammation (Russmann *et al*., 2010; Yuan and Kaplowitz, 2013; Garcia-Cortes *et al*., 2020).

ii. Direct and death receptor-mediated pathways leading to mitochondrial permeability transition

The change in the permeability transition of the mitochondria results from the beginning of cell stress and from specific reactions that involve the immune system. However, if the metabolites do not impair the function of the mitochondria directly, the MPT can occur via two pathways. These are the intrinsic and extrinsic pathways, also called the direct and indirect pathways, respectively. The direct pathway is associated with acute cell stress while the indirect pathway is associated with negligible cell stress. This MPT leads to further cell death (Russmann *et al*., 2010; Yuan and Kaplowitz, 2013; Garcia-Cortes *et al*., 2020).

iii. Apoptosis and necrosis

The cell undergoes necrotic or apoptotic cell death from an insufficient energy supply from impaired mitochondria. During apoptosis, the MPT causes release of cytochrome C which combines with other necrotic cells, forming a complex that cleaves other proteins in the cell, resulting in cell death. During necrosis, cytokines get released, leading to inflammation that activates neighbouring hepatocytes, leading to more liver injury (Russmann *et al*., 2010; Yuan and Kaplowitz, 2013; Garcia-Cortes *et al*., 2020).

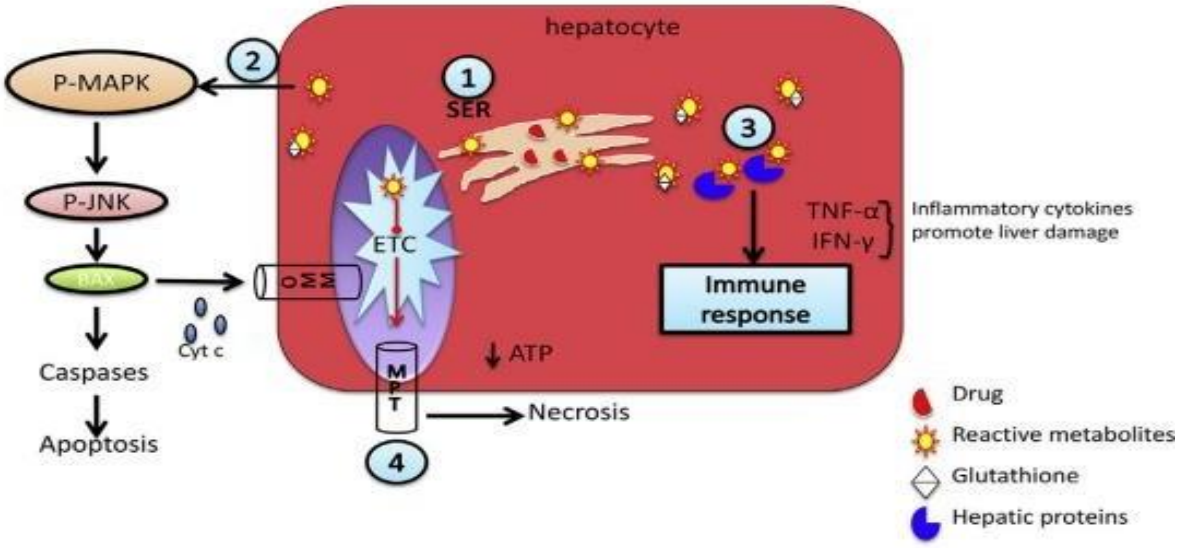

Figure 16: The 3-step mechanistic working model of DILI (Shehu *et al*., 2017)

1.5.3 Diagnosis and prognosis of DILI

There is no specific diagnostic procedure for DILI. It is associated with a variety of drugs, shares symptoms with other liver diseases and the patient may not disclose that they are taking other herbal and dietary supplements. However, laboratory tests like measurements (figure 17) of alanine transaminase (ALT), aspartate aminotransferase (AST), gamma-glutamyl transferase (GGT), alkaline phosphatase (ALP) and bilirubin are used to test for DILI. However, these biomarkers are not specific to DILI (Garcia-Cortes *et al*., 2020). In the 1900s, the Rouseel-Uclaf Casuality Assessment Method (RUCAM) was invented as a model to diagnoseDILI based on the ratio of ALT and ALP, denoted as the R-value (Maddur and Chalasani, 2011). According to this model, DILI can be hepatocellular, mixed or cholestatic (Stournaras and Tziomalos, 2015). However, the patient must be checked of any symptoms, pharmacological and clinical history before determination of the R-value. Once the R-value has been determined, first-line tests such as abdomen sonography are then performed to assess the liver and second line tests such as liver biopsy are done for liver tissue examination (Maddur and Chalasani, 2011; Chalasan *et al*., 2021).

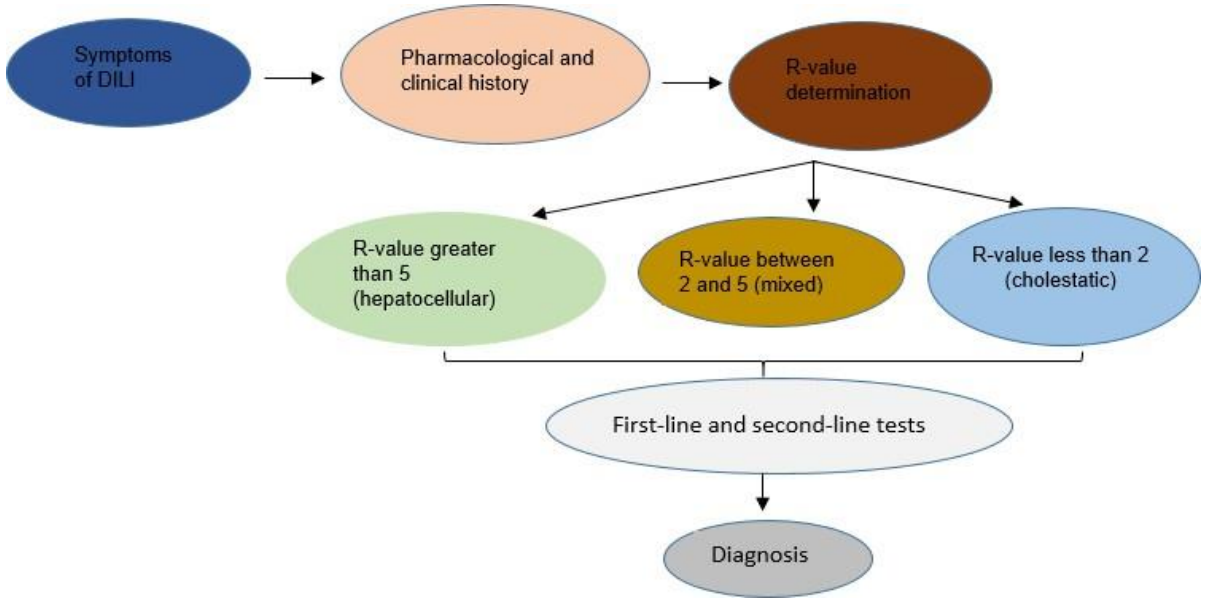

Figure 17: The stepwise approach to DILI diagnosis (modified from Chalasani *et al*., 2021; Garcia-Cortes *et al*., 2020)

1.5.4 DILI as a result of APAP

APAP is a commonly used therapeutic analgesic and antipyretic drug. APAP at therapeutic doses has very good safety profile. However, patients tend to deliberately or accidentally overdose on the drug, leading to the drug exceeding therapeutic levels (Rotundo and

Pyrsopoulos, 2020). As a result, these patients tend to suffer from liver injury, which could lead to liver failure (Jaeschke *et al*., 2020; Bruells *et al*., 2021). N-acetyl-p-benzoquinone imine (NAPQI) binds to GSH thereby decreasing the levels of GSH in the cell, which result in more accumulation of the NAPQI in the cell. This leads to the formation of protein adducts (Rotundo and Pyrsopoulos, 2020) that subsequently cause oxidative stress in the cell mitochondria and in the endoplasmic reticulum (ER). ER stress then cause DNA fragmentation (figure 18). High levels of oxidative stress cause c-Jun N-terminal kinase (JNK) protein to activate the electron transport chain (ETC) and translocate to a Sab protein on the cell mitochondria upon activation by phosphorylation. This then leads to the formation of peroxynitrite from the reaction of superoxide and mitochondrial nitric oxide (Rotundo and Pyrsopoulos, 2020). The peroxynitrite then causes the formation of a mitochondrial permeability transition and the release of apoptotic proteins from the mitochondria into the cytosol which then leads to hepatocyte damage (Jaeschke *et al*., 2020).

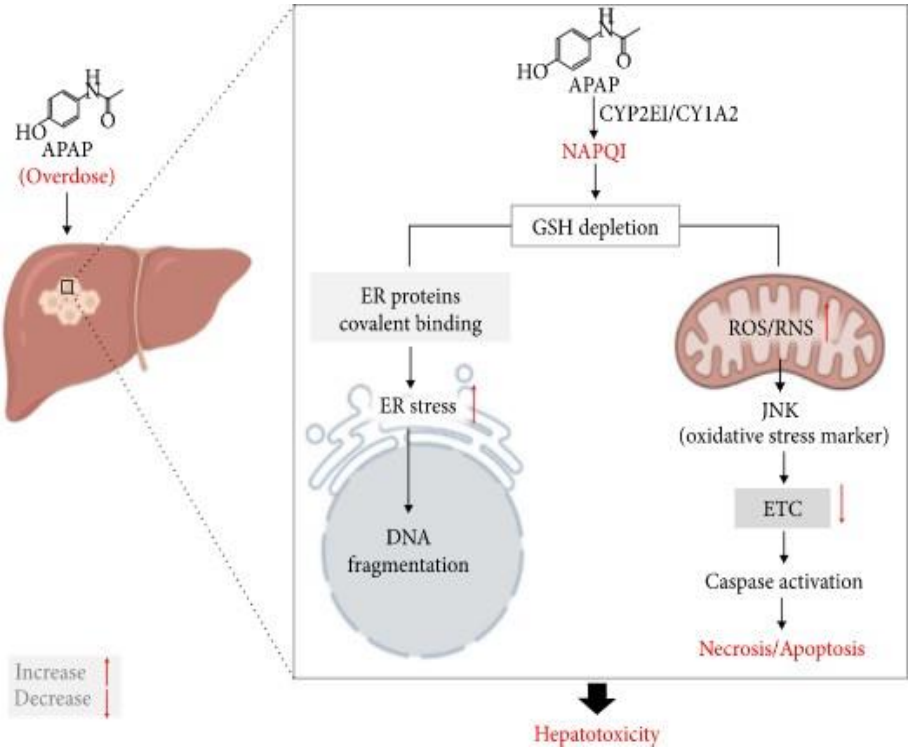

Figure 18: Mechanism of APAP in DILI (Ntamo *at al*., 2021)

1.5.4.1 Acetaminophen

i. Pharmacology

APAP, also known as N-acetyl-*para*-aminophenol or paracetamol (Figure 19) (Ghanem *et al*., 2016) can be taken orally at 50 – 75 mg/kg/day by children and at 4 g/day by adults (Rotundo and Pyrsopoulos, 2020). APAP can be taken via rectal administration, orally (Gerriets *et al*.,

2018) and intravenously, (Gerriets *et al*., 2018; Mazaleuskaya *et al*., 2015) and has a bioavailability of 80% with a half-life of 2-3 hours after oral administration (Rotundo and Pyrsopoulos, 2020).

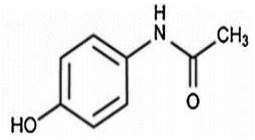

Figure 19: The chemical structure of APAP (Ghanem *et al*., 2016)

ii. Mechanism of action

APAP first gets deacetylated in the liver into p-aminophenol, which further gets metabolized by FAAH (Fatty acid amide hydrolase) enzyme in the brain into AM404 (N-arachidonoylaminopheno) (Mallet *et al*., 2017) by coupling p-aminophenol with arachidonic acid. Cannabinoid type 1 (CB1) receptors (from the Vanilloid system, cannabinoid system and calcium channels) work by binding the AM404 metabolite, reinforcing the initiation of the descending pathways (figure 20) that allow for the secretion of serotonin from the midline of the brainstem. The serotonin binds into the respective receptors of serotonin in the spinal cord that function in suppressing pain (Mallet *et al*., 2017; Bauerlein *et al*., 2021).

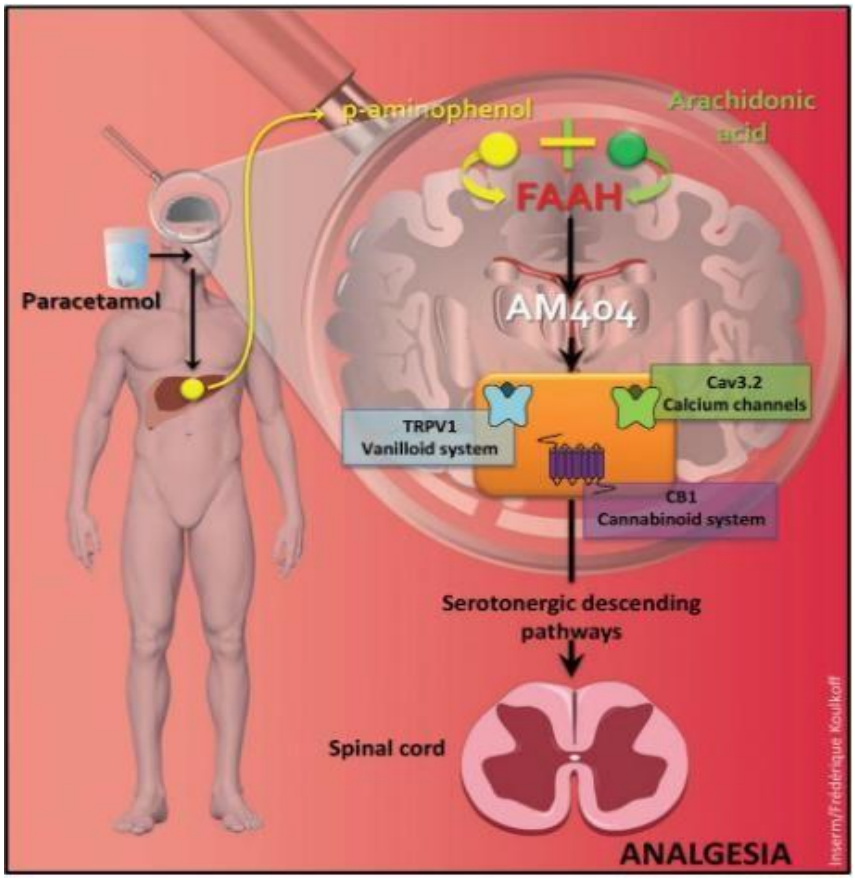

Figure 20: The mechanism of action of APAP (Mallet *et al*., 2017)

iii. Metabolism

The metabolism of APAP occurs more in the liver and less in the intestines and the kidneys (Mazaleuskaya *et al*., 2015) through the processes of sulfation, oxidation and glucuronidation (Ji *et al*., 2012). After administration, approximately 2% of APAP gets excreted unchanged. APAP further gets converted into inactive APAP-glucuronide and inactive APAP-sulfate that makes up 90% of metabolites in urine (figure 21). These non-toxic metabolites get excreted into the blood and bile and then further into the kidneys. However, approximately 5% of APAP further gets oxidised by cytochrome p450 (CYP450) isozymes in the liver into a very active and hepatotoxic NAPQI metabolite (Jiang *et al*., 2013). This metabolite binds to liver glutathione through conjugation to form non-toxic APAP-GSH that is readily excreted and eliminated via urine as APAP-cysteine and mercapturic acid (Mazaleuskaya *et al*., 2015).

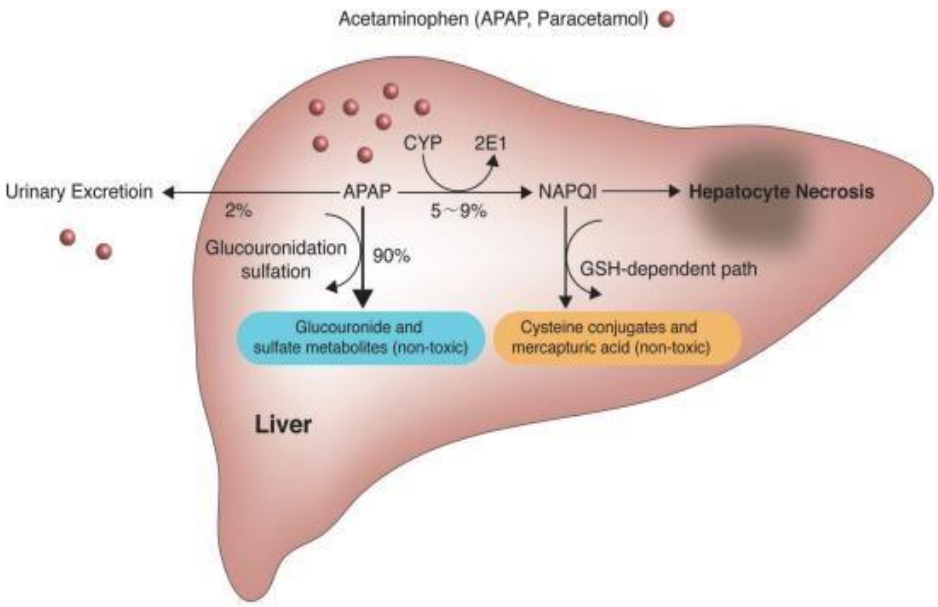

Figure 21: The metabolic pathway of APAP (Yoon *et al*., 2016)

iv. Side effects and contraindications

Despite being the standard antipyretic and analgesic drug for pain and fever, incorrect and longer use of paracetamol is also associated with adverse effects. These include gastrointestinal bleeding, hypertension, neurodevelopmental disorder (Ghanem *et al*., 20116), renal toxicity, and most commonly, hepatotoxicity (McCrae *et al*., 2018).

1.6 NAC in the management of DILI as a result of APAP overdose

1.6.1 N-acetyl cysteine

i. Pharmacology

NAC ((2R)-2-acetamido-3-sulfanylpropanoic acid (C_5H_9 NO_3S)) is a sour tasting white crystalline powder with an acetic odor. It is a thiol compound (figure 22) that serves as a precursor of l-cysteine. NAC can be administered orally or intravenously. Oral administration is usually at a dose of 2400 mg/day and reaches maximum plasma concentrations after 1-2 hours post oral administration. Oral NAC has a bioavailability of 5%, volume of distribution of 0.33-0.47 L/kg and a half-life of >6 hours (Adil *et al*., 2018) with 30% and 70% of its metabolites excreted in urine and faeces, respectively. Intravenous infusion is a two-bag regimen infusion over a 20-hour period that includes first, the administration of 200 mg/kg over 4hours followed by 100 mg/kg over 16 hours (Wong *et al*., 2020).

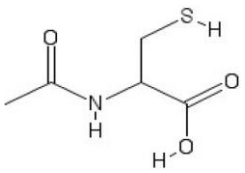

Figure 22: The chemical structure of NAC (Tardiolo *et al*., 2018)

ii. Mechanism of action

NAC exerts its effect as a direct antioxidant, indirect antioxidant and as an agent that breaks down disulphide bonds (Aldini *et al*., 2018). As an indirect antioxidant, NAC acts as a precursor for reduced glutathione (GSH) (Paschalis *et al*., 2018) by providing the amino acid cysteine (figure 23) that is required for the synthesis of GSH during the deacetylation reaction that is facilitated by acylase (Sadowska, 2012; Aldini *et al*., 2018). This GSH act as a direct antioxidant and as a substrate for other several antioxidant enzymes (Aldini *et al*., 2018, Pedre*et al*., 2021, Treweeke *et al*., 2012).

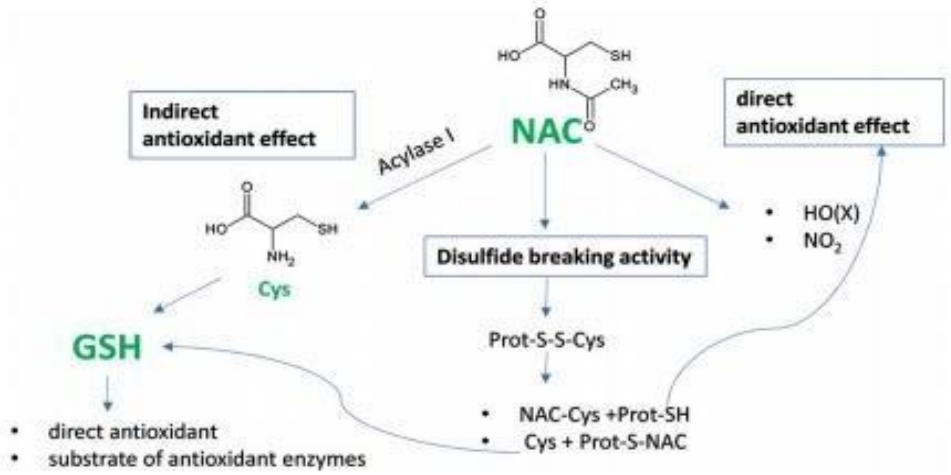

Figure 23: The mechanism of action of NAC (Aldini *et al*., 2018)

During times of GSH depletion due to excessive oxidative stress, NAC directly scavenges NO(X) (Nitrogen oxides) and NO_2 (Nitrogen Dioxide), preventing these oxidants from causing damage. NAC indirectly exerts its antioxidant activity by breaking down proteins that have undergone thiolation, thereby releasing thiols with more direct antioxidant effect compared to NAC and are important in the synthesis of more GSH (Aldini *et al*., 2018; North *et al*, 2012; Moosa *et al*., 2014).

iii. Metabolism

NAC undergoes first pass metabolism in the liver to produce glutathione (GSH), a reducing agent that works by scavenging harmful species using the free sulfhydryl group. NAC is firstly metabolised into cysteine (figure 24) which combines with the amino acids, glycine and glutamate to form the GSH antioxidant (Casanova and Garigliany, 2016).

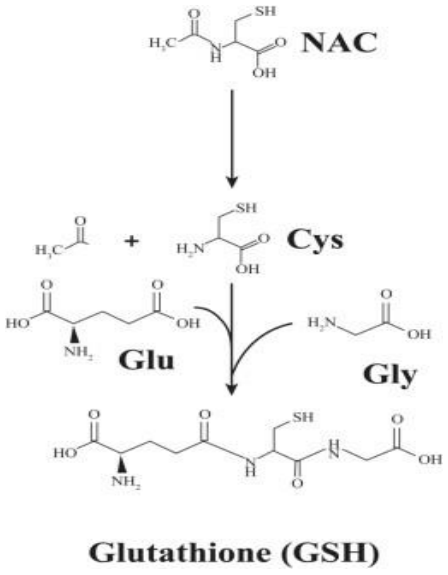

Figure 24: The metabolic pathway of NAC (Casanova and Garigliany, 2016)

iv. Side effects and contraindications

The adverse effects associated with oral NAC administration are less severe than those of intravenous NAC infusion (Heard and Dart, 2017). A higher than normal oral dose of NAC can result in side effects that include diarrhea, rash, edema, headache, epigastric pain, constipation, gastroesophageal reflux, nausea, and vomiting (Adil *et al*., 2018). Intravenous infusion of NAC can result in autoimmune disease and anaphylaxis (Janeczek *et al*., 2019). The use of NAC is contraindicated in patients on nitroglycerin as this may lead to vasodilation that can potentially lead to hypotension. NAC use is also contraindicated in pregnant or breastfeeding women as it can cross the placenta or get excreted via breast milk, leading to embryotoxicity (Aldini *et al*., 2018).

1.6.2 NAC as an intervention for DILI due to APAP overdose

Liver injury due to APAP overdose can be prevented by NAC from progressing to liver failure (Darweesh *et al*, 2017). This antioxidant works by supplying more GSH to the cell, which can bind to the NAPQI metabolite of APAP for excretion. Glutathione replacement protects hepatocytes from being attacked by the NAPQI metabolite (Pettie *et al*., 2019)

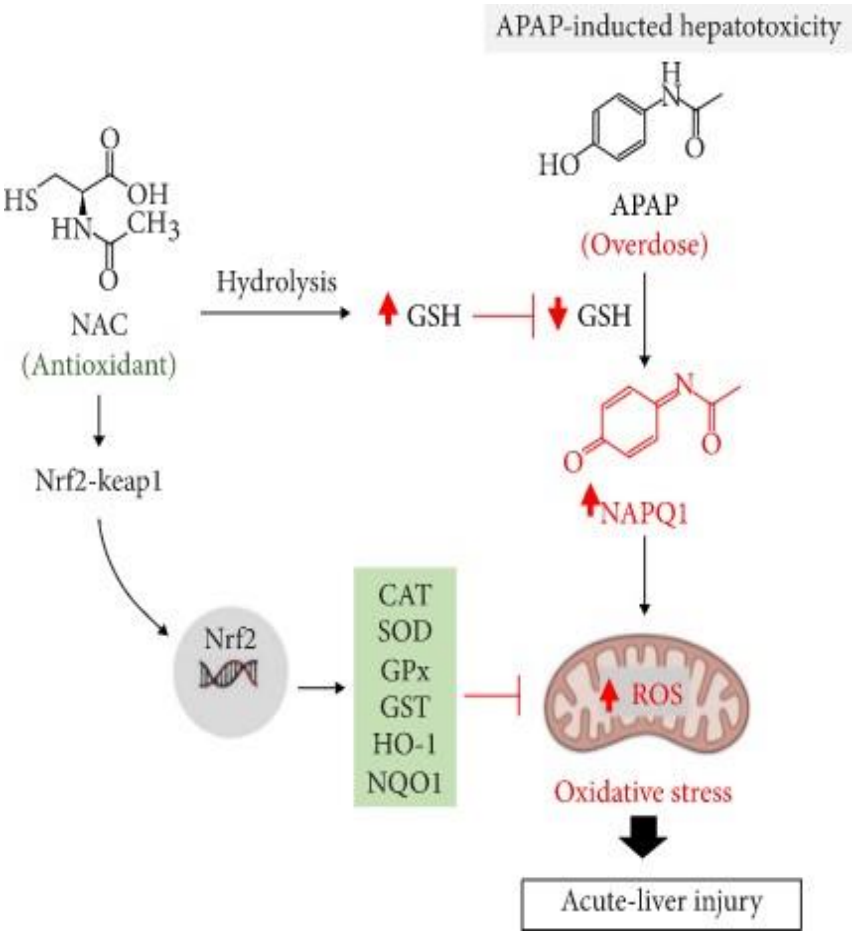

Figure 25: Mechanism by which NAC exerts its effect in APAP DILI (Ntamo *at al*., 2021)

Excess NAC forms part of the Krebs cycle intermediates that drive the metabolism of the mitochondria to generate more energy in the form of ATP. In addition, NAC can induce the reduction of NAPQI into APAP through sulfonation (Yoon *et al*., 2016). As an antioxidant, NAC can directly inhibit oxidative stress by stimulating a nuclear factor erythroid 2-related factor 2 (Nrf2) that is responsible for the upregulation of genes that code for antioxidants like glutathione-s-transferase (GST), superoxide dismutase (SOD) and NADPH quinone oxidoreductase 1 (NQO1) (figure 25).

The 21-hour intravenous 3 bag NAC regimen (150 mg/kg in 200 mL over 1 hour, 50 mg/kg over 4 hours and 100 mg/kg over 16 hours) for APAP overdose has been used for four decades (Wong *et al*., 2020). However, patients on this therapy presented with anaphylaxis and gastrointestinal system adverse reactions (Wong *et al*., 2020). To counteract this, physicians used to stop NAC therapy for a short time and introduce anti-histamine (such as epinephrine) to treat the adverse reactions and this led to administration errors due to the complexity of the3 bag regimen therapy (Pettie *et al*., 2019) and long hospital stays for patients (Au and Zakaria,2014). As part of an intervention, the 20-hour intravenous 2 bag NAC regimen (200 mg/kg over4 hours and 100 mg/kg over 16 hours) (Wong *et al*., 2020) was used instead, which is safe with reduced incidences of anaphylactic reactions and shows high efficacy in the treatment of APAP overdose (Pettie *et al*., 2019). NAC is highly active when given in the first 8 hours post APAP overdose (Ershad *et al*., 2019), which is estimated as the time before levels of ALT peakin serum (Heard and Dart, 2017). NAC can also be administered orally with a loading dose of 140 mg/kg followed by a maintenance dose of 70 mg/kg every 4 hours for 72 hours (Heard and Dart, 2017). Treatment should result in undetectable levels of APAP in blood. Prior to stopping treatment, it is recommended that APAP serum concentrations and ALT levels be measured to monitor if liver injury occurred or whether a liver transplant is needed (Heard andDart, 2017).

1.6.3 NAC in other types of DILI

The potential of NAC in preventing or reversing DILI as a result of cocaine and endotoxin (Labib and Abdel-Rahman, 2003) and acute carbon tetrachloride (Maksimchik *et al*, 2008) toxicity in animal models, to name a few, has been shown. Unclear results from an open-labeltrial were generated where NAC was co-administered with INH and RIF (Ramappa and Aithal,2013). This has led to the uncertainty of the potential of NAC in treating or preventing the development of DILI resulting from antituberculosis medication. Therefore, these findings needto be confirmed through other studies (Devarbhavi *et al*., 2011).

1.7 Zebrafish larvae as a model organism for DILI

Characterised by their striped, black and white zebra-patterned bodies, the zebrafish (*Danio rerio*) is a vertebrate that inhabits floodplains that are found in slow-moving waters like lakes or ponds (Bhandari, 2021). The first publication on zebrafish was made in the year 1822 by an Indian surgeon, Francis Hamilton (Hamilton, 1822). Following Hamilton's publication, a scientist from the University of Oregon by the name of George Streisinger, also known as the father of zebrafish research developed methods for manipulating the genome of zebrafish (Khan and Alhewairini, 2018). To this day, the zebrafish serves as the most widely used model in biomedical research, genetics, and biology. It is also used in the pharmaceutical industry to test the effect of drugs and chemicals (Cassar *et al*., 2019). The zebrafish model has been validated for modeling human diseases (Khan and Alhewairini, 2018) such as cancer (Ignatius *et al*., 2018), mycobacterial infections (Meijer and P Spaink, 2011) and liver steatosis (Dai *et al*., 2015). The zebrafish larval model for toxicology has been developed for use in research for many reasons and one of these is to test if the drugs are suitable to be administered in humans and to check the outcome after administration of the drug (Caballero and Candiracci,2018).
After fertilisation, the zygote grows into a pharyngeal that hatches as a larva at 72 hpf (hours post fertilisation). This larva then grows into an adult zebrafish at 90 dpf (days post fertilisation) (Hosen *et al*., 2013; van Wijk *et al*., 2016). The physiological processes, morphology (figure 26) and pathology of zebrafish are similar to those in humans (So *et al*., 2020). About 70% of human genes and 82% of genes associated with human diseases are similar to those of zebrafish (Bhandari, 2021). The zebrafish has a fully functional liver at 72 hpf (He *et al*., 2013; Garcia-Cortes *et al*., 2020; Verstraelen *et al*., 2016). The metabolic pathways in zebrafish are similar to those in humans, possessing a wide range of cytochrome P450 enzymes that allow metabolic reactions of hydroxylation, conjugation, oxidation and demethylation, thereby providing a suitable tool to study hepatotoxicity (Goessling and Sadler, 2015). There are many reports in literature on the use of zebrafish and zebrafish larva in investigating the potential of hepatotoxicants in developing DILI (Jia *et al*., 2019; Zhang *et al*., 2016; Zhang *et al*., 2017) and also interventions that have been used to reverse DILI (North *et al*, 2010).

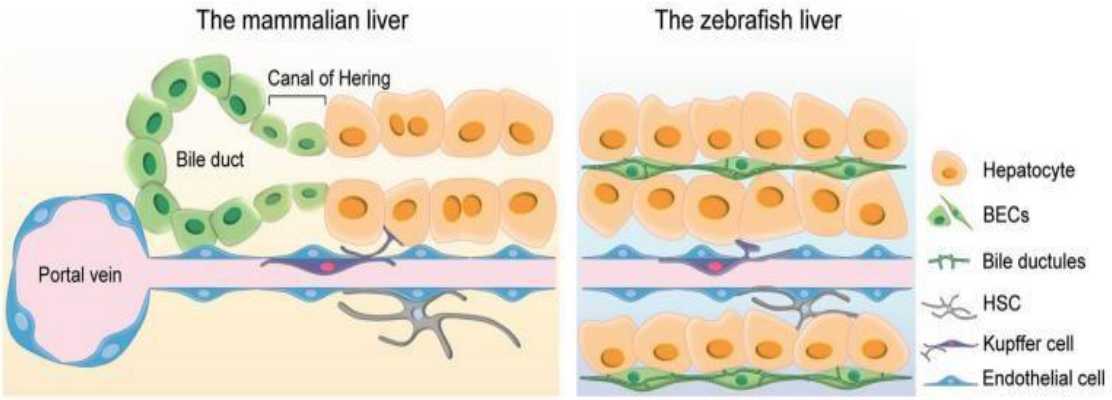

Figure 26: The structures of zebrafish and mammalian liver (So *et al*., 2020)

1.7.1 Quantification of liver injury in zebrafish larvae

Liver histopathology tests are performed in zebrafish to check whether after treatment, there is normal liver cell structure, shape and tight cell-cell contacts in zebrafish larval tissue. Histopathology that has been observed is the appearance of mitochondria shaped like a clover leaf, presence of fatty droplets following staining such as Oil red O and Nile red stains (Zheng *et al*., 2015), macro vesicular triglyceride droplets (Braunbeck *et al*., 1990) and cell death (North *et al*., 2010). The websites www.zfin.org and zfatlas.psu.edu contain information on normal zebrafish tissue to assist in the detection of any changes that may arise from treatment. The phenotypic endpoints that indicate liver toxicity in a zebrafish larval model are retention ofthe yolk sac, modification of the size of the liver and abnormality of the morphology of the liver (Vliegenthart *et al*., 2014). The locomotor activity of zebrafish is also assessed to check the distance that is moved by the zebrafish over a period of five minutes to indicate toxicity (Reuter *et al*., 2016). Zhang and colleagues have also used methods of acridine orange staining as a way of detecting cell death, oxidative stress tests, Real Time polymerase chain reaction (RT-PCR) and the production of ROS to assess hepatotoxicity (Zhang *et al*., 2017). In addition, liver injury can be quantified by measuring liver enzymes such as ALT, AST and Gamma- glutamyl transferase (GGT) in blood using respective diagnostic kits in both zebrafish and in humans (Zhang and Gong, 2014). The zebrafish larvae serve as a better model for studying human diseases such as DILI over other animal models (Zhang *et al*., 2017). Table 2 below summarises the advantages of using zebrafish larvae for modelling human disease

Table 2: Advantages of the zebrafish model over other research models

Characteristic	Advantage	Reference
Develop and reproduce rapidly	✓ Allow for larger sample size and prevention of spending long time for research	Zhang *et al*., 2017; Diekmann and Hill, 2013; He *et al*., 2013
Transparency	✓ Allows for easy visualisation of internal organs such as the liver	Van Wijk *et al*., 2020; Goessling and Sadler, 2015; He *et al*., 2013; van Wijk *et al*, 2016
Inexpensive	✓ Allows for preservation of resources	Goessling and Sadler, 2015; Poon *et al*., 2017
Fully developed and functional organs at 72hpf	✓ Allows for processes such as metabolic processes to occur	Vliegenthart *et al*., 2014 ; Mesens *et al*., 2015 ; Pandya *et al*., 2016
Similar metabolic processes as in humans	✓ Suitable model for studying liver toxicity	Zhang *et al*., 2017; So *et al*., 2020; Vliegenthart *et al*., 2014
Embryo develop in the exterior environment	✓ Protection from any effects that may come from the mother ✓ Allows for screening of different compounds at different developmental stages	Zou *et al*., 2017; Goessling and Sadler, 2015
Small size	✓ Allows for easy handling and growing of many larvae on each well of a multi-well plate ✓ Allows for use of a small drug quantity for treatment	Caballero and Candiracci., 2018; Goessling and Sadler, 2015; He *et al*., 2013; Jia *et al*., 2019
Many offspring	✓ Allows for screening of a range of compounds in a short period ✓ Allows for repetition of experiments to improve validity of results	Goessling and Sadler, 2015; Zou *et al*., 2017
Treatment absorption via the gills, skin and gut	✓ Allows for easy addition of treatment in fish medium	He *et al*., 2013; Diekmann and Hill, 2013

1.8 Analytical methods and software

Daniovision and EthoVision software

The DanioVision is an instrument equipped with EthoVision software that is used for tracking the movement of tiny organisms including zebrafish larvae to study their behavioural activity (Oren *et al*., 2015; Abdelrahman *et al*., 2018).

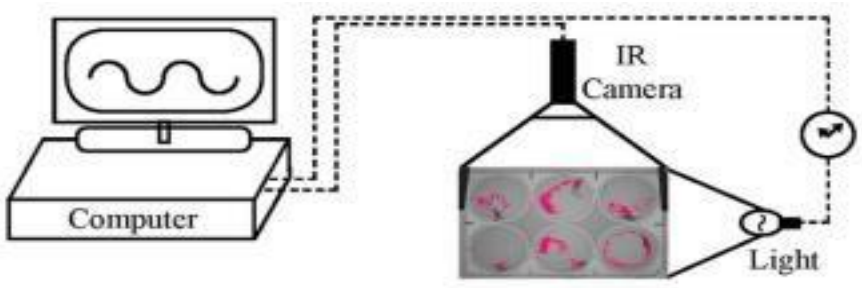

Figure 27: DanioVision set-up with EthoVision software (Oren *et al*., 2015)

This system is equipped first, with a chamber for observing the organism, which is comprised of: a multi-well plate holder, a highly sensitive camera with the highest speed and light source allowing for easy light and dark condition adjustments and for stimulating a response in other assays or organisms that require flash light in order to respond; secondly, with a unit for controlling the temperature (usually set at 28.5˚C); and lastly, a computer with an EthoVision XT software (figure 27) for controlling the light source and to generate a video for tracking the movement of the organism in the plate (Oren *et al*., 2015). Apart from the light stimulus, the DanioVision is also equipped with a tapping device that can generate sound and vibrations in order to stimulate a response (Oren *et al*., 2015).

1.8.1 High performance Liquid chromatography (HPLC)

Chromatography is defined as the separation of parts of a mixture that is exerted into a stationary phase, facilitated by a mobile phase that flows through a column.

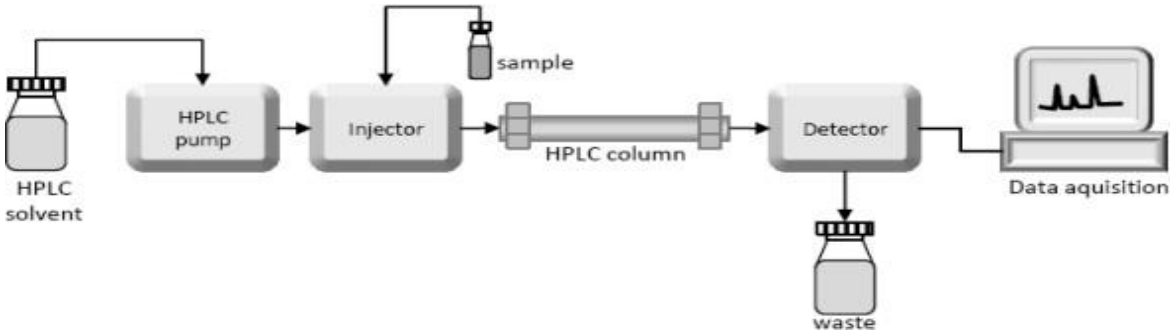

Figure 28: The components of an HPLC system (Czaplicki, 2013)

In HPLC, a high-pressure pump is attached into the column through an injector (figure 28) that inject the sample into the column at high pressure (Coskun, 2016). The column is packed with a small particle sized absorbent material. In the column, high efficiency of separation increases giving high resolution of the peaks. The separation of the molecules is dependent on the molecular weight and the affinity of these molecules to the stationary phase as well as the temperature and the composition, pH, polarity and flow rate of the mobile phase. (Sahu *et al*., 2018). With the help of a detector connected that collects the information and report it on a computer a peak, the concentration and the identity of the analytes can be measured. The can be done by running the samples against a standard curve of calibration standards of known concentration. With an increase in concentration of the analyte of interest, the area under the curve in the peaks increases. The use of HPLC is advantageous as the results after a run can be stored and retrieved any time after every analysis (Gowramma *et al*., 2019).
HPLC can either be normal with a polar stationary phase with a non-polar mobile phase or reversed phase (RP) with a non-polar stationary phase and a polar mobile phase. The polar stationary phase of the normal phase (NP-HPLC) is due to the Si-OH in the silica molecules in the stationary phase therefore, resulting in the retention of polar molecules in the stationary phase while the non-polar molecules move down the column in the mobile phase. However, in RP-HPLC, the non-polar molecules get retained in the stationary phase while the polar molecules move down the column in the mobile phase. Other type of HPLC include size exclusion and Ion exchange HPLC separating the molecules based on the size and molecular charge, respectively.

Once an HPLC method is developed, it needs to be validated according to the International Council for Harmonisation (ICH) and the Food and Drug Administration (FDA) guidelines to ensure that the suitability of the method for purpose. HPLC has been used in the pharmaceutical industry to test the stability of a variety of compounds in different conditions. The aim of conducting a stability test on a drug is to test how the value of that particular drug changes over time (Ciobanu *et al*., 2017; Osman and Elbashir, 2017). The factors that can influence the stability of the drug include light, temperature and humidity (Osman and Elbashir, 2017).

1.8.2 Liquid chromatography-mass spectrometry (LC-MS)

Liquid chromatography-mass spectrometry is a conjugation of liquid chromatography with mass spectrometry and is a widely used technique in the pharmaceutical industry for analysing analytes or biomarkers in biological or other samples. The LC-MS instrument comprises of a liquid chromatography and mass spectrometry unit such as the HPLC and a mass

spectrometer. The sample components (figure 29) are first separated in the HPLC column based on their affinity to the stationary phase.

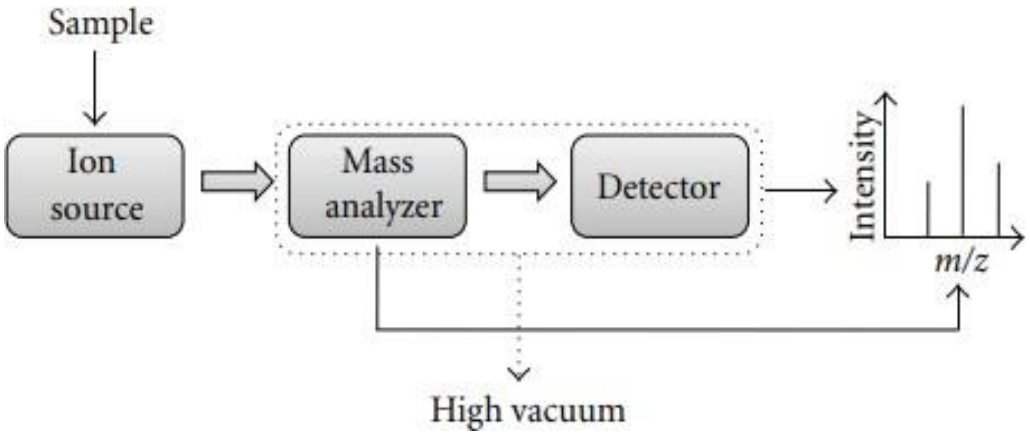

Figure 29: The components of LC-MS system (Banerjee and Mazumdar, 2012)

The separated sample then gets sprayed into an Atmospheric Ion Source (API) where they get converted into ions in the gas phase and most of the eluent gets pumped into waste. The ion source is the most significant component of any MS analysis because it helps in the generation of ions for the analysis. The most common ion sources include Atmospheric Pressure Chemical Ionization (APCI) and the Electrospray Ionization (ESI). The choice of an ion source depends upon the polarity of the analyte of interest. Then the ions get sorted according to theirmass to charge (*m/z*) ratio (Pitt, 2009) in a high vacuum by a mass analyzer. Types of mass analysers include quadrupole, time of flight, ion trap and magnetic sector. Thereafter, the concentration of these separated ions is measured by a detector and the results get displayedas a mass spectrum on a computer that is connected to the LC-MS instrument. Commonly used mass detectors include electron multiplier, dynode, multichannel plate and photodiode detector (Banerjee and Mazumdar, 2012). Once an LC-MS method is developed, validation according to FDA and ICH guidelines is required to prove that the method is accurate and precise. Method validation parameters include system suitability, specificity, linearity, precision, accuracy, limit of detection, limit of quantification and robustness. LC-MS can be used in testing the stability of drugs in conditions such as at different temperatures by measuring the drug concentrations at these conditions at a specific time point (Desmarchelier*et al*. 2018; Rochani *et al*., 2020).

Chapter 2

Rationale, hypothesis, aim and objectives

2.1 Rationale and hypothesis

Many studies on humans (Huang *et al*., 2018) and animal models like mice (Mohar *et al*., 2014), rats (Aycan *et al*., 2014) and zebrafish larvae (North *et al*, 2012) have reported the potential of APAP in causing DILI after overdose of the drug, making APAP a known inducer of liver injury. Many studies on NAC intervention to DILI as a result of certain drugs have beenconducted in humans (Moosa *et al*., 2021) and animal models like mice (Saito *et al*., 2010), rats (Attri *et al*., 2000) and zebrafish larvae (North *et al*, 2012). APAP overdose can be reversedby the infusion of NAC within 8 hours after overdose (Ershad *et al*., 2019), otherwise liver injuryis prone to occur and progress to liver failure (Bruells *et al*., 2021). In addition, NAC has beenreported to be effective in treating APAP overdose poisoning after oral administration (Pedre *et al*., 2021). Out of the four highly effective first line TB drugs, INH (Sachar *et al*., 2016; Lootset *al*., 2005; Jia *et al*., 2019; Zhang *et al*., 2017), PZA (Loots *et al*., 2005; Younossian *et al*., 2005; Zhang *et al*., 2016) and RIF (Sahu *et al*, 2015; Loots *et al*., 2005; Saukkonen *et al*., 2006) are known to be associated with adverse drug reactions, the most common of which isDILI, especially during the start of the highly intensive phase of antituberculosis chemotherapy (Combrink and du Preez, 2020). However, no information has been reported on the hepatotoxicity potential of EMB (Ramappa and Aithal, 2013). This therefore requires that during antituberculosis chemotherapy, therapeutic drug monitoring must be performed (Ramappa and Aithal, 2013). However, therapeutic drug monitoring is not done frequently (Babalik *et al*., 2011).

Unclear evidence exists for the potential of NAC in treating or preventing the development of drug induced liver injury due to TB drugs (Ramappa and Aithal, 2013). It is therefore hypothesized that NAC is able to reverse liver injury due to first line TB medication since it has been shown to be highly effective in the treatment of DILI associated with APAP and has in fact become the standard of care (Chughlay *et al*., 2016) and forms part of the vital medicinesas reported by the WHO (WHO, 2019). This means that the risk of introducing it as a treatmentis low. Therefore, a zebrafish larval model for DILI due to these drugs, individually and in combination needs to be developed and the potential of NAC in reversing the DILI needs to be investigated in the same model.

2.2 Research question

Can NAC prevent and reverse hepatotoxicity associated with first-line TB drugs, as well as combinations thereof?

2.3 Aim

This study aims to evaluate drug-induced hepatotoxicity as a result of first-line antituberculosis medication, and combinations thereof, and to test the efficacy of NAC in the prevention and treatment of hepatic injury caused by antituberculosis drugs using a zebrafish larval model.

2.4 Objectives

- Conduct solubility and stability assessment for APAP and all first line TB drugs
- Perform toxicity assays for NAC, APAP, INH, PZA, RIF and EMB to determine the safe dose (for NAC) and the dose produce most damage for each drug, using Oil red O liver stains and EthoVision movement tracking software (for NAC) as endpoints
- Develop a zebrafish larval model for DILI as a result of first-line TB medication by using APAP as a positive control
- Investigate the potential intervention of N-acetyl cysteine for the prevention of DILI by evaluating Oil red O liver stain reduction

Chapter 3

Materials and methods

3.1 Reagents and Chemicals

Absolute ethanol was purchased from B & M Scientific (B & M Scientific, Cape Town, South Africa). Reference standards of N-acetyl cysteine, Acetaminophen, isoniazid, ethambutol, Oil Red O, L-ascorbic acid, Tween 20, Phosphate-buffered saline (PBS), glycerol and agarose were purchased from Sigma-Aldrich (St Louis, MO, USA). Reference standards of Rifampicin and Pyrazinamide were purchased from Toronto Research Chemicals (Toronto, Canada). Ammonium formate and formic acid were obtained from Fisher Chemical (Madrid, Spain & Norcross, United State of America). Methanol and Acetonitrile were obtained from Romil Pure Chemistry (Johannesburg, South Africa). Burdick and Jackson Isopropanol was purchased from Honeywell Burdick & Jackson (Muskegon, United State of America).

3.2 Zebrafish embryos care and maintenance

Fertilised zebrafish eggs were sourced from the Zebrafish Research Facility at Stellenbosch University at the Division of Clinical Pharmacology, Faculty of Medicine and Health Sciences. Following collection, zebrafish eggs were transferred into clean petri dishes with fish water (E3) (which was refreshed after every 24 hours) and then incubated at 28˚C. The E3 embryo water was made up of 15 mM NaCl, 0.5 mM KCl, 1 mM $CaCl_2$, 1 mM $MgSO_4$, 0.05 Mm Na_2CO_2,3 drops per litre Methylene blue and distilled water with a pH between 7.20 and 7.80. These conditions allow for proper development of the embryos. After every 24 hours, the embryos were assessed for any abnormalities or fatalities by observation under the stereomicroscope and dead or abnormal embryos were removed from the dishes. Zebrafish embryos at 2 dpf were used for further experiments.

3.3 Instrumentation

The masses of all drugs, salts and stains used during experiments were weighed out using the BOECO Balance BXX (Axiology Lab, RSA). Zebrafish larvae were tracked by a Daniovision larval activity tracking equipment coupled with an Ethovision software (Noldus, Wageningen, Netherlands). Samples and mobile phases were sonicated using an ultrasonic bath (United Scientific, South Africa). Acetaminophen, as well as the first line TB drugs (Isoniazid, Pyrazinamide and Rifampicin), were analysed on the Shimadzu HPLC (Shimadzu LC-2050C 3D coupled with a binary pump, autosampler, column compartment and Photodiode-Array (PDA) detector and Ex-Bioanalytics software). The wavelength of acetaminophen was determined prior to method development using the DU® 640 Spectrophotometer, Beckman. Ethambutol was analysed on the Shimadzu LC-MS instrument (Shimadzu LC-20AD XR binary pump, SIL-20_AC XR Autosampler; Shimadzu CTO-20A column compartment and Shimadzu 8040 triple quadrupole mass spectrometer and Lab solutions software). Distilled water was

obtained from a Milli-Q® water purification system coupled with Synergy® UV system (Molsheim, France).

3.4 Methods

3.4.1 HPLC method development and validation

For stability testing of the three first line TB drugs (INH, PZA and RIF) in E3 medium, the following HPLC methods that have been previously developed and validated by Mr Cassius Phogole from Stellenbosch University for the completion of his MSc in Pharmacology have been used. For assessing the stability of EMB in E3 embryo water, a previously developed and validated LC-MS method was used. Below is a summary of the HPLC and LC-MS methodsused for the analysis of test samples. The chromatograms of the analytes are depicted in figure30 below.

i. Isoniazid:

Quantification of isoniazid was performed on an HPLC system coupled with a detector set at a wavelength of 264 nm. Chromatographic separation was accomplished by isocratic elution of 95: 5 (A: B; v/v) using a Poroshell 120 EC-C18 (4.6 x 100 mm, 2.7 µm) column at 0.550 mL/min flow rate. The mobile phase A was prepared with water + 2 mM ammonium acetate + 0.1% acetic acid, and mobile phase B was prepared with methanol: water (95:5, v/v) + 2 mM ammonium acetate + 0.1% acetic acid. The mobile phase was filtered before use. The column temperature was maintained at ambient conditions and the injection volume was 20 µl.

ii. Pyrazinamide:

The analysis of pyrazinamide was carried out on an HPLC system consisting of a quaternary pump, autosampler, and UV detector. Separations were performed on a Poroshell 120 EC-C18 (4.6 x 100 mm, 2.7 µm) column. UV detection was at 265 nm. Mobile phase A was a mixture of water + 0.1% formic acid and mobile phase B was a mixture of acetonitrile + 0.1% formic acid. Isocratic elution at 3.4 min was achieved by composition of 40: 60 (A: B; v: v). The flow rate was 0.350 mL/min, and the injection volume was 5 µl.

iii. Rifampicin:

The chromatographic quantification of rifampicin was carried out on an HPLC system coupled with a UV detector. Chromatographic separation was accomplished on a Venusil XBP C18 (2) (4.6 x 150 mm, 5 µm) column at room temperature. The analysis was performed at 334 nm using optimized mobile phase A consisting of water: acetonitrile (95:5, v/v) + 10 mM ammonium formate + 0.1% formic acid and mobile phase B consisting of acetonitrile: methanol: water (65:30:5, v/v/v) + 10 mM ammonium formate + 0.1% formic acid. The mobile phase flow rate was 0.500 mL/min, injection volume 10 µL and run time was 11 min. Gradient elution mode was achieved at 55-95% B over 6 minutes; 95-55% B over 7 minutes; and re- equilibration over 11 minutes.

iv. Ethambutol:

EMB is a small compound that has poor UV absorbance, making it difficult to develop a reversed phase HPLC method for the quantification of this compound (Jyothi *et al*., 2016). Therefore, a previously developed LC-MS method has been used for the analysis of standards (STDs), quality controls (QCs) and test samples for EMB. Quantification was carried out using a Shimadzu LC-MS instrument. Chromatographic separation was achieved using a Poroshell 120 EC-18 column (3, 0 X 100mm, 2.7µm) with gradient elution of 5% B over 1 min; 5-40% B over 1.25 min; 40-5% B over 0.5 min, equilibration at 5% B over 3 min. Mobile phase A consisted of 0.1% acetic acid in water and mobile phase B consisted on acetonitrile. A multiple reaction monitoring method in the positive ion mode was developed following the transitions m/z 205.0000→ 116.1500 and 205.0000→ 98.1000. The injection volume was 5 µL. Source settings were maintained at -15 eV collision energy, dwell time of 97 msec, Q1 Pre Bias of -12 V and QC Pre Bias of -12 V.

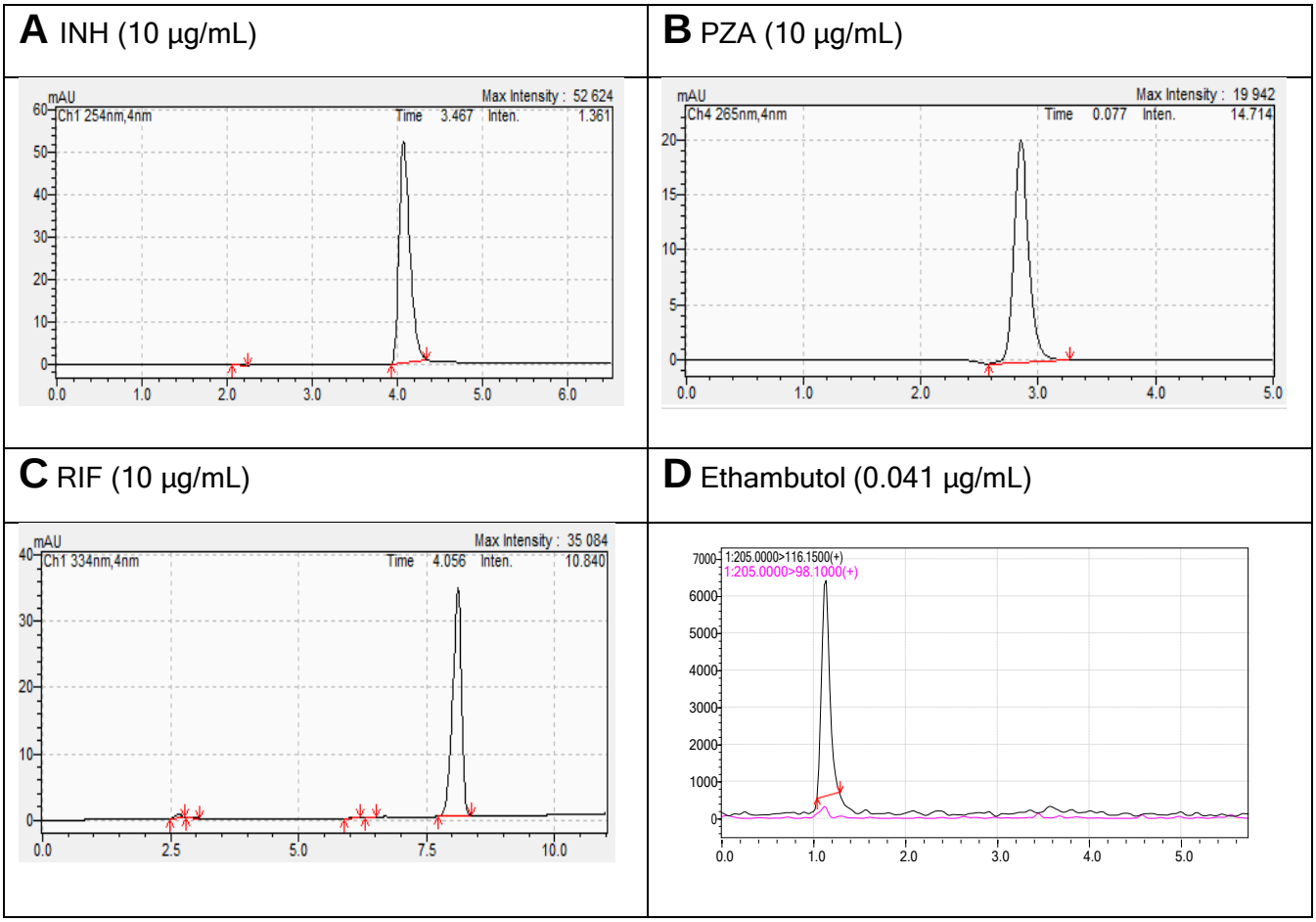

Figure 30: Chromatograms for (**A**) INH; (**B**) PZA; (**C**) RIF and (**D**) EMB

3.4.2 APAP HPLC method development

An accurate and precise HPLC method was developed and validated for APAP. Prior to method development, a suitable wavelength (between 200 and 800 nm) for detection of APAPwas determined using the spectrophotometer. APAP was prepared at a concentration of 10 µg/mL and the maximum absorbance wavelength of 247 nm was used for developing the method.

APAP was analyzed on a Shimadzu HPLC system coupled with an ultraviolet detector. Successful separation was achieved by isocratic elution on a reverse-phase Venusil XBP C18 (4.6 X 100 mm, 5 µm) column, using a mobile phase consisting of 0.1% formic acid in water and acetonitrile (82:18; A: B; v: v) at 0.650 mL/min flow rate, detection wavelength of 247 nm, column oven temperature of 28°C and injection volume of 10 µL. The chromatographic retention time was consistent at 3.26 min with excellent chromatographic peak, as shown in figure 31 below.

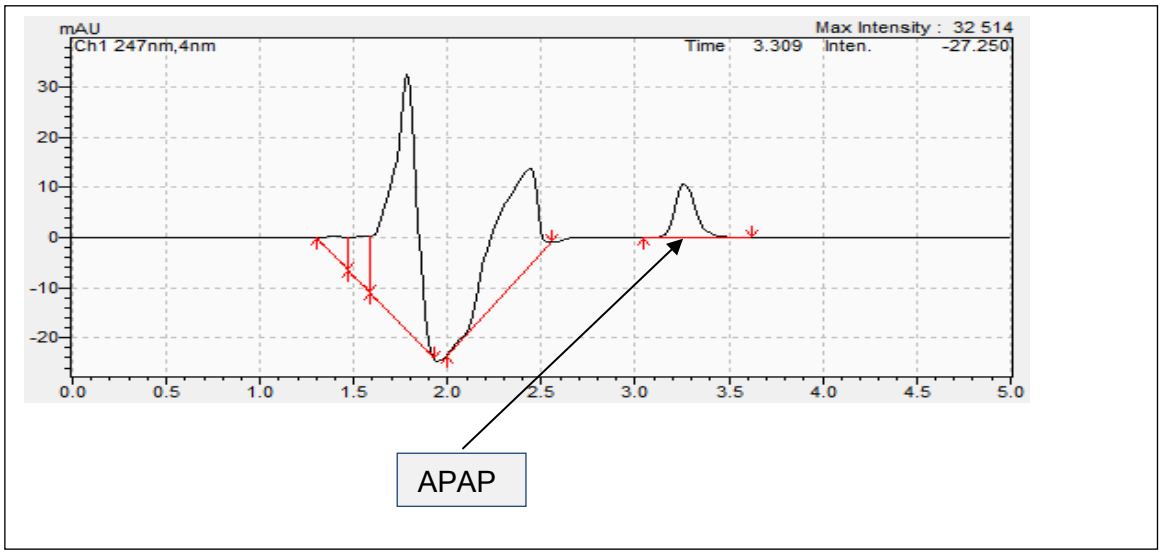

Figure 31: Chromatogram of APAP (1 µg/mL)

3.4.3 Analytical Method pre-validation

Validation of an HPLC method is crucial to prove the reliability and reproducibility of the method. For a method to be considered as valid in pre-clinical settings, the accuracy and precision of all STDs and QCs needs to be measured and must fall within acceptable limits as recommended by the FDA guidelines. Accuracy is the measure of how close the observed concentration is to the nominal concentration while precision (%CV), also known as the coefficient of variation, is the measure of how close the observed concentration replicates are to one another. The accuracy for all STDs and QCs in a batch must be between 85-115%, whereas for the LLOQ, it must be between 80-120%. However, the precision must be within 15% for all STDs and QCs and within 20% for the LLOQ in a batch. For the purpose of this study, a pre-validation was performed by construction of a calibration curve using the STDs and QCs.

i. Preparation of reference stock solutions for the drugs

Reference standards (SS) of each drug were weighed out and used to prepare reference stock solutions in the recommended solvent as outlined on the certificate of analysis. Each reference stock solution was prepared at a concentration of 1 mg/mL by adjusting the mass weighed out to purity (table 3). Samples were vortexed to get the drugs into solution. After preparation, the prepared stock solutions were then stored at -80˚C until use.

Table 3: Preparation of reference stock solutions for the drugs

Analyte	Mass weighed out (mg)	Mass adjustment (mg)	% Purity	Solvent	Solvent volume (mL)	Concentration (mg/mL)
Isoniazid	1.08	0.940	99.0	Water	0.931	1.00
Pyrazinamide	1.20	1.07	99.0	Acetonitrile	1.06	1.00
Rifampicin	1.21	1.15	97.0	Methanol	1.12	1.00
Ethambutol	1.15	1.13	99.0	Water	1.12	1.00
Acetaminophen	2.14	2.03	99.0	Methanol	2.01	2.00

ii. Preparation of calibration standards and quality control samples

For the preparation of calibration standards, seven working stock solutions of each drug of concentrations between 31.3 µg/mL to 2000 µg/mL were prepared in 1.5 mL microcentrifuge tubes by serial dilution using the reference stock solution. Calibration standards 1 to 7 were then prepared by spiking 50 µL of working stock solution into 950 µL of solvent to make the respective calibration standard. Vortexing of the samples for a minute was used to get the drugs into solution. The calibration standards concentration range was selected based on the drug concentration range used to dose the zebrafish larvae. Calibration standards were storedat -80˚C until use. Tables 4 and 5 below shows the preparation of the STDs and QCs of APAP.

Table 4: The preparation of the calibration standards from the working stock solutions of APAP

Sample ID	Volume of solvent (µL)	WS	Concentration of WS (µg/mL)	Amount spiked (µL)	Total volume of solvent and spiking solution (mL)	Final concentration (µg/mL)
STD 1	950	ws 1	2000	50.0	1.00	200
STD 2	950	ws 2	1000	50.0	1.00	100
STD 3	950	ws 3	500	50.0	1.00	50.0
STD 4	950	ws 4	250	50.0	1.00	25.0
STD 5	950	ws 5	125	50.0	1.00	12.5
STD 6	950	ws 6	62.5	50.0	1.00	6.25
STD 7	950	ws 7	31.3	50.0	1.00	3.13

STD: Standard; WS: Working solution

iii. Preparation of quality controls

Quality controls (QCs) were prepared at high, medium and low concentrations, using the same reference stock solution that was used to prepare the calibration standards. Prior to the preparation of the QCs, working stock solutions at 1600 µg/mL, 800 µg/mL and 90 µg/mL were prepared in the respective solvent. The QCH, QCM and QCL were prepared at a concentration of 160 µg/mL, 80 µg/mL and 9 µg/mL by spiking 100 µL of working stock solution to 900 µL of solvent, respectively. Working stock solution 3 (WSQ3) at 400 µg/mL was only used to facilitate the dilution steps. All samples were vortexed to solubilize the drug. All QCs were stored at -80˚C until use.

Table 5: The preparation of QCs from the working stock solutions of APAP

WS	Source solution	Solvent volume (µL)	Spiking solution (µL)	WS concentration (µg/mL)	QC	WS volume spiked in solvent (µL)	Solvent volume (µL)	QC concentration (µg/mL)
WSQ1	SS	200	800	1600	**QCH**	100	900	160
WSQ2	WS 1	500	500	800	**QCM**	100	900	80.0
WSQ3	WS 2	500	500	400	**-**	-	-	-
WSQ4	WS 3	775	225	90.0	**QCL**	100	900	9.00

3.4.4 Stability assessment of INH, PZA and RIF

For this study, solubility and stability studies were carried out to test whether the analytes were soluble in E3 medium and also stable when the samples are placed in the laboratory incubator set at 28 ˚C for three consecutive days. For the toxicity and intervention experiments, the drugs would be added to the zebrafish larvae in the E3 medium, and solubility and stability in this medium at 38°C is vital information. For the stability assessment of the analytes, the samples at high and low QC levels were prepared and placed at 28°C as this is the optimal temperature in which the larvae live. For a test sample to be considered stable, the percentage difference between the test sample and the reference sample must be within 15%.

i. Preparation of calibration standards from drug working stock solutions

For the preparation of calibration standards, seven working stock solutions of each drug covering a range of 0.156 µg/mL to 10 µg/mL were prepared by serial dilution using the reference stock solution prepared as described in section 3.4.3 in table 3, prepared in the appropriate solvent listed in the certificate of analysis for optimal solubility. Calibration standards 1 to 7 were then prepared by spiking a 50 µL of working stock solution to a 950 µL of solvent to make the respective calibration standard using the respective working stock solution. Samples were solubilized through vortexing. The calibration standards concentration range was selected based on the drug concentration range used to dose the zebrafish larvae. Calibration standards were stored at -80˚C until use.

Table 6: The preparation of the calibration standards from the INH, PZA and RIF working stock solutions

Sample ID	Volume of solvent (µL)	WS	Concentration of WS (µg/mL)	Amount spiked (µL)	Total volume of solvent and spiking solution (mL)	Final concentration (µg/mL)
STD 1	950	ws 1	200	50.0	1.00	10.0
STD 2	950	ws 2	100	50.0	1.00	5.00
STD 3	950	ws 3	50.0	50.0	1.00	2.50
STD 4	950	ws 4	25.0	50.0	1.00	1.25
STD 5	950	ws 5	12.5	50.0	1.00	0.625
STD 6	950	ws 6	6.25	50.0	1.00	0.313
STD 7	950	ws 7	3.13	50.0	1.00	0.156

ii. Preparation of quality controls

QCs were prepared at high, medium and low concentrations using the same reference stock solution that was used to prepare the calibration STDs. Prior to the preparation of the QCs, working stock solutions at 160 µg/mL, 80 µg/mL and 8 µg/mL were prepared in the respective solvent. The working stock solutions were then used to prepare the QCs at QC-Low, QC-Medium and QC-High at a concentration of 8 µg/mL, 4 µg/mL and 0.4 µg/mL by spiking a 50 µL of working stock solution into 950 µL of solvent. Samples were solubilized by means of vortexing. The QCs were stored at -80˚C until use.

Table 7: The preparation of INH, PZA and RIF QCs from the working stock solutions

WS	Solvent volume (µL)	Source solution	Spiking solution volume (µL)	WS concentration (µg/mL)	QC	WS volume spiked in solvent (µL)	Solvent volume (µL)	QC concentration (µg/mL)
WSQ1	840	**SS**	160	160	**QCH**	50.0	950	8.00
WSQ2	500	**WSQ1**	500	80.0	**QCM**	50.0	950	4.00
WSQ3	900	**WSQ2**	100	8.00	**QCL**	50.0	950	0.400

iii. Preparation of test samples in E3 embryo water

For the preparation of the test samples, working stock solutions of each drug were prepared at high (160 µg/mL) and low (8 µg/mL) QC concentrations by serial dilution using the respective solvent (for RIF, 1 mg/mL of ascorbic acid in methanol was used). Using the working stock solutions, test samples were prepared at low and high QC concentrations at 8.00 µg/mL and 0.400 µg/mL by spiking 200 µL of working stock solution into 3800 µL of E3 embryo water. Working stock solution 2 (WSQ2) at 80 µg/mL was only used to facilitate the dilution steps. Thereafter, the test samples were stored in the laboratory incubator at 28˚C over 3 days. After every 24 hours, test samples were sampled from the incubator and were stored at -80˚C until analysis. The samples at time 0 were used to assess the baseline stability and solubility of the analyte in E3 embryo water.

Table 8: The preparation of INH, PZA and RIF test samples in E3 embryo water from the working stock solutions

WS	Solvent volume (µL)	Source solution	Spiking solution volume (µL)	WS concentration (µg/mL)	QC	WS volume spiked in E3 (µL)	E3 volume (µL)	QC concentration (µg/mL)
WSQ1	840	**SS**	160	160	**QCH**	200	3800	8.00
WSQ2	500	**WSQ1**	500	80.0		-	-	-
WSQ3	900	**WSQ2**	100	8.00	**QCL**	200	3800	0.400

3.4.5 Stability assessment of RIF in E3 embryo water with ascorbic acid at 20 µg/mL

The solubility of RIF in an aqueous environment has been shown to improve by the addition of ascorbic acid (Phogole, 2022). Therefore, in an attempt to improve the solubility of RIF in E3 embryo water over time, the RIF test samples were prepared at high and low QC concentrations in E3 embryo water with 20 µg/mL of ascorbic acid. Working stock solutions of RIF were prepared by serial dilution using the RIF stock solution (20 µg/mL RIF in methanol with ascorbic acid). Test samples were prepared at low and high concentrations of QC at 8.00 µg/mL and 0.400 µg/mL by spiking 200 µL of working stock solution in 3800 µL of E3 embryo water. Working stock solution 2 (WSQ2) at 80 µg/mL was only used to facilitate the dilution steps. Samples were vortexed in order to get the drug into solution. Thereafter, the test samples were stored in the laboratory incubator at 28˚C over 3 days. After every 24 hours, testsamples were taken from the incubator and stored at -80˚C until analysis. The samples at time0 were used to assess the baseline stability and solubility of the analyte in E3 embryo water.

Table 9: Table showing the preparation of RIF test samples in E3 embryo water from the working stock solutions

WS	Solvent volume (µL)	Source solution	Spiking solution volume (µL)	WS concentration (µg/mL)	QC	WS volume spiked in solvent (µL)	Solvent volume (µL)	QC concentration (µg/mL)
WSQ1	840	**SS**	160	160	**QCH**	200	3800	8.00
WSQ2	500	**WSQ1**	500	80.0		-	-	-
WSQ3	900	**WSQ2**	100	8.00	**QCL**	200	3.8×10^3	0.400

3.4.6 Stability assessment of EMB

An ethambutol-D4 internal standard at 200 ng/mL was included in the preparation of the STDs, QCs and test samples for EMB. The internal standard was diluted to 0.2 µg/ml. This was done to compensate for any error that might have occurred during sample preparation. Test samples were prepared in E3 embryo water and placed in the incubator set at 28˚C for 3 days. The test samples were sampled from the incubator after every 24 hours and were placed at -80˚C until analysis. On the day of analysis, test samples were analyzed on the LC-MS instrument against the freshly prepared STDs and QCs in the solvent recommended on the certificate of analysis. Tables 10-12 below show how the STDs, QCs and test samples for EMB were prepared.

Table 10: The preparation of the calibration standards from the EMB working stock solutions

Sample ID	Volume of solvent (µL)	WS	Concentration of WS (µg/mL)	Amount spiked (µL)	Total volume of solvent and spiking solution (mL)	Final concentration (µg/mL)
STD 1	150	ws 1	10.0	50.0	0.200	2.50
STD 2	150	ws 2	5.00	50.0	0.200	1.25
STD 3	150	ws 3	2.50	50.0	0.200	0.625
STD 4	150	ws 4	1.25	50.0	0.200	0.313
STD 5	150	ws 5	0.625	50.0	0.200	0.156
STD 6	150	ws 6	0.313	50.0	0.200	0.0783
STD 7	150	ws 7	0.156	50.0	0.200	0.0390

Table 11: The preparation of EMB QCs from the working stock solutions

WS	Solvent volume (µL)	Spiking solution volume (µL)	WS concentration (µg/mL)	QC	WS volume spiked in solvent (µL)	Solvent volume (µL)	QC concentration (µg/mL)
WSQ1	950	50.0	10.0	**QCH**	50.0	150	2.50
WSQ2	950	50.0	0.400	**QCL**	50.0	150	0.100

Table 12: The preparation of EMB test samples in E3 embryo water from the working stock solutions

WS	Solvent volume (µL)	Source solution	Spiking solution volume (µL)	WS concentration (µg/mL)	QC	WS volume spiked in solvent (µL)	Solvent volume (µL)	QC concentration (µg/mL)
WSQ1	3600	**SS**	400	8.00	**QCH**	50.0	150	2.00
WSQ2	3960	**SS**	40.0	0.400	**QCL**	50.0	150	0.100

3.4.7 Concentration range finding experiments (Dose response experiment)

The purpose of performing dose range finding experiments in toxicology is to determine the well-tolerated and toxic doses of the drugs in a zebrafish larval model. The optimal concentrations will then be used to answer the research question. For the purpose of this study, dose range finding experiments for all the drugs (NAC, APAP, INH, PZA, RIF and EMB) were performed. To do this, previously reported hepatotoxic concentrations of APAP, INH and PZA and safe concentration of NAC were used as references for the dose range finding experiments (Zhang *et al*., 2017; North *et al*., 2010). For EMB and RIF, there were no previously reported hepatotoxic doses for the drugs, therefore the doses were adjusted based on the human dose of the drugs.

i. Dose response experiments for APAP, INH, PZA, EMB and RIF

Zebrafish larvae at 48 hpf were pipetted into each well of a 6-well plate with 12 replicates per concentration. For preparation of treatment, a reference stock solution was prepared in E3 and 2.4% Dimethyl sulfoxide (DMSO) and was then used for the preparation of the other treatments by serial dilution. For the positive control (2% ethanol) and each test concentration, 3 mL (2400 µL of fish water and 600 µL of treatment) was added to each well of a 6-well plate. For the

negative control group 3 mL of E3 was added to the well. Each treatment was changed after every 24 hours for 3 days and after every change in treatment, the plate was placed in a laboratory incubator set at 28˚C. At 4 days post exposure (dpe), the larvae were fixed with 4% formaldehyde and kept overnight at 4˚C. On the next day, the 4% formaldehyde was removed, and the larva were stained with Oil red O (ORO) stain and were then taken for visualisation under the microscope. Reference stock solutions of the drugs were prepared in E3 embryo water with 2.4% DMSO of the total volume and were adjusted for purity. DMSO was used in order to facilitate the uptake of the drugs by the zebrafish larvae.

Table 13: Preparation of reference stock solutions of the drugs in E3 embryo water with 2.4% DMSO

Drug	Concentration of ref stock (mg/mL)	Amount weighed out (mg)	Volume of E3 embryo water (mL)	Volume of 2.4% DMSO (mL)	Total volume (mL)
INH	10.0	100	9.76	0.240	10.0
PZA	10.0	100	9.76	0.240	10.0
RIF	1.00	1.00	0.976	0.0240	1.00
EMB	3.00	30.0	9.76	0.240	10.0
APAP	1.00	10.0	9.76	0.240	10.0
NAC	1.00	10.0	9.76	0.240	10.0

Table 14: Preparation of INH treatment used to dose the zebrafish larvae at 48 hpf for 3 days in a 6-well plate

Concentration (mM)	Total volume (mL)	Amount taken out of previous sample (mL)	Volume of E3 (mL)
20.0	7.00	-	-
16.0	6.00	4.80	1.20
12.0	5.00	3.75	1.25
8.00	4.00	2.67	1.33
4.00	3.00	1.50	1.50
1.00	2.00	0.500	1.50

Table 15: Preparation of PZA treatment used to dose the zebrafish larvae at 48 hpf for 3 days in a 6-well plate

Concentration (mM)	Total volume (mL)	Amount taken out of previous sample (mL)	Volume of E3 (mL)
8.00	7.00	-	-
7.00	6.00	5.25	0.750
5.00	5.00	3.57	1.43
4.00	4.00	3.20	0.800
2.00	3.00	1.50	1.50
1.00	2.00	0.670	1.33

Table 16: Preparation of RIF treatment used to dose the zebrafish larvae at 48 hpf for 3 days in a 6-well plate

Concentration (mM)	Total volume (mL)	Amount taken out of previous sample (mL)	Volume of E3 (mL)
12.0	7.00	0.346	6.65
10.0	6.00	5.00	1.00
8.00	5.00	4.00	1.00
6.00	4.00	3.00	1.00
4.00	3.00	2.00	1.00
2.00	2.00	1.00	1.00

Table 17: Preparation of EMB treatment used to dose the zebrafish larvae at 48 hpf for 3 days in a 6-well plate

Concentration (mM)	Total volume (mL)	Amount taken out of previous sample (mL)	Volume of E3 (mL)
2.00	7.00	6.53	0.470
1.60	6.00	4.80	1.20
1.20	5.00	3.75	1.25
0.800	4.00	2.67	1.33
0.400	3.00	1.50	1.50
0.200	2.00	1.00	1.00

Table 18: Preparation of APAP treatment used to dose the zebrafish larvae at 48 hpf for 3 days in a 6-well plate

Concentration (mM)	Total volume (mL)	Amount taken out of previous sample (mL)	Volume of E3 (mL)
1.00	11.0	8.80	2.20
0.900	10.0	9.00	1.00
0.800	9.00	8.00	1.00
0.700	8.00	7.00	1.00
0.600	7.00	6.00	1.00
0.500	6.00	5.00	1.00
0.400	5.00	4.00	1.00
0.300	4.00	3.00	1.00
0.200	3.00	2.00	1.00
0.100	2.00	1.00	1.00

ii. Dose response experiment for NAC

Individual zebrafish larvae were pipetted into a 96-well plate with 12 replicates per concentration. The negative control consisted of 250 µL of E3 embryo water while the positive tox control had 0.02 mg/mL 3,4-Dichloroalanine. For each test concentration, 200 µL of E3 embryo water with each larva was pipetted and then 50 µL of treatment (N-acetyl-cysteine) was added to make a total volume of 250 µL. The 96-well plate was then placed in a laboratory incubator set at 28˚C. After an hour, each larva was visualised under the microscope to check for any injuries that occurred during the pipetting stage. After observation, the plate was placed back into the incubator. After 24 hpe (hours post exposure), the movement of each fish was tracked on the EthoVision movement tracking software to evaluate the response to treatment.

Table 19: The preparation of NAC treatment used to dose the zebrafish larvae at 72 hpf for 24 hours in a 96-well plate

Concentration (mM)	Total volume (mL)	Amount taken out of previous sample (mL)	Volume of E3 (mL)
20.0	7.00	-	-
16.0	6.00	4.80	1.20
12.0	5.00	3.75	1.25
8.00	4.00	2.67	1.33
4.00	3.00	1.50	1.50
2.00	2.00	1.00	1.00

iii. Oil red O staining procedure:

Oil red O (ORO) is a lipophilic dye that stains lipids and triglycerides. To make up the stain, 0.250 g of ORO was dissolved in 50 mL of 100% isopropanol (0.5% ORO). For staining, zebrafish larvae were first tricained and then fixed overnight with 4% paraformaldehyde (PFA). Next, the paraformaldehyde was washed off 3 times with 500 µL of 1 X Phosphate Buffered Saline with Tween (1 X PBST), each for 5min. Once the washes were completed, zebrafish larva were stained with 300 µL of 0.5% ORO solution and 200 µL of distilled water and then incubated at room temperature for 15 min. After incubation, the stain was washed off 3 times using 500 µL of 1 X PBST for 5 min each. For thorough washing of the stain, 500 µL of 60% isopropanol was used twice for 5 min each. Thereafter, isopropanol was briefly rinsed off once with 1 X PBST. After washing, the zebrafish larvae were fixed with 4% PFA and were mounted in glycerol/ low melting point agarose prior to observation under the stereomicroscope.

Chapter 4

Results

4.1 Results for method pre-validation

In order to prove that the HPLC method for quantification of APAP was accurate and precise, a single validation batch of the APAP STDs (in duplicates from STD 1 to STD 7) and QCs (in 6-fold at QC-Low, QC-Medium and QC-High) was run. The data obtained fit a linear regression weighed 1/c (c=concentration).

Criteria: The accuracy (85-115%) and precision (within 15%) of the STDs and QCs were all within acceptable criteria as recommended by the FDA guidelines (FDA, 2014).
The tables 20 and 21 below shows the accuracy and precision of the STDs and QCs for APAP.

Table 20: Calibration standard accuracy and precision of APAP

Sample ID	STD 1	STD 2	STD 3	STD 4	STD 5	STD 6	STD 7
Nominal concentration (µg/mL)	200	100	50.0	25.0	12.5	6.25	3.13
Replicates	Observed concentration (µg/mL)						
1	205	97.0	50.3	26.2	13.7	6.42	2.86
2	198	96.0	50.2	25.8	13.1	6.36	2.71
Average	202	96.5	50.3	26.0	13.4	6.39	2.79
STDEV	4.95	0.707	0.0707	0.283	0.424	0.0424	0.106
% CV	2.5	0.7	0.1	1.1	3.2	0.7	3.8
% Accuracy	100.8	96.5	100.5	104.0	107.2	103.8	89.0

STDEV: Standard deviation; %CV: Coefficient of variation- precision

Table 21: Quality control accuracy and precision of APAP

Sample ID	QCH	QCM	QCL
Nominal concentration (µg/mL)	160	80.0	9.00
Replicates	Observed concentration (µg/mL)		
1	154	74.6	8.35
2	151	72.8	8.48
3	146	75.6	8.39
4	154	73.2	8.45
5	145	75.0	8.37
6	139	72.3	8.68
Average	148	73.9	8.45
STDEV	5.91	1.33	0.121
% CV	4.0	1.8	1.4
% Accuracy	92.6	92.4	93.9

The results above show that all the STDs and QCs were within 85-115% accuracy, with precision less than 15% at all concentrations. Based on these results, it can therefore be concluded that the calibration range of 3.13 µg/mL to 200 µg/mL is valid for the quantitative analysis of the analyte.

4.2 Results for solubility and stability assessment of INH, PZA, RIF, EMB and APAP

The test samples were evaluated against a valid calibration curve to assess whether there was degradation of the analytes when placed in the incubator over 3 days. The test samples at time 0 were used to test the solubility of the analytes in E3 embryo water and were also used as the reference against which degradation of the analytes in the E3 embryo water was determined. The analytes APAP, INH, EMB and PZA were shown to be stable in E3 embryo water for 3 days. This is indicated by the %difference that was within 15% of the time 0 for all four analytes. However, RIF was shown to solubilize over time in E3 embryo water and was also deemed unstable at 28°C. Table 22-23 below shows the accuracy and precision of the STDs and QCs and also the % Difference between the reference test samples (time 0) and the test samples at the different time points. The QCs were analysed in duplicate and this was deemed valid for a pre-clinical experiment.

Table 22: Calibration standard accuracy and precision of INH from a re-instatement validation experiment

Sample ID	STD 1	STD 2	STD 3	STD 4	STD 5	STD 6	STD 7
Nominal concentration (µg/mL)	10.0	5.00	2.50	1.25	0.625	0.313	0.156
Replicates	Observed concentration (µg/mL)						
1	9.77	4.79	2.33	1.29	0.606	0.296	0.145
2	9.73	[6.06]*	2.40	1.23	0.600	0.290	0.142
Average	9.75	4.79	2.37	1.26	0.603	0.293	0.144
STDEV	0.0283	n/a	0.0495	0.0424	0.00424	0.00424	0.00212
% CV	0.3	n/a	2.1	3.4	0.7	1.5	1.5
% Accuracy	97.5	95.8	94.6	101	96.5	93.6	92.0

**Denotes on-bench error, excluded from statistics*

Table 23: Quality control accuracy and precision of INH from a re-instatement validation experiment

Sample ID	QCH	QCM	QCL
Nominal concentration (µg/mL)	8.00	4.00	0.400
Replicates	Observed concentration (µg/mL)		
1	7.65	3.89	0.377
2	7.76	3.93	0.382
Average	7.71	3.91	0.380
STDEV	0.0778	0.0283	0.00354
% CV	1.0	0.7	0.9
% Accuracy	96.3	97.8	94.9

The results in tables 22 and 23 above show that with the exception of STD 2, all the accuracy of all the STDs and QCs for INH were within 85-115%, with precision less than 15%. The error in the concentration of one of the STD 2 is based on on-bench error and the STD 2 was excluded when calculating averages. On-bench error refers to mistakenly spiking the working

stock solution to prepare the standard. The standard will have a different concentration from the concentration that the standard was supposed to be at. This occurs while the analyst is still preparing the samples prior to injection. The criteria for a batch to pass is that 75% of the STDs must pass. Therefore, the 92.9% of STDs that had passed in the batch indicate that the batch passed. Based on these results, it can therefore be concluded that the calibration range of 0.156 µg/mL to 10.0 µg/mL is valid for the quantitative analysis of INH.

Table 24: Solubility and stability assessment of INH at 28°C at 0, 18, 24, 48 and 72 hours

Time (hours)	**0**		**18**		**24**		**48**		**72**	
Nominal concentration (µg/mL)	**8.00**	**0.400**	**8.00**	**0.400**	**8.00**	**0.400**	**8.00**	**0.400**	**8.00**	**0.400**
Replicates	**Observed concentration (µg/mL)**									
1	7.61	0.484	7.40	0.483	7.06	0.443	7.83	0.431	7.61	0.438
2	7.91	0.483	[4.92]*	0.490	7.40	0.440	7.00	0.421	7.68	0.437
3	7.82	0.445	7.38	0.455	7.10	0.419	7.85	0.418	7.47	0.436
Average	7.72	0.417	7.39	0.426	7.19	0.434	7.56	0.423	7.59	0.437
STDEV	0.105	0.00222	0.0141	0.0185	0.186	0.0131	0.485	0.00681	0.107	0.00100
%CV	1.4	4.7	0.2	3.9	2.6	3.0	6.4	1.6	1.4	0.2
% Difference	-3.5	4.3	-14.9	1.1	-6.9	-7.8	-10.7	-10.1	-14.6	-13.5

**Denotes on-bench error*

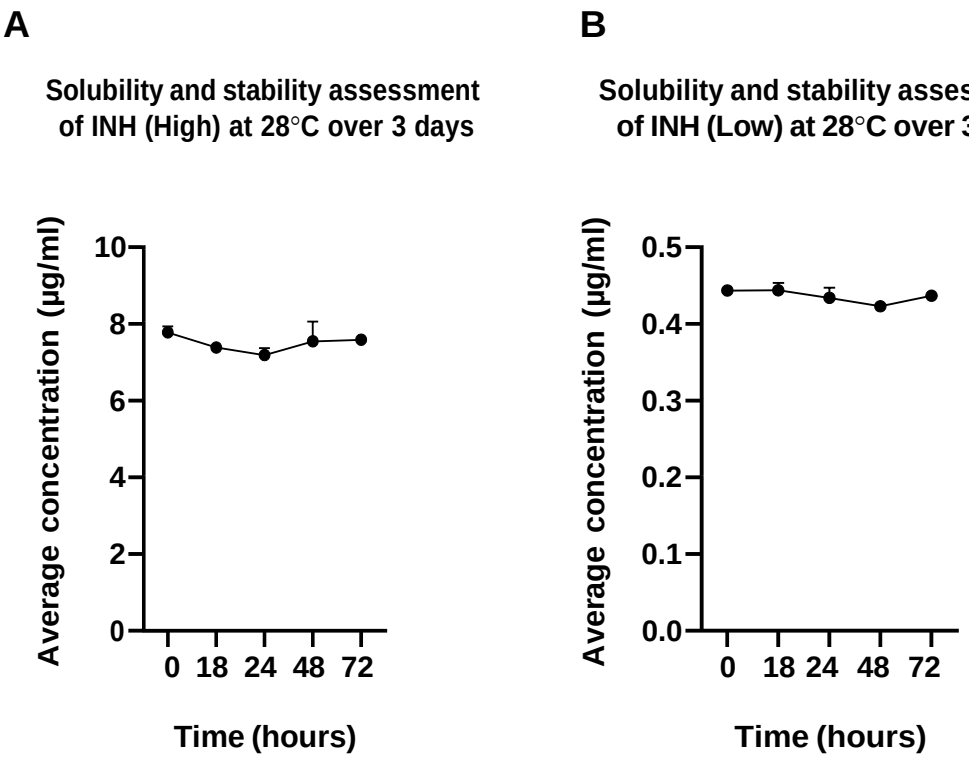

Figure 32: Solubility and stability assessment of INH in E3 embryo water at 28˚C over 3 days. Test samples were prepared at relatively high (**A**) and relatively low (**B**) QC concentrations. Error bars represent ±SD of n = 3

INH test samples were prepared in E3 embryo water at concentrations of QCL and QCH using a 1 mg/mL INH stock solution and were used to test INH solubility in E3 embryo water and stability at 28°C. Sampling was done after every 24 hours and samples were placed at -80°C until analysis. The results in table 24 and figure 32 above shows that the %difference of the INH test samples at time 18, 24, 48 and 72 hours and the test samples at time 0 hours was below 15%, suggesting that INH was soluble in E3 embryo water and stable at 28°C for 3 days.

Table 25: Calibration standard accuracy and precision of PZA from a re-instatement validation experiment

Sample ID	STD 1	STD 2	STD 3	STD 4	STD 5	STD 6	STD 7
Nominal concentration (µg/mL)	10.0	5.00	2.50	1.25	0.625	0.313	0.156
Replicates	Observed concentration (µg/mL)						
1	10.0	5.15	2.37	1.30	0.618	0.324	0.159
2	9.96	5.12	2.33	1.23	0.639	0.320	0.149
Average	9.98	5.14	2.35	1.27	0.629	0.322	0.154
STDEV	0.0283	0.0212	0.0283	0.0495	0.0148	0.00283	0.00707
% CV	0.3	0.4	1.2	3.9	2.4	0.9	4.6
% Accuracy	99.8	102.8	94.0	101.6	100.6	102.9	98.7

Table 26: Quality control accuracy and precision of PZA from a re-instatement validation experiment

Sample ID	QCH	QCM	QCL
Nominal concentration (µg/mL)	8.00	4.00	0.400
Replicates	Observed concentration (µg/mL)		
1	8.14	4.33	0.431
2	8.31	4.40	0.408
Average	8.23	4.37	0.418
STDEV	0.120	0.0495	0.0233
% CV	1.5	1.1	3.9
% Accuracy	102.9	109.3	104.5

As shown in the tables 25 and 26 above, the STDs and QCs for PZA had an accuracy that was between 85 -115% and a precision of less than 15% at all concentrations. Based on these results, it can therefore be concluded that the calibration range of 0.156 µg/mL to 10.0 µg/mL is valid for the quantitative analysis of PZA.

Table 27: Solubility and stability assessment of PZA at 28°C at 0, 18, 24, 48 and 72 hours

Time (hours)	0		18		24		48		72	
Nominal concentration (µg/mL)	8.00	0.400	8.00	0.400	8.00	0.400	8.00	0.400	8.00	0.400
Replicates	Observed concentration (µg/mL)									
1	7.13	0.421	7.17	0.448	7.19	0.446	7.14	0.431	7.14	0.445
2	7.16	0.460	7.17	0.449	7.11	0.447	7.11	0.415	7.16	0.454
3	7.15	0.460	7.17	0.447	7.18	0.446	7.14	0.442	7.18	0.415
Average	7.15	0.447	7.17	0.448	7.16	0.446	7.13	0.429	7.16	0.438
STDEV	0.0153	0.0225	0.000	0.0100	0.0436	0.0577	0.0173	0.0136	0.0200	0.0204
%CV	0.2	5.0	0.0	0.2	0.6	0.1	0.2	3.2	0.3	4.7
% Difference	-10.4	11.8	0.3	2.5	-0.1	-3.4	-0.4	-8.5	0.4	-2.0

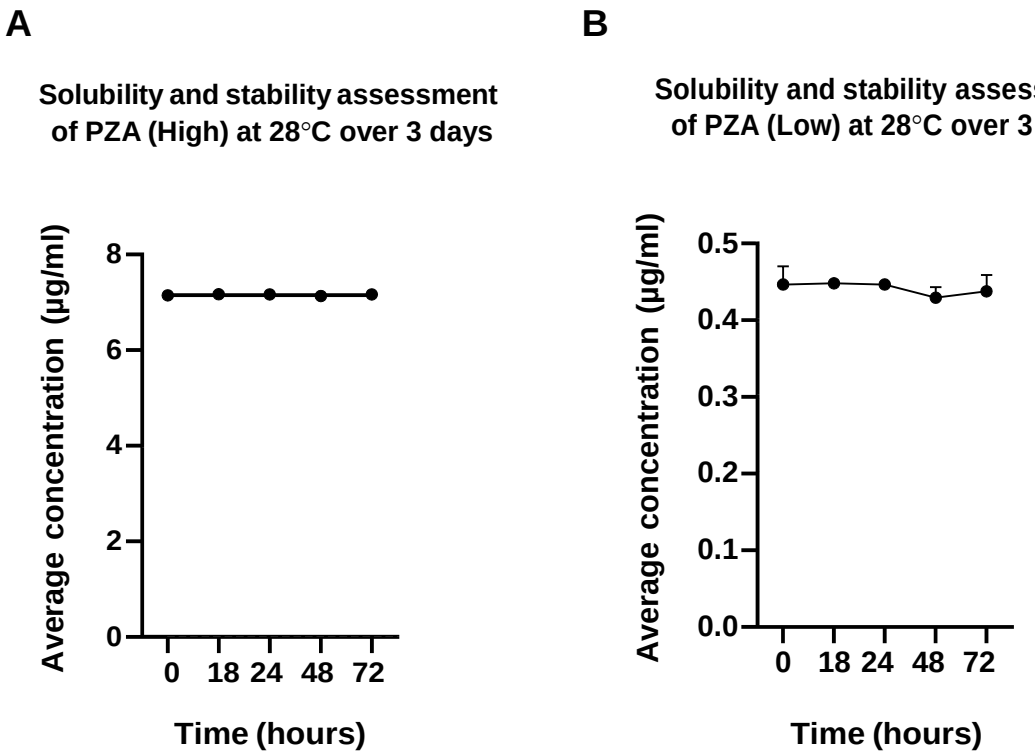

Figure 33: Solubility and stability assessment of PZA in E3 embryo water at 28˚C over 3days. Test samples were prepared at relatively high (**A**) and relatively low (**B**) QC concentrations. Error bars represent ±SD of n = 3

The test samples for PZA were prepared in E3 embryo water at QCL and QCH concentrations using a 1 mg/mL PZA reference stock solution and were used to test the solubility of PZA in E3 embryo water and stability at 28°C. After every 24 hours, a reasonable volume of the samples was sampled into a microcentrifuge tube and was stored at -80°C until analysis. The results in table 27 and figure 33 above shows that the %difference of the test samples at time 18, 24, 48 and 72 hours and the test samples at time 0 hours was below 15%, suggesting that INH was soluble in E3 embryo water and stable at 28°C for 3 days.

Table 28: Calibration standard accuracy and precision of RIF from a re-instatement validation experiment

Sample ID	STD 1	STD 2	STD 3	STD 4	STD 5	STD 6	STD 7
Nominal concentration (µg/mL)	10.0	5.00	2.50	1.25	0.625	0.313	0.156
Replicates	Observed concentration (µg/mL)						
1	9.97	5.16	2.47	1.24	0.633	0.331	0.150
2	9.97	5.05	2.36	1.24	0.639	0.331	0.146
Average	9.97	5.11	2.42	1.24	0.636	0.331	0.148
STDEV	0.00	0.0778	0.0778	0.00	0.00	0.00	0.00283
% CV	0.0	1.5	3.2	0.0	0.7	0.0	1.9
% Accuracy	99.7	102.2	96.8	99.2	101.8	105.8	94.9

Table 29: Quality control accuracy and precision of RIF from a re-instatement validation experiment

Sample ID	QCH	QCM	QCL
Nominal concentration (µg/mL)	8.00	4.00	0.400
Replicates	Observed concentration (µg/mL)		
1	8.40	4.16	0.360
2	8.40	4.47	0.371
Average	8.40	4.32	0.366
STDEV	0.00	0.219	0.00778
% CV	0.0	5.1	2.1
% Accuracy	105.0	108.0	91.5

Tables 28 and 29 above show that all the STDs and QCs for RIF were within 85-115% accuracy, with precision of less than 15%. Based on these results, it can therefore be concluded that the calibration range of 0.156 µg/mL to 10.0 µg/mL is valid for the semi-quantitative analysis of RIF.

Table 30: Solubility and stability assessment of RIF without ascorbic acid in E3 at 28°C at 0, 18, 24, 48 and 72 hours

Time (hours)	0		18		24		48		72	
Nominal concentration (µg/mL)	8.00	0.400	8.00	0.400	8.00	0.400	8.00	0.400	8.00	0.400
Replicates	Observed concentration (µg/mL)									
1	7.55	0.113	5.88	0.000	3.89	0.00400	1.33	0.000	0.000	0.000
2	7.85	0.0910	5.32	0.0290	3.42	0.00200	1.63	0.000	0.603	0.000
Average	7.70	0.102	5.60	0.0145	3.66	0.000	1.48	0.000	0.302	0.000
STDEV	0.212	0.0156	0.396	0.0205	0.332	0.00141	0.212	0.000	0.325	0.0212
%CV	2.8	15.3	7.1	141	9.1	47.1	14.3	0.0	141	13.7
% Difference	-0.4	-7.5	-27.3	-85.8	-52.5	-97.1	-80.8	-100.0	-96.1	-84.8
% Solubility	96.3	25.5	70.0	3.6	45.8	0.0	18.5	0.0	3.8	3.9

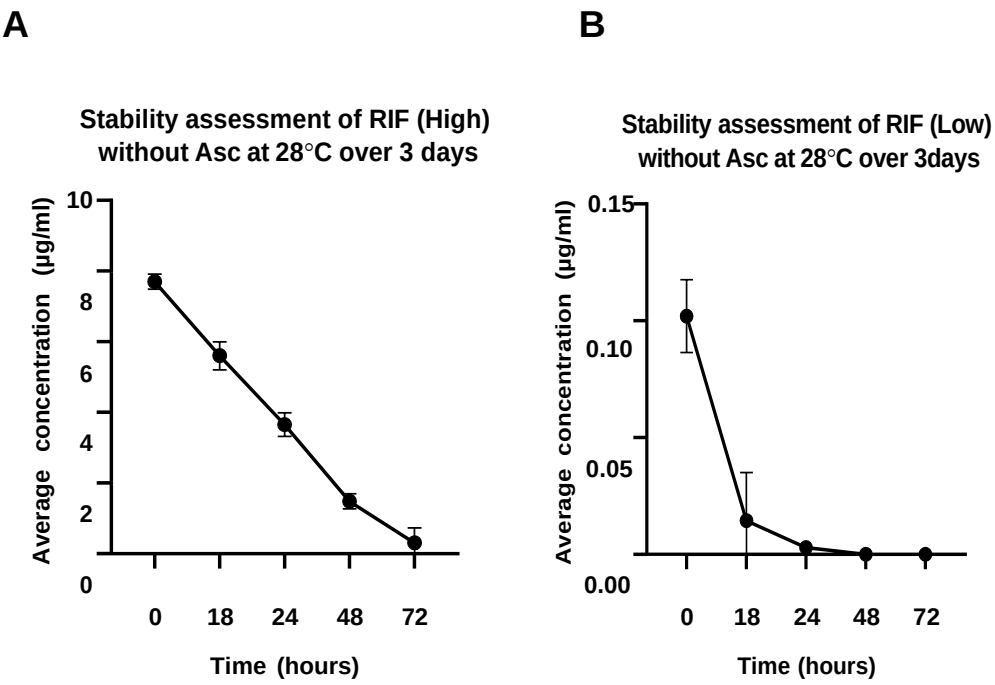

Figure 34: Solubility and stability assessment of RIF in E3 embryo water at 28˚C over 3 days. Test samples were prepared at relatively high (**A**) and relatively low (**B**) QC concentrations. Error bars represent ±SD of n = 2

RIF test samples were prepared in E3 embryo water at QCL and QCH concentrations using a 1 mg/mL RIF stock solution in methanol with ascorbic acid and were placed in the laboratory incubator set at 28˚C. The samples were used to test the solubility of RIF in E3 embryo water and stability at 28°C. Sampling was performed after every 24 hours for 3 days and samples were stored at -80°C until analysis. The results in table 30 and figure 34 above shows that the even in the presence of ascorbic acid, RIF was poorly soluble in E3 medium. Furthermore, RIF concentrations declined over 3 days at 28°C.

Table 31: Solubility and stability assessment of RIF with 20 µg/mL ascorbic acid at 28°C at 0, 18, 24, 48 and 72 hours

Time (hours)	**0**		**18**		**24**		**48**		**72**	
Nominal concentration (µg/mL)	8.00	0.400	8.00	0.400	8.00	0.400	8.00	0.400	8.00	0.400
Replicates	**Observed concentration (µg/mL)**									
1	6.21	0.086	4.35	0.0550	4.06	0.0470	3.03	0.0480	1.95	0.0310
2	6.01	0.082	4.39	0.0580	4.05	0.0370	2.98	0.0280	1.93	0.0310
3	6.06	0.0790	4.28	0.0560	3.93	0.0380	2.99	0.0410	1.90	0.0310
Average	6.09	0.084	4.34	0.0560	4.01	0.0407	3.00	0.0390	1.93	0.0310
STDEV	0.104	0.00351	0.0557	0.00153	0.0723	0.00551	0.0265	0.0101	0.0252	0.00
%CV	1.7	4.3	1.3	2.7	1.8	13.5	0.9	26.0	1.3	0.0
% Difference	-23.9	-79.0	-28.8	-31.6	-34.1	-50.6	-50.8	-52.6	-68.4	-62.3
% Solubility	76.2	21.0	54.3	14.0	50.1	10.2	37.5	9.8	24.1	7.8

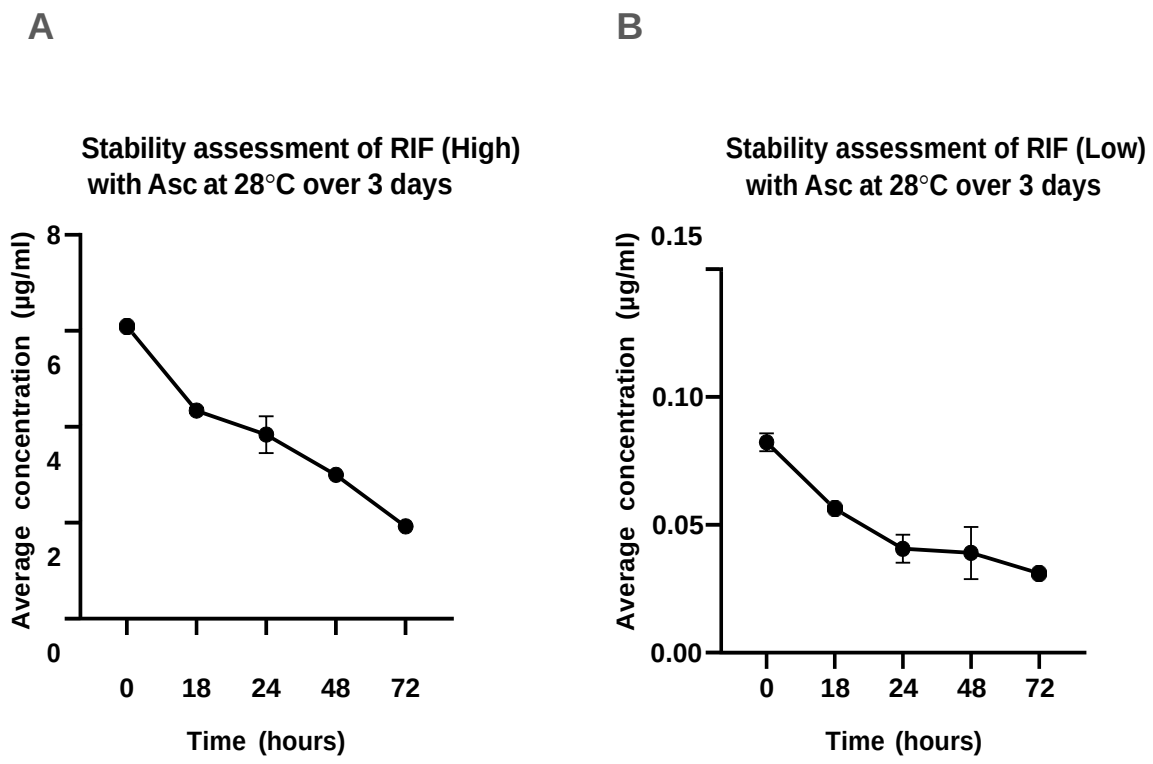

Figure 35: Solubility and stability assessment of RIF in E3 embryo water with 20 µg/mL ascorbic acid at 28˚C over 3 days. Test samples were prepared at relatively high (**A**) and relatively low (**B**) concentrations of QC. Error bars represent ±SD of n = 3

A 1 mg/mL RIF stock solution in methanol with ascorbic acid was used in the preparation of the RIF test samples in E3 embryo water with 20 µg/mL ascorbic acid. The test samples were prepared at QCL and QCH concentrations and were stored in the laboratory incubator set at 28˚C. The samples were used to test the solubility of RIF in E3 embryo water with 20 µg/mL ascorbic acid and stability of RIF at 28°C. Sampling was performed after every 24 hours for 3 days and samples were stored at -80°C until analysis. The results in table 31 and figure 35 above show that the %difference of the RIF test samples at time 18, 24, 48 and 72 hours and the test samples at time 0 hours was still above 15%. This suggests that even in the presence of ascorbic acid, RIF was still poorly soluble in E3 medium and degraded over time (%difference between -79.0% and -23.9%).

Table 32: Calibration standard accuracy and precision of EMB from a re-instatement validation experiment

Sample ID	STD 1	STD 2	STD 3	STD 4	STD 5	STD 6	STD 7
Nominal concentration (µg/mL)	2.50	1.25	0.625	0.313	0.156	0.0783	0.0390
Replicates	Observed concentration (µg/mL)						
1	2.40	1.23	0.615	0.329	0.164	0.0764	0.0382
2	2.62	1.26	0.595	0.325	0.165	0.0772	0.0373
Average	2.51	1.24	0.605	0.327	0.164	0.0768	0.0377
STDEV	0.157	0.0236	0.0146	0.00265	0.000990	0.000530	0.000600
% CV	6.3	1.9	2.4	0.8	0.6	0.7	1.6
% Accuracy	100.4	99.5	96.8	104.5	105.1	98.1	96.7

Table 33: Quality control accuracy and precision of EMB re-instatement validation experiment

Sample ID	QCH	QCM	QCL
Nominal concentration (µg/mL)	2.50	1.00	0.100
Replicates	Observed concentration (µg/mL)		
1	2.71	1.17	1.101
2	2.74	1.13	0.101
Average	2.73	1.15	0.101
STDEV	0.0153	0.0246	0.000280
% CV	0.6	2.1	0.3
% Accuracy	109.0	115.0	101.0

The STDs and QCs for EMB had an 85-115% accuracy, with a precision that was within 15% for all concentrations as shown in the tables 32 and 33 above. The concentration of QCH is 2.5 µg/mL because it was accidentally prepared at the concentration of STD 1 (2.5 µg/mL) as shown in table 11 of section 3.4.6. The results therefore prove that the calibration range of 0.156 µg/mL to 10.0 µg/mL is valid for quantitative analysis of EMB.

Table 34: Solubility and stability assessment of EMB at 28°C at 0, 18, 24, 48 and 72 hours

Time (hours)	0		18		24		48		72	
Nominal concentration (µg/mL)	2.00	0.100	2.00	0.100	2.00	0.100	2.00	0.100	2.00	0.100
Replicates	Observed concentration (µg/mL)									
1	2.21	0.105	2.20	0.110	2.14	0.110	2.17	0.108	2.11	0.109
2	2.17	0.110	2.23	0.110	2.11	0.111	2.18	0.111	2.10	0.108
Average	2.19	0.107	2.21	0.111	2.13	0.110	2.18	0.109	2.11	0.108
STDEV	0.0300	0.00343	0.0128	0.000424	0.0212	0.00110	0.00721	0.00166	0.00707	0.000141
%CV	1.4	3.2	0.6	0.4	1.0	1.0	0.3	1.5	0.3	0.1
% Difference	9.5	7.5	1.1	2.3	-3.0	2.8	-0.7	1.9	-3.9	0.9

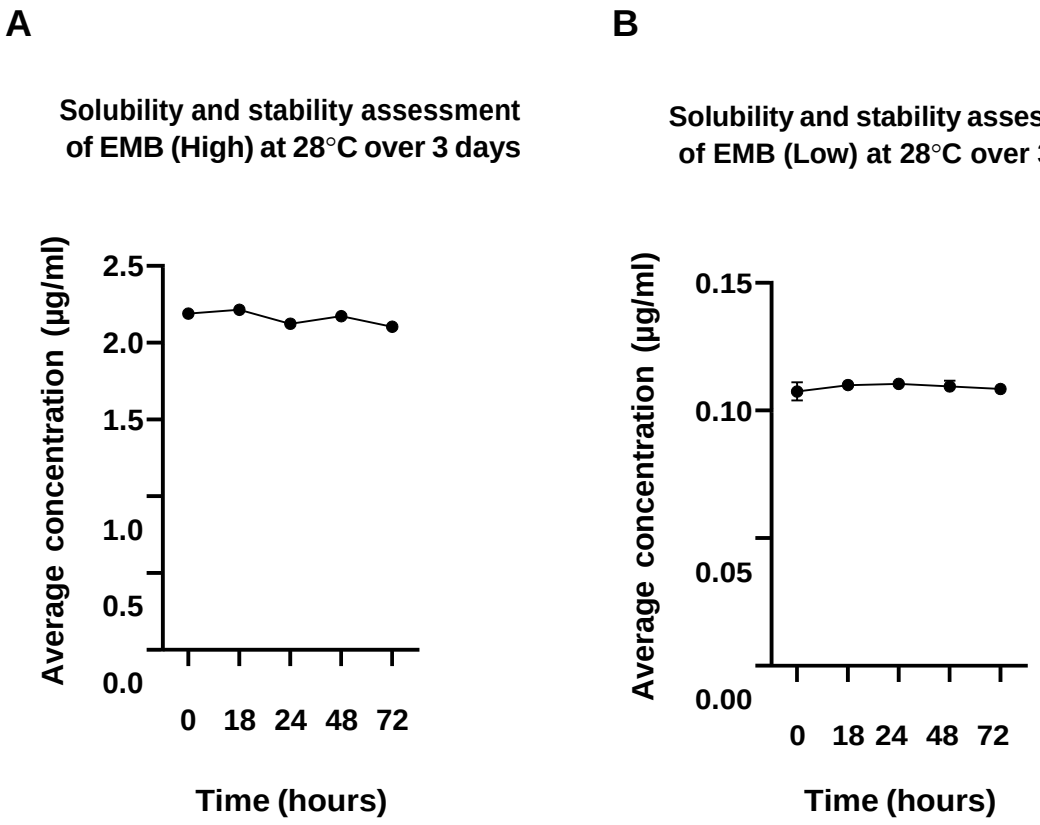

Figure 36: Solubility and stability assessment of EMB in E3 embryo water at 28˚C over 3days. Test samples were prepared at relatively high (**A**) and relatively low (**B**) QC concentrations. Error bars represent ±SD of n = 2

EMB test samples were prepared in E3 embryo water at high and low QC using an EMB stock solution of 2 mg/mL in water. Samples were stored at 28°C and sampling was performed after every 24 hours. After sampling, the samples were stored at -80°C until analysis. The results in table 34 and figure 36 above shows that the %difference of the EMB test samples at time 18, 24, 48 and 72 hours and the test samples at time 0 hours was below 15%, suggesting thatEMB was soluble in E3 embryo water and stable at 28°C for 3 days.

4.3 APAP stability assessment

The test samples of the APAP were run against the STDs ad QCs that were used for validating the HPLC method for APAP.

Table 35: Calibration standard accuracy and precision of APAP from a re-instatement validation experiment

Sample ID	STD 1	STD 2	STD 3	STD 4	STD 5	STD 6	STD 7
Nominal concentration (µg/mL)	200	100	50.0	25.0	12.5	6.25	3.13
Replicates	Observed concentration (µg/mL)						
1	205	96.4	50.6	26.1	13.8	6.48	2.73
2	198	95.1	49.1	26.4	13.3	6.40	2.68
Average	201	95.8	49.9	26.3	13.6	6.44	2.71
STDEV	4.95	0.919	1.06	0.212	0.354	0.0566	0.0354
% CV	2.5	1.0	2.1	0.8	2.6	0.9	1.3
% Accuracy	100.5	95.8	99.7	105.2	108.8	103.0	86.4

Table 36: Quality control accuracy and precision of APAP in a re-instatement validation experiment

Sample ID	QCH	QCM	QCL
Nominal concentration (µg/mL)	160	80.0	9.00
Replicates	Observed concentration (µg/mL)		
1	151	74.5	8.04
2	158	76.9	7.96
Average	155	75.7	8.00
STDEV	4.95	1.70	0.0566
% CV	3.2	2.2	0.7
% Accuracy	96.6	94.6	88.9

The STDs and QCs for APAP had an accuracy between 85-115% and a precision that was less than 15% at all concentrations as shown in the tables 35 and 36 above. The results therefore prove that the calibration range of 0.156 µg/mL to 10.0 µg/mL is valid for the semi-quantitative analysis of APAP.

Table 37: Solubility and stability assessment of APAP at 28°C at 0, 18, 24, 48 and 72 hours

Time (hours)	0		18		24		48		72	
Nominal concentration (µg/mL)	160	9.00	160	9.00	160	9.00	160	9.00	160	9.00
Replicates	Observed concentration (µg/mL)									
1	161	8.62	160	8.58	160	8.53	160	8.55	160	8.64
2	160	8.59	160	8.52	160	8.55	161	8.55	160	8.60
3	160	8.89	161	8.56	160	8.58	160	8.50	160	8.58
Average	160	8.70	160	8.55	160	8.55	160	8.53	160	8.61
STDEV	0.577	0.165	0.577	0.0306	0.000	0.0252	0.577	0.0289	0.000	0.0306
%CV	0.4	1.9	0.4	0.4	0.0	0.3	0.4	0.3	0.0	0.4
% Difference	0.0	-3.3	0	-1.7	0	-1.7	0	-2.0	0	-1.0

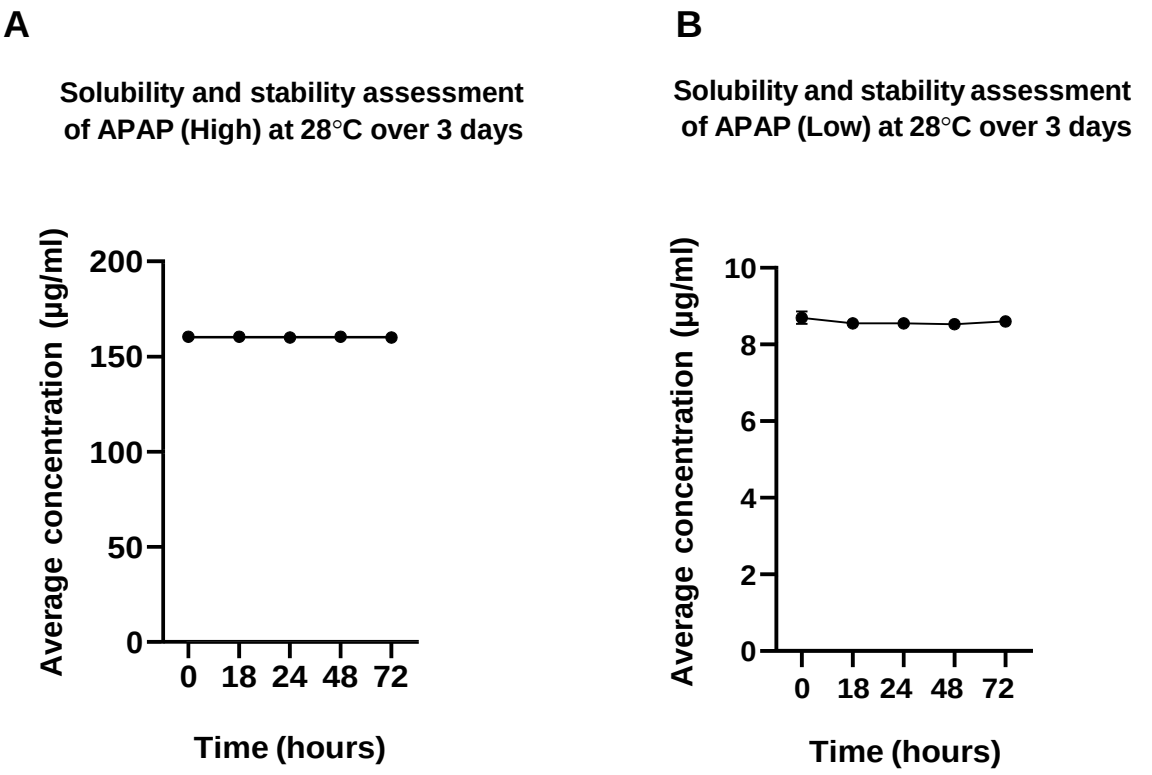

Figure 37: Solubility and stability assessment of APAP in E3 embryo water at 28˚C over 3 days. Test samples were prepared at relatively high (**A**) and relatively low (**B**) QC concentrations. Error bars represent ±SD of n = 3

APAP test samples were prepared in E3 embryo water using a 1 mg/mL APAP stock solution in E3 embryo water at high and low QC concentration. After preparation, the test samples were placed in the laboratory incubator at 28°C for 72 hours. Sampling was done after every 24 hours and samples were placed at -80ºC until analysis. Table 37 and figure 37 above showthat the %difference between the concentration of APAP at time 0 and time 18, 24, 48 and 72hours is below 15%. This suggests 3-day stability of APAP at 28ºC in E3 embryo water.

4.4 Dose range finding experimental results

Dose range finding experiments were performed on zebrafish larvae at 48 hpf (for INH, PZA, RIF and EMB) and 72 hpf (for NAC) in order to determine the safe dose for NAC and to determine the dose that results in liver damage for APAP, INH, RIF and EMB. Moreover, for APAP, INH, RIF and EMB, Oil red O liver stains were used as the endpoint whereasEthoVision movement tracking software was used as an endpoint for NAC. Figures 38-49 below represent the results obtained from these experiments.

4.4.1 INH

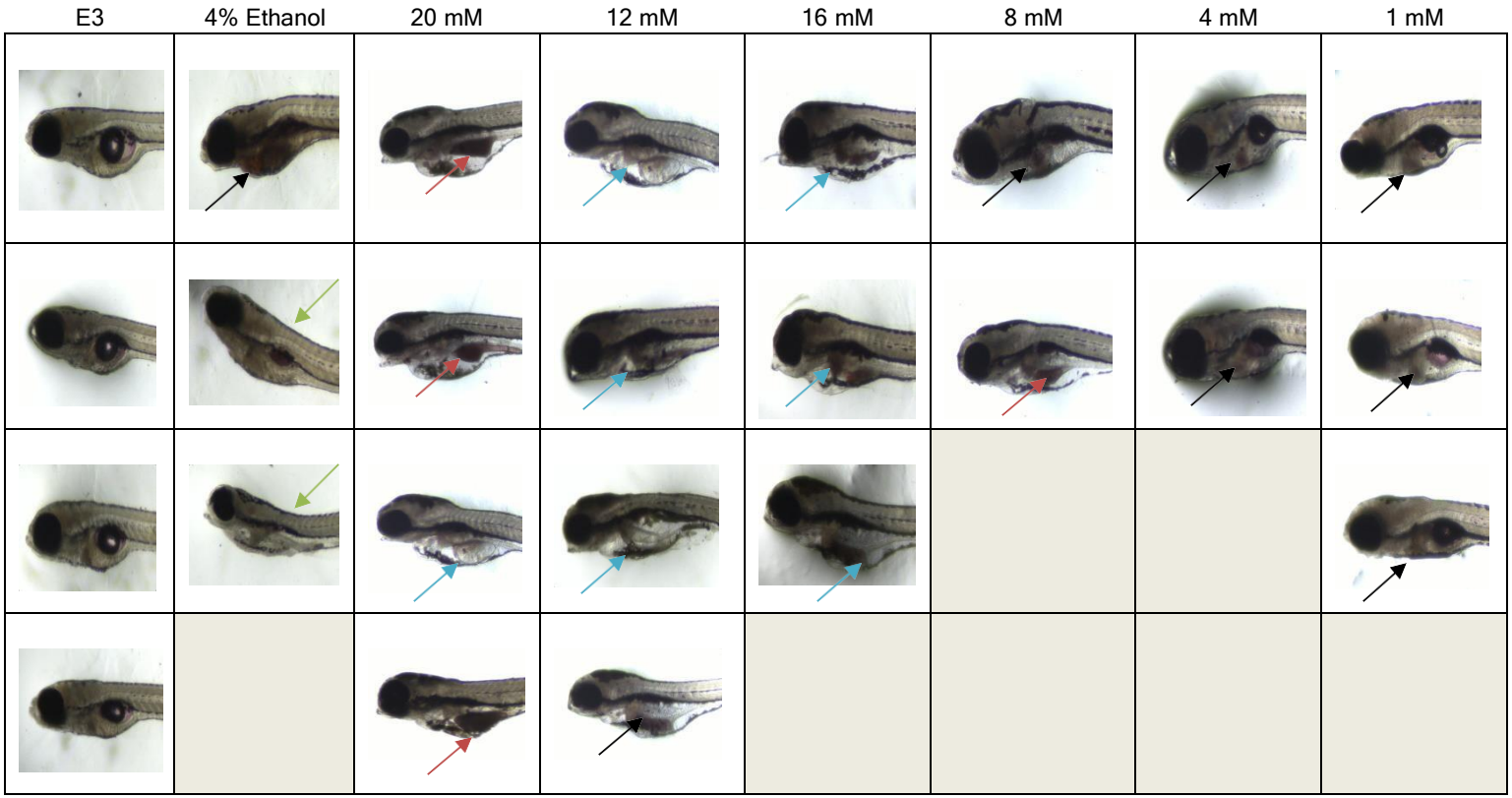

Figure 38: Zebrafish larvae treated with 2% Ethanol (n=4) and INH at 1 mM (n=4), 4 mM (n=4), 8 mM (n=3, 12 mM (n=2), 16 mM (n=2) and 20 mM (n=3). The negative control group only contained E3 embryo water (n=3). Number of larvae shown represent the total number of larvae that were left in each group after staining procedure. Blue, red, green and black arrows indicate yolk sac edema, ORO positive staining of internal organs, s-shaped larvae and ORO positive liver stains, respectively

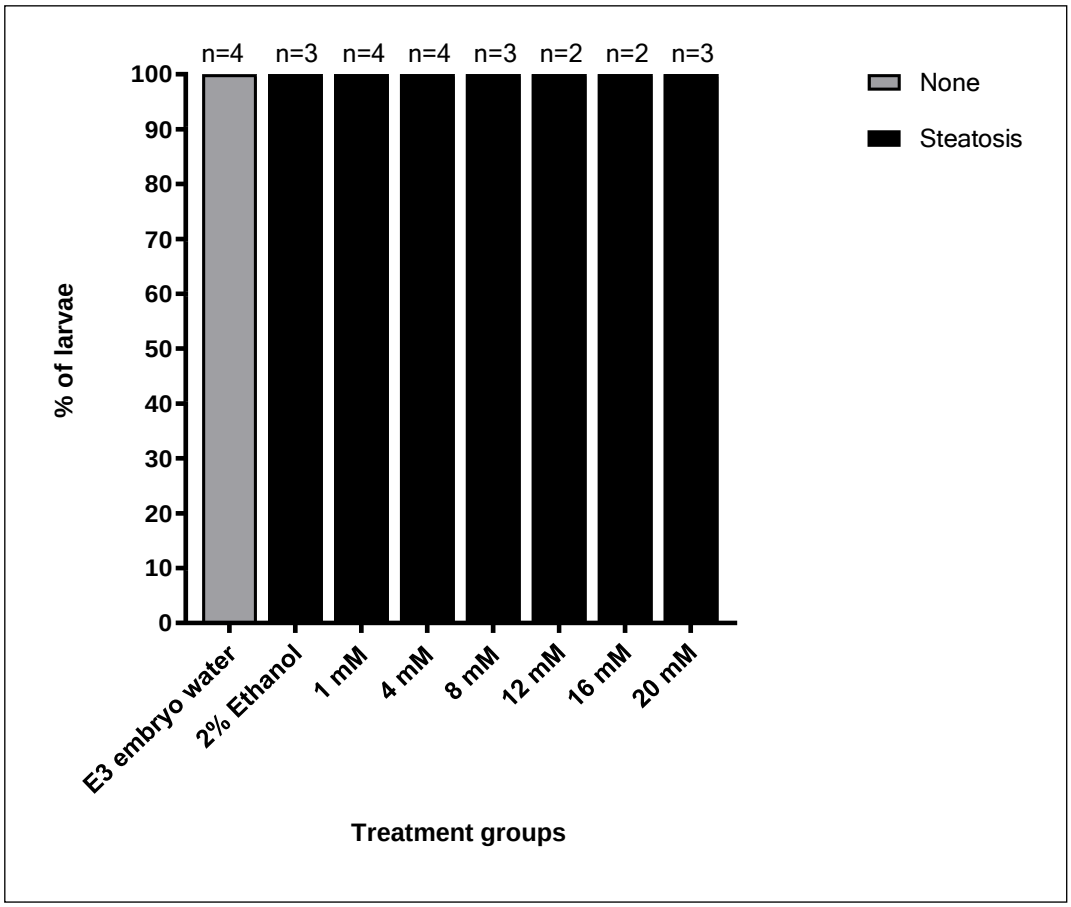

Figure 39: Percentage of zebrafish larvae with Oil red O positive stained livers. Zebrafish larvae at 2 dpf were treated with INH at 1 mM, 4 mM, 8 mM, 12 mM, 16 mM and 20 mM concentration for 3 days. Zebrafish larvae were fixed overnight and stained with 0.5% Oil red O. All treatment groups had Oil red O lipid stains in the liver ($P < 0.05$)

Figure 38 above shows that all the larvae in all treatment groups had Oil red O liver stains. Moreover, larvae treated with doses of 8 mM, 12 mM, 16 mM and 20 mM had severe yolk sac oedema and Oil red O lipid stains in the gut, indicating lethal levels of INH. Zebrafish larvae treated with 4 mM and 1 mM INH showed Oil red O positive lipid stains in the liver area and no signs of oedema. The 1 mM dose of INH resulted in most damage.

4.4.2 PZA

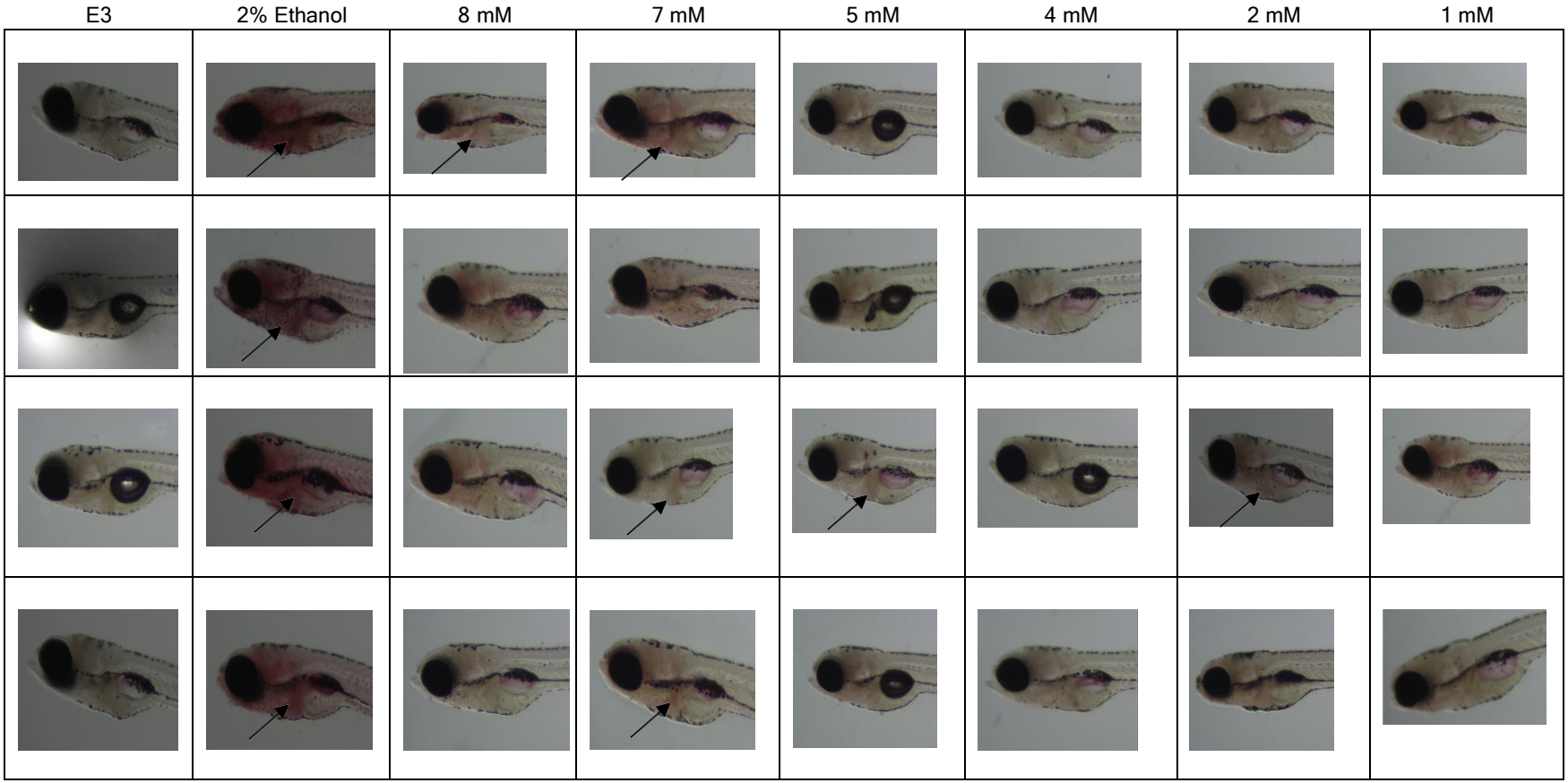

Figure 40: Zebrafish larvae treated with 2% Ethanol (n=6) and PZA at 1 mM (n=6), 2 mM (n=6), 4 mM (n=6), 5 mM (n=6), 7 mM (n=6) and 8 mM (n=6). The negative control group only contained E3 embryo water (n=6). Number of larvae shown is not a representative of the total number of larvae that was in each group after staining. Black arrows indicate Oil red O positive staining of livers

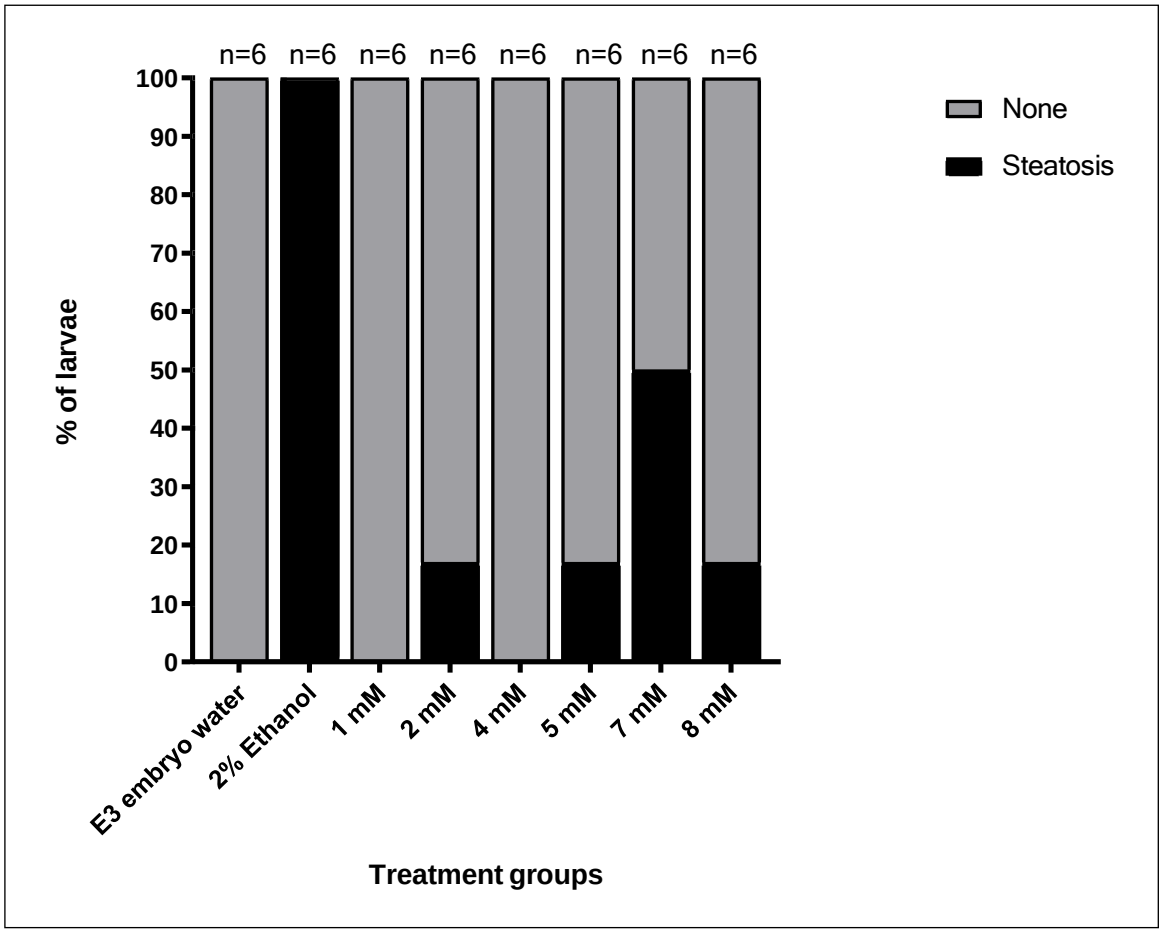

Figure 41: Percentage of zebrafish larvae with Oil red O positive staining livers. Zebrafish larvae at 2 dpf were treated for 3 days with PZA at concentrations of 1 mM, 2 mM, 4 mM, 5 mM, 7 mM and 8 mM. Zebrafish larvae were fixed overnight and then stained with 0.5% Oil red O. The 7 mM treatment group showed more larvae with the Oil red O positive staining livers compared to other groups ($P > 0.05$)

The 7 mM dose of PZA showed more larvae with Oil red O positive lipid droplets compared to other groups ($P > 0.05$) as shown in figure 40 and 41 above, suggesting that 7 mM PZA was the dose that produced the most liver damage in zebrafish larvae. This dose was then chosen as the PZA dose causing DILI to use in the study.

4.4.3 RIF

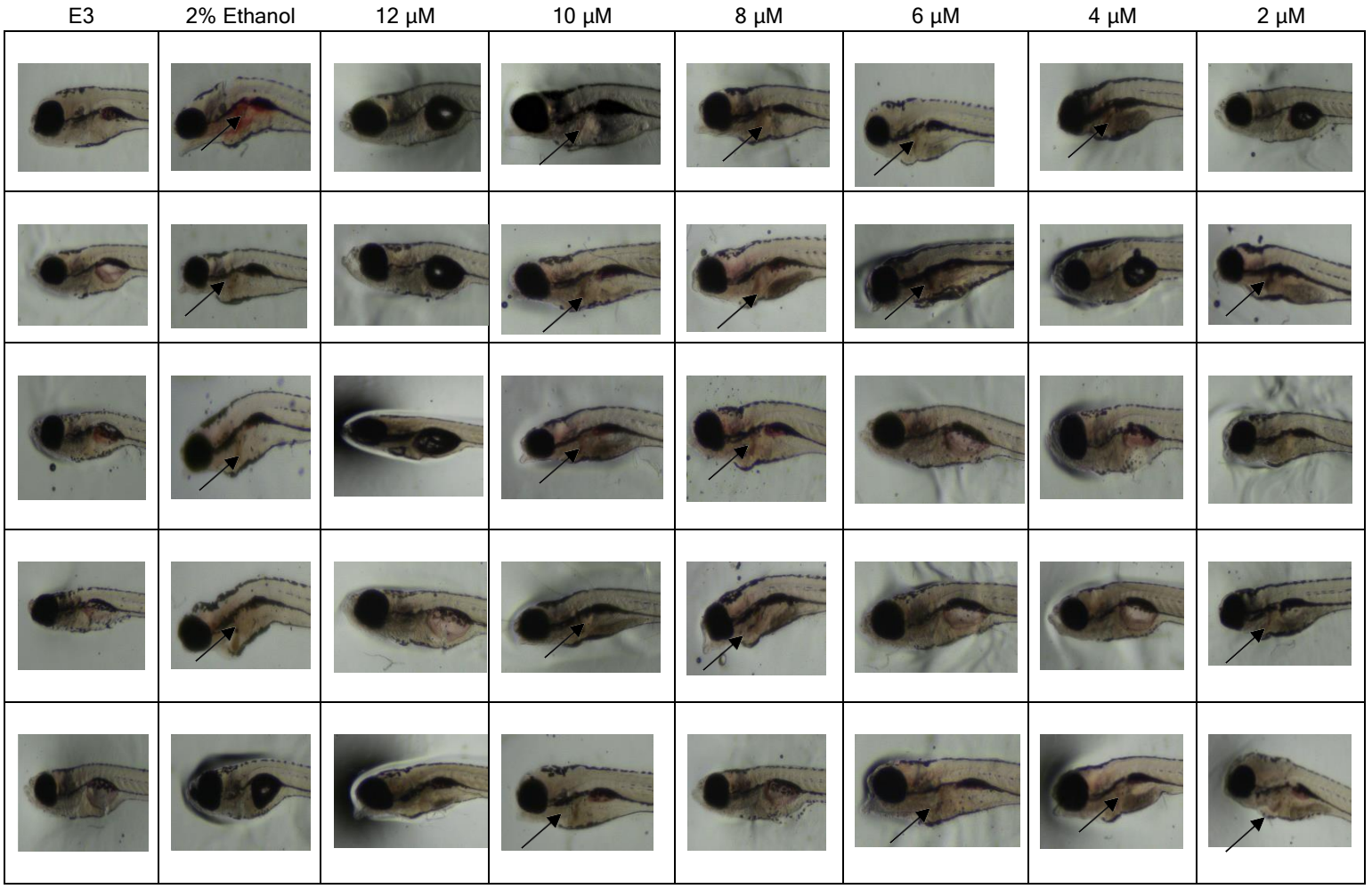

Figure 42: Zebrafish larvae treated with 2% Ethanol (n=8) and RIF at 2 µM (n=7), 4 µM (n=5), 6 µM (n=5), 8 µM (n=7), 10 µM (n=6) and 12 µM (n=9). The negative control group only contained E3 embryo water (n=10). Number of larvae shown does not represent the total number of larvae that was in each group after the staining procedure. Oil red O postive staining of livers is indicated by black arrows

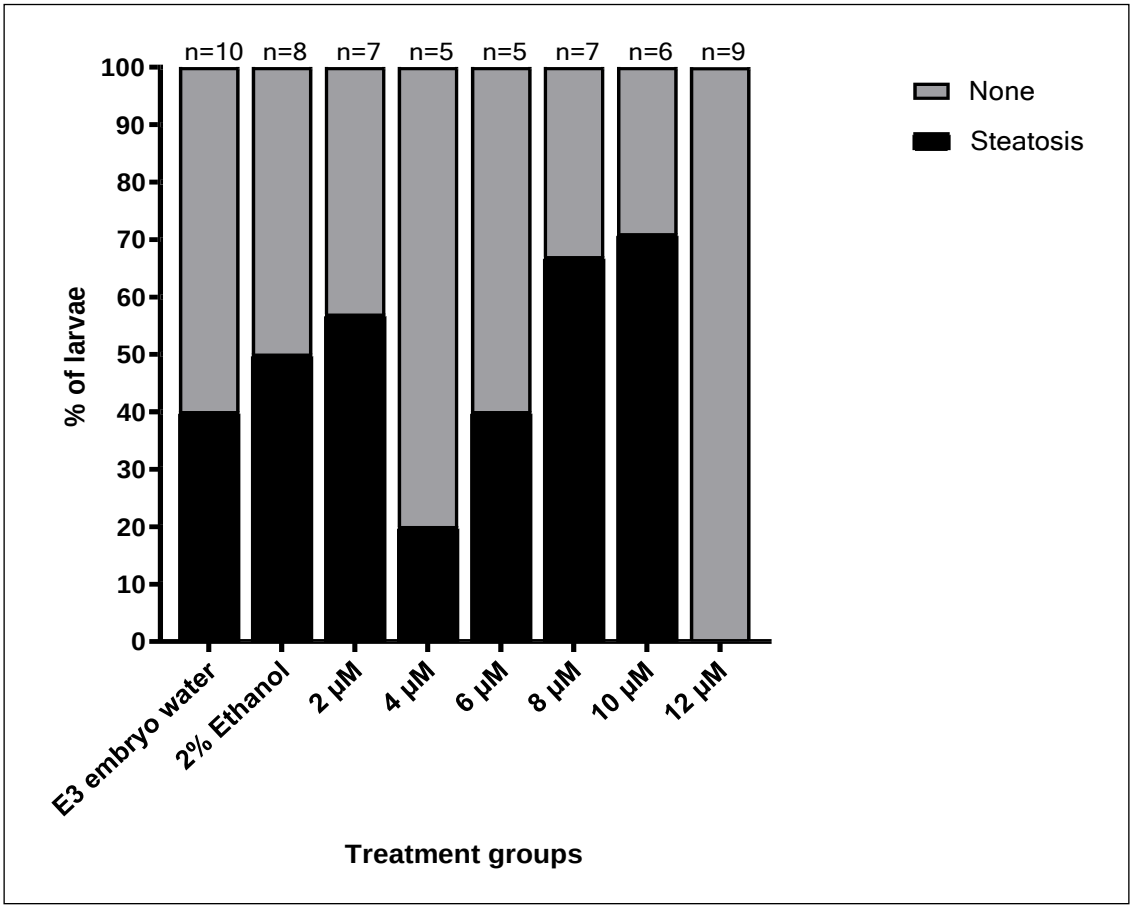

Figure 43: Percentage of zebrafish larvae with Oil red O positive staining livers. Zebrafish larvae at 2 dpf were treated for 3 days with RIF at 2 µM, 4 µM, 6 µM, 8 µM, 10 µM and 12 µM concentrations. Zebrafish larvae were fixed overnight and then stained with 0.5% Oil red O. The 10 µM treatment group showed more larvae with the Oil red O lipid stains compared to other groups ($P > 0.05$).

Figures 42 and 43 above show that more zebrafish larvae in the 10 µM treatment group had larvae with the Oil red O positive stained livers compared to the other groups ($P > 0.05$). Hence, the 10 µM dose of RIF was chosen as the dose that induced most damage in zebrafishlarval livers and was used for further experiments in the study.

4.4.4 EMB

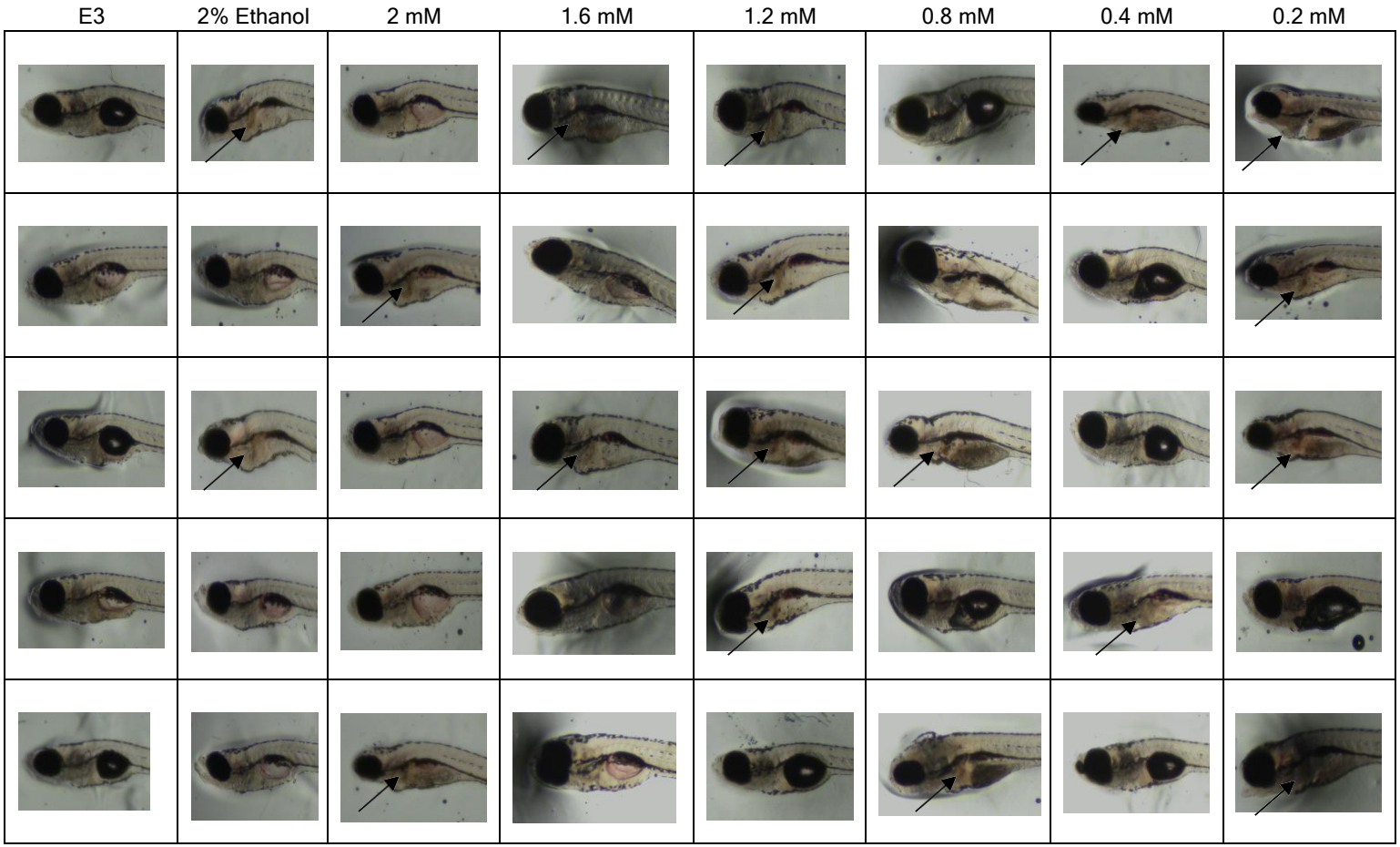

Figure 44: Zebrafish larvae treated with 2% Ethanol (n=9) and EMB at 0.2 mM (n=10), 0.4 mM (n=9), 0.8 mM (n=8), 1.2 mM (n=10), 1.6 mM (n=8) and 2 mM (n=7). Negative control group only contained E3 embryo water (n=8). Number of larvae shown is not a representative of the total number of larvae that was in each group after staining with Oil red. Black arrows indicate Oil red O positive staining of larval livers

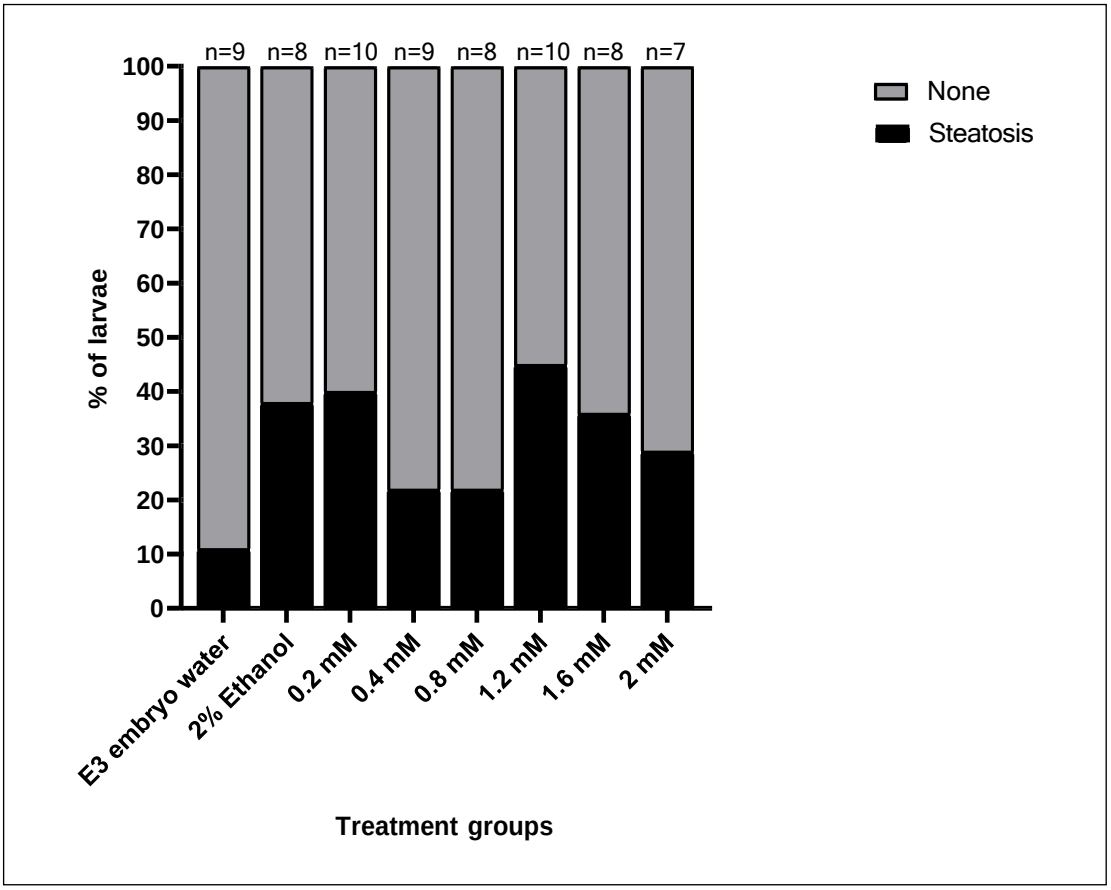

Figure 45: Percentage of zebrafish larvae with Oil red O positive stained livers. Zebrafish larvae at 2 dpf were treated for 3 days with EMB at concentrations of 0.2 mM, 0.4 mM, 0.8 mM, 1.2 mM, 1.6 mM and 2 mM. Zebrafish larvae were fixed overnight and then stained with 0.5% Oil red O. The 1.2 mM treatment group showed more larvae with the Oil red O lipid stains compared to other groups ($P < 0.05$).

As depicted in figures 44 and 45 above, the 1.2 mM EMB treatment group showed more zebrafish larvae with the positive ORO stained livers as compared to other groups. Hence, the 1.2 mM dose of EMB was chosen as the dose that had brought about most of the liver damage in larval zebrafish for use in the study.

4.4.5 APAP

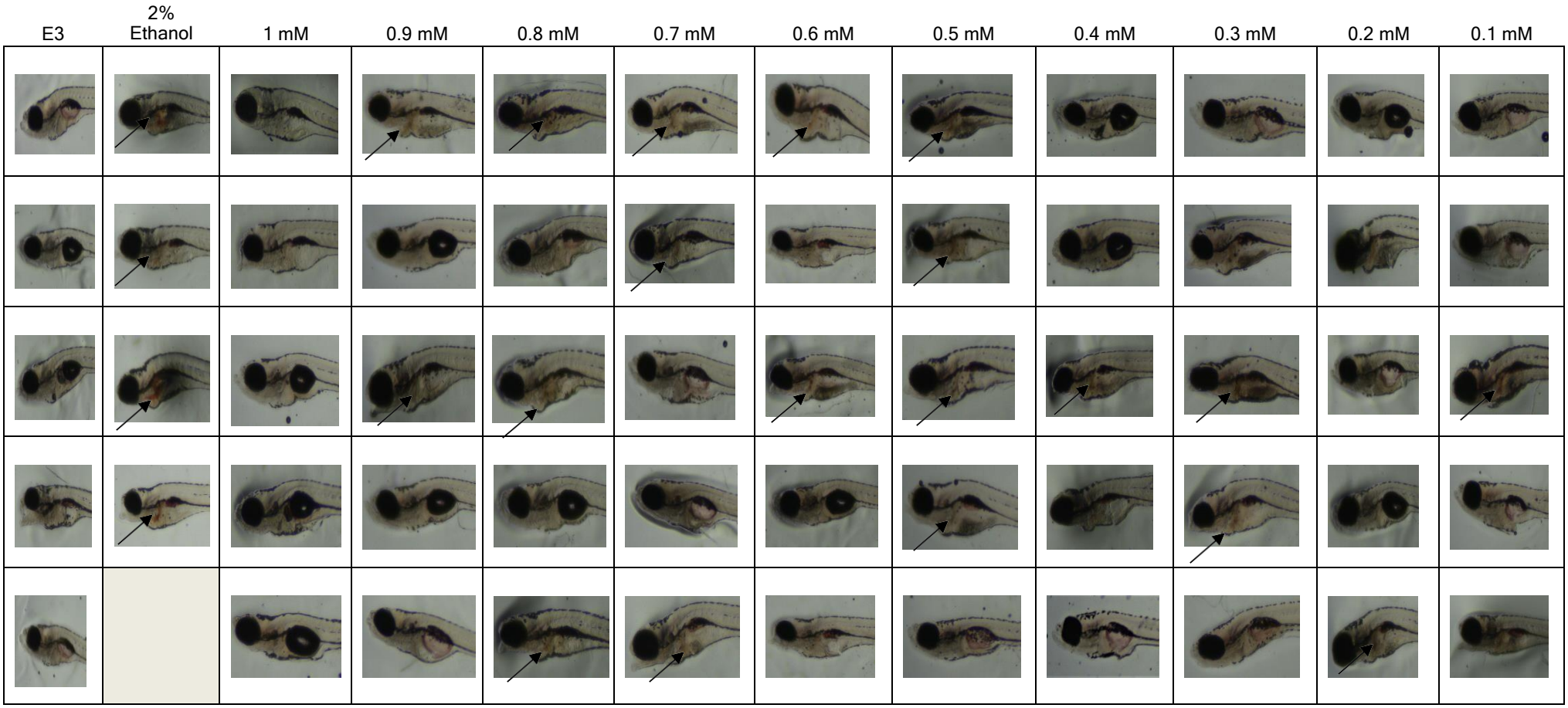

Figure 46: Zebrafish larvae treated with 2% Ethanol (n=7) and APAP at 0.1 mM (n=7), 0.2 mM (n=7), 0.3 mM (n=7), 0.4 mM (n=7), 0.5 mM (n=7), 0.6 mM (n=7), 0.7 mM (n=7), 0.8 mM (n=7), 0.9 mM (n=7) and 1 mM (n=7). The negative control group only contained E3 embryo water (n=7). Number of larvae shown is not representative of the total number of larvae that was in each group after staining with 0.5% Oil red O. Oil red O positive staining of zebrafish larval livers is indicated by black arrows

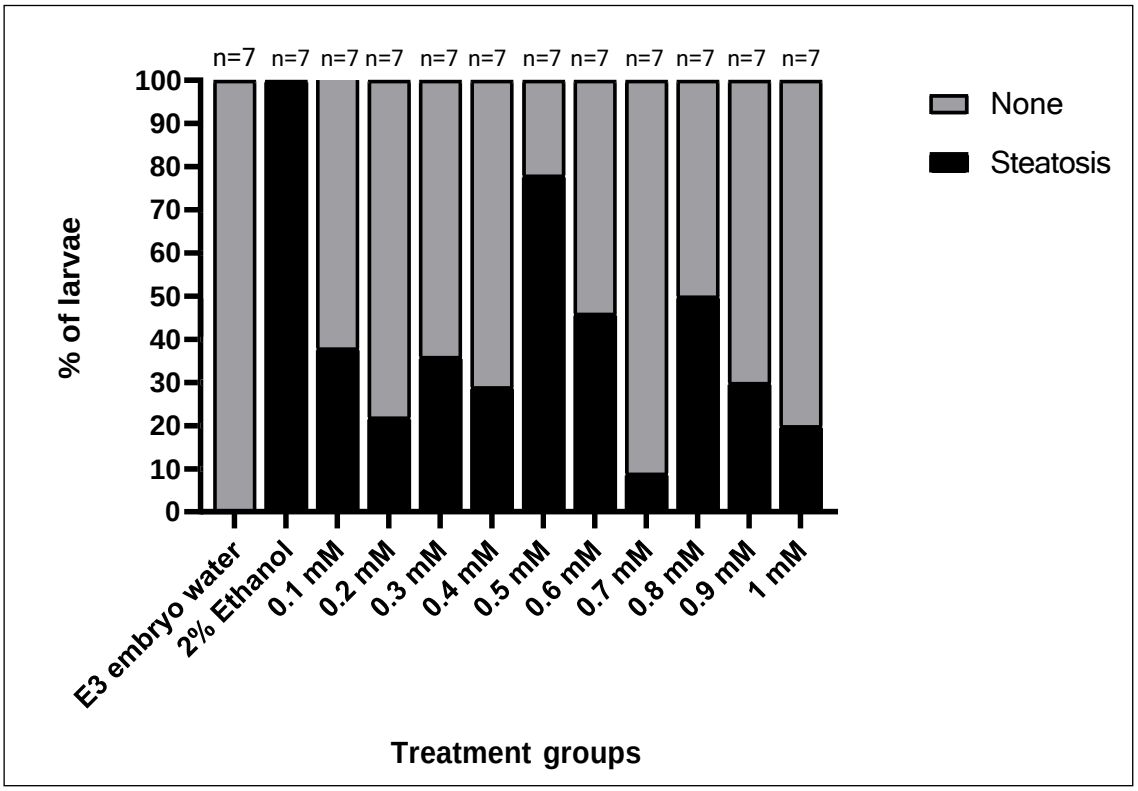

Figure 47: Percentage of zebrafish larvae with Oil red O positive staining livers. Zebrafish larvae at 2 dpf were treated for 3 days with APAP at concentrations of 0.1 mM, 0.2 mM, 0.3 mM, 0.4 mM, 0.5 mM, 0.6 mM 0.7 mM, 0.8 mM, 0.9 mM and 1 mM. Zebrafish larvae were fixed overnight and then stained with 0.5% Oil red O. The 0.5 mM treatment group showed more larvae with the Oil red O positive staining livers compared to other groups ($P > 0.05$)

APAP dose of 0.5 mM showed more larvae with Oil red O lipid droplets in the liver compared to other treatment groups ($P > 0.05$), as shown in figures 46 and 47 above. This dose was then used selected for use in further experiments.

4.4.6 NAC dose response

Zebrafish larvae at 3 dpf were treated with six different concentrations of NAC for 24 hours as part of a dose range finding experiment. The negative control group had only fish water in each well of a 96-well plate and the positive control group had 0.02 mg/mL 3,4-Dichloroalanine. After the 24 hour incubation period at 28˚C, zebrafish larvae were taken for tracking of movement in response to treatment on the EthoVision software. The results showed that when the fish were dosed with 16 µM, their movement decreased, suggesting oxidative damage to the fish and therefore toxicity of NAC to the larva at this concentration. In contrast, a concentration of 12 µM appeared to be the safe dosage with an increase in movement with the higher NAC concentration. Therefore, concentrations of 2 µM, 4 µM and 8 µM of NAC were to be used for further experiments in the study. Figure 48 below shows the average distance moved by each group of larvae at the different concentrations at different time points for 10 min at 24 hpe.

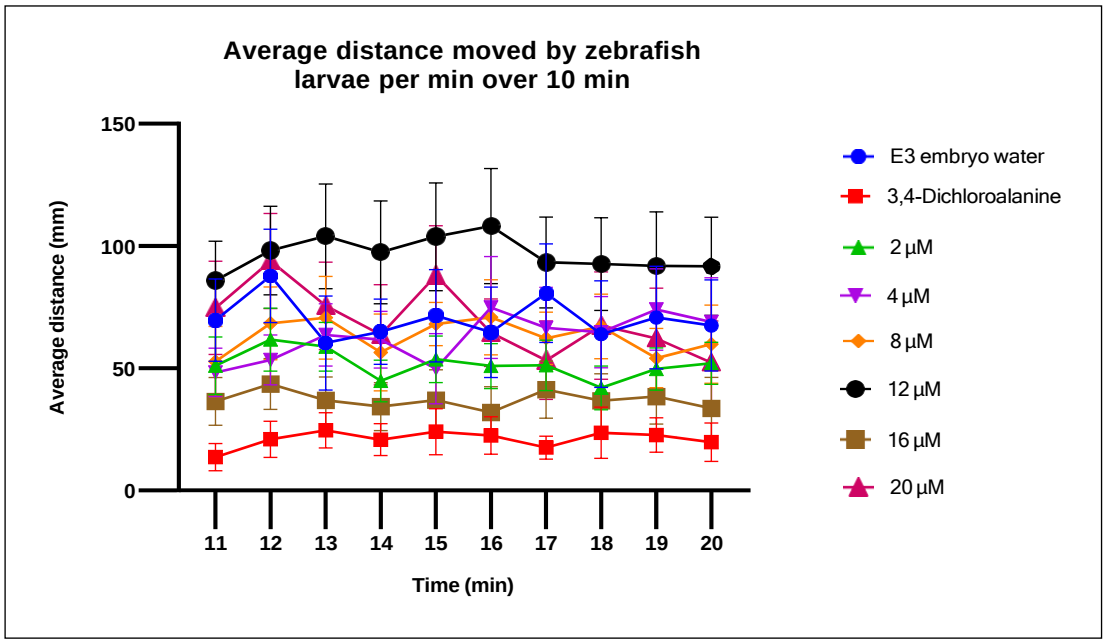

Figure 48: Average distance moved over 10 min by zebrafish larvae dosed with different concentrations of NAC, as tracked by the EthoVision. Each error bar represents ±SEM of n = 11 zebrafish larvae for each concentration

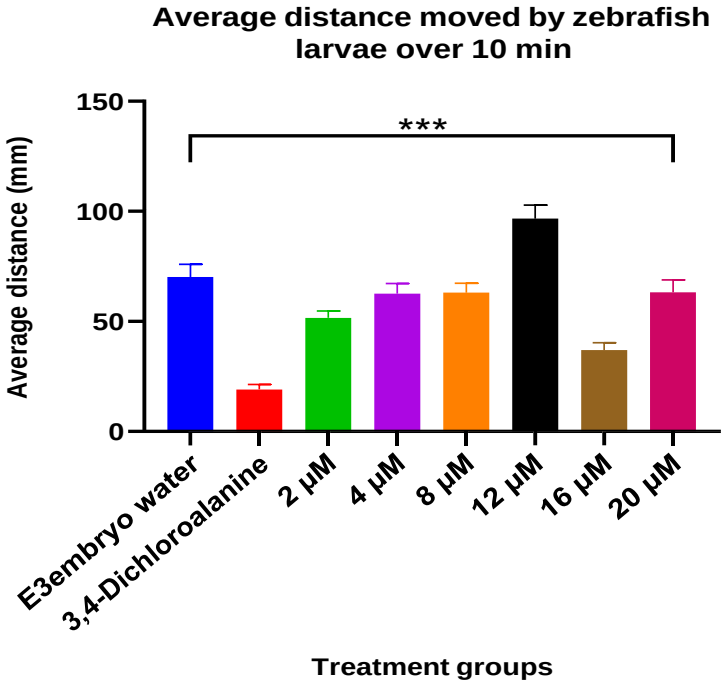

Figure 49: Average distance moved by zebrafish larvae treated with various concentrations of NAC. Error bars represents ±SEM of n = 11 zebrafish larvae for each concentration. The standard error of the mean (SEM) here was used because it measures variability across all the groups. In contrast to SEM, standard deviation (SD) measures variability across one group or one sample. Statistics: repeated measures ANOVA (analysis of variance) showed main effect of treatment dose, ($P < 0.001$). Tukey post hoc: n = 11;***$P < 0.001$

NAC at various concentrations was given to zebrafish larvae at 3 dpf over 24 hours. After 24 hours, the movement of each larvae at each concentration group was tracked for 20 minutes. Only results from the last 10 minutes were used for analysis as this is the time that the zebrafish larval movement was shown to be at baseline. The data in figure 48 and figure 49 above shows that the 12 µM and 16 µM groups experienced irritation and toxicity, respectively. The 20 µM dose resulted in the development of seizures and fatigue in zebrafish larvae. Zebrafish larvae at this concentration start to die off and this is shown by the erratic movement of zebrafish larvae as shown in the figure 48 above. However, the 8 µM group was shown to be consistent with the negative control. Therefore, 8 µM NAC was selected as the safe dose.

Chapter 5

Discussion

5.1 Zebrafish larval model for TB-DILI

TB is ranked as the second most deadly infectious disease worldwide. Despite the availability of drug regimens that are used to treat the disease, a wide range of adverse drug reactions occur due to these treatments. The most common and most serious adverse effect is DILI. DILI usually occurs in the intensive phase of treatment and is mostly due to INH, RIF and PZA (Ambreen *et al*., 2014). INH is metabolized and cleared in the liver. INH hepatotoxicity is linked to the accumulation of INH and its toxic acetyl hydrazine metabolite due to slow acetylation (Bouz and Hasawi, 2019). RIF undergoes hepatic metabolism to non-toxic agents. However, RIF has the potential to induce CYP450 enzymes, thereby exacerbating the toxic effects of some drugs (Bouz and Hasawi, 2019). When used in combination with INH during antituberculosis therapy, RIF increases INH toxicity by inducing the production of acetyl hydrazine from the hydrolysis of INH by slow acetylators (Bouz and Hasawi, 2019). PZA undergoes hepatic metabolism and the metabolites are excreted through the kidneys. The hepatotoxicity of PZA follows a dose-dependent pattern (Bouz and Hasawi, 2019). No data has been reported on the hepatotoxicity potential of EMB. Some authors reported PZA as themost hepatotoxic drug when used in combination with RIF, INH and EMB (Schechter *et al*., 2006; Yew and Leung, 2006) while others reported that DILI from antituberculosis treatment was due to INH when used in combination with PZA and RIF (Lei *et al*., 2021).

Since TB medication has been shown to be associated with the development of DILI, it is important that during antituberculosis chemotherapy, therapeutic drug monitoring should be performed, especially during the initiation of therapy. Discontinuation of treatment serves as the best option to immediately manage antituberculosis drug induced liver injury, but as soon as liver biochemistry normalizes, therapy is re-initiated due to the efficacy of first line antituberculosis therapy (Saha *et al*., 2016). In addition to elevated liver enzymes as one of the symptoms of DILI, DILI can lead to severe liver injury leading to the patient requiring a liver transplant, or even death (Devarbhavi, 2011). A few studies in humans (Schechter *et al*., 2006; Moosa *et al*., 2021) and animal models (Saito *et al*., 2010; Attri *et al*., 2000; North *et al*, 2012) have confirmed the usefulness of NAC in managing DILI. Characterized by its mucolytic property, NAC act as an L-cysteine and glutathione precursor that scavenges free radicals. Free radicals cause oxidative stress that potentially causes the depletion of intracellular glutathione. Therefore, as an antioxidant, NAC works by replenishing intracellular glutathione such as in hepatocytes (Santus *et al*., 2014). However, this beneficial effect of NAC still needs to be investigated through more studies. Therefore, new models are needed for predicting DILI in humans. Moreover, markers of DILI and mediators that would protect against liver injury as a result of first-line TB medication need to be identified.

Zebrafish larvae have been used for screening and studying the mechanism of action of hepatotoxic compounds *in vivo*. Both the mammalian liver and the zebrafish liver are similar in structure and perform the same function. Zebrafish liver morphogenesis completes as early as 2 dpf and the liver is fully functional at 3 dpf with metabolism occurring and driven by the CYP450 enzymes, especially the CYP3A4 and CYP2D6 enzymes (He et al., 2013). The CYP2E1 enzymes in zebrafish larvae are associated with the hepatotoxicity of acetaminophen. Therefore, the larval zebrafish can be used to study hepatotoxicants such as APAP and TB drugs in vivo by screening the compounds using multi-well plates

Hepatotoxicity is defined as injury to the liver or impairment to the function of the liver as a result of exposure to hepatotoxicants such as medicines, chemicals, or herbal or dietary supplements. These agents cause liver injury via different mechanisms that produce a variety of toxic phenotypes of the liver. The most common include necrosis, steatosis and cholestasis. As the largest organ in the body, the liver is involved in the processing of macronutrients and in the detoxification and biliary excretion of xenobiotics and endobiotics. Even though the tissue of the zebrafish liver differs in nature with regards to its cellular and extracellular compartments from the mammalian liver, it contains all the same cell types as the mammalianliver (So *et al*., 2020). Of the four types of liver cells, the hepatocytes make up 70- 80% of the mass of the liver and contain organelles like the mitochondria that play a role in the metabolism and excretion of substances. This therefore makes the liver more susceptible to inflammation and damage from insults. Liver injury can be reversed by stopping the offending drug until liver enzymes normalise. In the case of DILI due to first-line TB medication, INH, RIF and PZA canbe stopped and be replaced by streptomycin until liver enzymes normalise. However, in the case of irreversible liver damage, hepatocyte cell death can occurin the form of either apoptosis or necrosis (Cullen and Stalker, 2016).

5.2 ORO for liver injury quantification

ORO (figure 50) has emerged as a useful dye for staining of tryglycerides and lipids for over a decade. The use of ORO is advantageous over other lipid stains such as Nile red since it is cost effective, less toxic and the staining procedure is rapid with a quick response (Liu and Chen, 2019). The use of ORO as a qualitative and quantitative measure of lipids does not only save money but it also saves resources (Yoganantharajah, 2018). ORO is a fat-soluble dye that is highly sensitive and soluble in lipids, lipoproteins and cholesterol esters and stains them red. The azo (-N=N-) group of the ORO prevent the stain from undergoing ionization and hence facilitate its high lipid solubility (Bumbrah *et al*., 2019; Bharati *et al*. 2022).

The current study showed that acetaminophen and the first-line TB drugs cause steatosis, an indicator of liver injury, in zebrafish larva stained with ORO at 6 dpf. Steatosis is a type of liver

injury in which an abnormal retention of fats/lipids occur within the liver that is cause by an increase in fatty acid synthesis or a decrease in the secretion of lipids or inhibition of β-oxidation (Driessen *et al*., 2015). This cost-effective and convenient vertebrate model can bridge the gap between mammalian models and cell-based models (He *et al*., 2013). Moreover, the zebrafish larval model for DILI as a result of antitubercular drugs can be furtherused with pharmacokinetic based models to find ways to adjust treatment doses of hepatotoxicants in patients suffering from liver injury (Bouz and Al Hasawi, 2018; Lokhande, 2017).

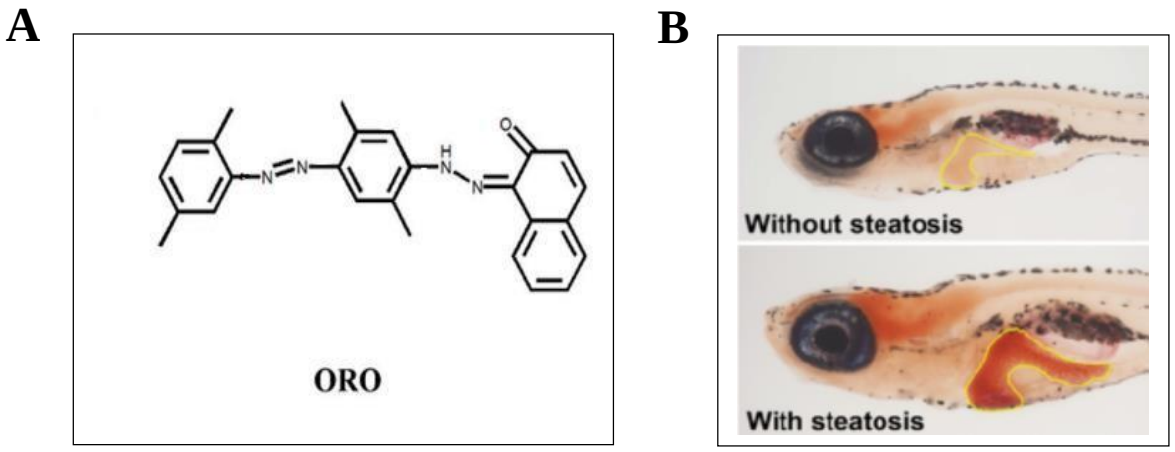

Figure 50: (**A**) Chemical structure of ORO (Liu and Chen, 2019); (**B**) Zebrafish larvae with and without steatosis (Dai *et al*., 2015)

In this study, a time efficient, economical zebrafish larval model for DILI was successfully developed. This study revealed that INH, PZA, RIF and EMB produced hepatotoxicity in zebrafish larvae at concentrations of 1 mM, 7 mM, 10 µM and 1.2 mM, respectively. The intensity and allocation of the stain in the liver area on the APAP treatment group compared to groups treated with TB drugs was used as an endpoint for liver damage. It is difficult to study the pathogenesis of DILI and the mechanism of action of the agents that are associated with the disease. New models are needed to predict which therapeutic agents are associated with DILI and new markers and mediators of DILI need to be identified.

Studies have shown the potential of ethanol in inducing liver disease (Lai *et al*., 2018; Dai *et al*., 2022; Lin *et al*., 2017; Liu *et al*., 2021; Passeri *et al*., 2009). The mechanism in which ethanol induces liver disease lies in the metabolism of ethanol to an acetaldehyde which is toxic to hepatocytes. The toxicity of acetaldehyde causes damage to the hepatocyte, inducing their release of Danger-Associated Molecular Patterns (DAMPs) which further induce cells of

the adaptive and innate immune system to cause more liver damage through inflammation (Dunn and Shah, 2016). Ethanol is further oxidised into acetic acid by alcohol dehydrogenase. Acetic acid further gets oxidised into CO_2 and H_2O. The overall metabolism of ethanol in the liver produces NADH (nicotinamide adenine dinucleotide (NAD) + hydrogen) and NAD+, which induce the synthesis of more fatty acids and decrease the oxidation of fatty acids, respectively. Ethanol also induces the CYP450 E2 enzymes in the liver, leading to more oxidation of the liver, subsequently leading to more liver damage (Lu *et al*., 2008).

5.3 Acetaminophen method development and partial validation

A simple, rapid and specific HPLC method for a quantification of APAP was developed and partially validated according to the FDA guidelines. The method yielded excellent chromatography as shown in the figure 31 in section 3.4.2. An HPLC method should be simple, accurate and robust. When developing an HPLC method for the detection of an analyte, the polarity of the compound is important in selecting the mobile phase composition, the column as well as the flow rate (Kumar *et al*., 2013). APAP is a polar molecule and therefore a mobile phase of higher aqueous was therefore needed for elution of the analyte at 3.26 min. This was also observed in similar studies (Narayanan and Austin, 2016; Koblová; Narayanan and Austin, 2016). However, others have used a higher organic mobile phase and produced excellent chromatographic peaks with good retention (Chandrasekhar and Manikandan, 2020; Kanthale *et al*., 2020).

Since the method developed was not used to analyze patient samples, a batch of APAP STDs and QCs was run to ensure that the method was accurate and precise. All the STDs and QCs for APAP had an accuracy between 85-115% and a precision of less than 15%. This therefore suggested that the method was fit for quantitative analysis of the APAP samples covering the range of 3.13 µg/mL to 200 µg/mL. This range was selected based on the initial concentration range of 2 mM to 20 mM APAP that was used in the determination of the dose that would result in liver damage for APAP to use in further experiments for the study.

5.4 Solubility and stability assessment of APAP, INH, RIF, PZA and EMB

Since zebrafish can only survive in E3 embryo medium that is made up of specific chemicals and reagents that are healthy to the fish, treatments therefore need to be prepared in the same solvent as the fish medium. This requires that the drug be soluble in the fish water. Solubility is the ability of a solute (e.g drug) to dissolve in a solvent (e.g fish water) to form a homogeneous solution. Since the treated larvae were kept for 3 days in the laboratory incubator set at 28˚C during the dose response experiments, samples were assessed for stability at 28˚C for 3 days. According to our knowledge, no data has been published on the

solubility and stability of the test samples under the conditions (28°C). It is important to evaluate this to mimic how clinical drug administration would occur. Moreover, other drugs are not water-soluble and therefore, in order to make the right conclusions about the experiments, solubility and stability assessment of the drugs was carried out on HPLC and LC-MS. APAP, INH, PZA and EMB all had accuracy between 85-115% with precision and %differences which were within 15%. It can therefore be concluded the APAP, INH, PZA and EMB were soluble in E3 embryo water and stable when placed in the laboratory incubator set at 28˚C for 3 days. APAP, INH, PZA and EMB are polar compounds and the polar portions of their molecules form covalent bonds with water (Hojjati and Rohani, 2006). However, the RIF test samples failed to meet acceptable criteria when placed in the incubator at 28˚C for three days. Both the %CV and the %difference of RIF were outside the 15% threshold. It can therefore be concluded that the RIF was poorly soluble in E3 embryo water and degraded over the experimental time. RIF is a hydrophobic drug and therefore its solubility in water is a challenge (Ellard and Fourie, 1999). However, ascorbic acid (also known as Vitamin C) has been shown to improve the solubility of RIF in water over time (Phogole, 2022). Ascorbic acid is a water-soluble vitamin that is found in fruits and vegetables that act as an antioxidant that is responsible for tissue repair and a scavenger for oxidative radicals that are produced by the body (Devaki and Raveendran, 2017). Hence it is responsible for preventing RIF from degrading in solution (Rajaram *et al*., 2014), thereby improving the stability and solubility of RIF. A study by Wu *et al.,* 2015 showed that a concentration of 20 µg/mL ascorbic acid protects against zebrafish larvae hair cell loss induced by neomycin (Wu *et al* 2015), suggesting good tolerability at this concentration in a zebrafish model. Hence 20 µg/mL ascorbic acid in E3 embryo water was used to prepare the RIF test samples. However, the addition of 20 µg/mL ascorbic acid did not prevent the degradation of RIF. This is indicated by the drastic decrease of RIF concentration over time as shown in figure 35 in section 4.2. It is suspected that the temperature of 28°C was too high and the ascorbic acid concentration might have been too low to protect against degradation. However, 28°C is the optimal temperature for survival of zebrafish larvae and a higher concentration of ascorbic acid increases the acidity of the E3 embryo medium, which is toxic to zebrafish larvae.

5.5 Dose range finding experiments and previous zebrafish larval doses

To determine the dose (s) that resulted in most damage for each drug, dose-response experiments were performed on zebrafish larvae by using a range of concentrations that cover the previously reported zebrafish larval doses of each drug (Ali *et al*., 2012; Dalto *et al*., 2016; North *et al*., 2010; Zhang *et al*., 2016; Zhang *et al*., 2017). It is difficult to translate zebrafish larval doses to human doses and vice versa because the administration of drugs in zebrafish larvae is by adding of the drugs in the medium. Although the concentration of the drug in the

embryo medium is known, it is difficult to get the exact amount of drug taken up by the zebrafish larvae (Vliegenthart *et al*., 2014). As shown in section 4.4, the doses that resulted in liver damage for INH, PZA, RIF, EMB and APAP were 1 Mm, 7 mM, 10 µM, 1.2 mM and 0.5 mM. These doses were selected because a large number of zebrafish larvae showed an ORO positive staining of livers as a sign of steatosis in the respective groups after Oil red O staining. The doses that resulted in most damage for INH and PZA were lower than previously reported hepatotoxic doses for these drugs. Zhang *et al* has reported that INH induced hepatotoxicity at 16 mM and PZA induced hepatotoxicity at 2.5 mM and 5 mM in zebrafish larvae. However, a Tg (L-FABP: EGFP) transgenic zebrafish larvae was used for the study with no use of Oil red O as a measure of the degree of liver injury. For the current study, a wild type zebrafish strain was used. Similarly, with APAP, the 0.5 mM dose was lower than the reported APAP hepatotoxic dose of 10 mM that was reported by North *et al* in 2010. A Tg (-2.8fabp10: GFP)^{as3} zebrafish line was also used in the study, which was different from our study (Wild type stain).

NAC is a known antioxidant that works by replenishing cellular glutathione. However, antioxidants such as NAC can also act as pro-oxidants (Rahal *et al*., 2014). Hence, EthoVision is a better method in analysing results for an antioxidant such as NAC because with NAC, a trend of irritation and toxicity can be clearly observed. The EthoVision data in section 4.4.1 show that zebrafish larvae exposed to different doses expressed different distances moved by each group at different time points. The results showed that the 12 µM concentration of NAC resulted in irritation while the concentration of 16 µM resulted in toxicity. However, the group that was treated with 20 µM concentration of NAC was regarded as an outlier as it did not correlate with what was expected. The 8 µM concentration of NAC seemed to produce a consistent effect and was therefore chosen as the dose for further experiments to evaluate protection against liver injury in zebrafish larvae. This is however different to the previously reported safe dose (10 mM) for NAC (North *at al*, 2010). This could be due to the fact that a transgenic zebrafish strain (Tg (-2.8fabp10: GFP)^{as3}) had been used as well.

Test organisms need to be in a habitat with environmental conditions that are suitable for their survival. These include the right temperature and availability of nutrients (Krell and Schmidt, 2020). Therefore, it is very crucial for one to work as quickly as possible when treating the zebrafish larvae. The small size and hence vulnerability of the zebrafish larvae makes it difficult to position it for proper visualization and therefore requires time and proper handling. Zebrafish are also sensitive to noise and vibrations which makes the zebrafish too stressed to breed. Moreover, the water needs to be of good quality and free of any oxygen scavenging microorganism or any waste build up in the breeding tank (Zhang, 2017). However, the 8 µM dose of NAC can be used in future work to evaluate the potential of NAC in reversing TB-drug associated DILI.

Chapter 6

Conclusion, limitations and future work

6.1 Conclusion

The development of drug induced liver injury is not only a challenge to patients, but also to physicians and the pharmaceutical industry. Patients on TB medication experience DILI, especially in the intensive phase of therapy. The treatment of drug-sensitive TB is a combination regimen consisting of INH, PZA, RIF and EMB, and each of these drugs causes hepatotoxicity via a different mechanism of action. INH hepatotoxicity is due to the acetyl hydrazine metabolite and through slow acetylation. Hepatotoxicity due to PZA is dose dependant while RIF has the potential to induce liver enzymes such as the cytochrome P450 enzymes. RIF also induces INH directly, leading to an increase in the hepatotoxicity potential of INH. However, most studies have confirmed that the hepatotoxicity due to the TB medication is due to PZA when the drugs are used in combination. Close monitoring of the patients during therapy is therefore recommended.

The current study aimed to develop an *in vivo* zebrafish larval model for DILI within the Division of Clinical Pharmacology and to use the model to investigate whether NAC is able to reverse/prevent TB-drug associated DILI. NAC was chosen because it is an effective antidote for DILI due to APAP poisoning. The current study showed that 1 mM INH, 7 mM PZA, 10 µM RIF and 1.2 mM EMB are associated with DILI as evaluated by ORO positive staining in the liver, indicative of steatosis. Due to the high incidence rate of DILI from TB medication, a preventative strategy needs to be put in place in order to prevent the DILI from occurring rather than to wait until the patient gets sick. This study showed that 8 µM NAC could be a dose that can reverse hepatotoxicity as a result of TB medication in zebrafish larvae as shown by the figures 48-49 in section 4.4.6. Due to delays during zebrafish breeding and time constraints, the aims of the current study could not be achieved. The zebrafish larval model for DILI was developed. However, the model still needs refinement for further evaluation in the Division of Clinical Pharmacology. However, investigation of the potential intervention of NAC in TB-drug associated DILI has now emerged as a potential project for another student.

6.2 Limitations

The stability issue of RIF serves as a limitation that needs to be overcome when evaluating DILI as a result of RIF and experiments need to be conducted over short periods of time. Working with zebrafish larvae, like other animal models, comes with some challenges. Some of these challenges include perishing of the test organisms due to intolerance to cold for long periods. Some zebrafish larvae were lost during the staining procedure due to the dark colour of the stain, especially in the INH group. There is a distinct possibility that the lost larvae also displayed the positive ORO staining in the livers, indicating liver steatosis. Initially, each group of zebrafish larvae had twelve replicates. During the course of treatment (3 days), about 40% of the zebrafish larvae had died in each group. After staining, a minimum of 42% and a

maximum of 80% of zebrafish larvae had survived in each group. Therefore, the chosen dose (s) of the drugs were only based on the total number of zebrafish larvae left after staining. As a consequence of difficulties in breeding and handling of vulnerable zebrafish larvae, a large number of up to 50% of the zebrafish larvae had died before the completion of the project. This posed a great challenge in the completion of the project and therefore, the current study could not prove the protective effect of NAC in reversing DILI as a result of TB medication.

6.3 Future work

The potential protective effect of NAC in TB-drug associated hepatic injury needs to be investigated in zebrafish larvae using the well-tolerated dose of 8 µM to evaluate whether NAC can protect/ reverse the hepatotoxic effects of each first-line TB drug. Drugs needs to be evaluated individually and in combination. Since NAC is used as an antidote for APAP poisoning in humans, the risks of introducing it as an intervention in a human clinical trial are low. Moreover, this can also prevent using doses of NAC that are associated with adverse effects such as anaphylaxis. A paper on a study done at the University of Cape Town was found where the efficacy of the 21-hour 3-bag regimen of NAC was tested in TB patients with DILI. NAC was able to reduce length of hospital stay but patients experience adverse effects. Therefore, in future, perhaps the better tolerated 20-hour 2 bag NAC regimen can be investigated in future.

References

1. Abbara, A., Chitty, S., Roe, J.K., Ghani, R., Collin, S.M., Ritchie, A., Min Kon, O., Dzvova, J., et al. n.d. Drug-induced liver injury from antituberculous treatment: a retrospective study from a large TB centre in the UK. DOI: 10.1186/s12879-017-2330-z.
2. Abdelrahman, M., Burritt, D.J. & Tran, L.S.P. 2018. The use of metabolomic quantitative trait locus mapping and osmotic adjustment traits for the improvement of crop yields under environmental stresses. *Seminars in Cell and Developmental Biology*. 83:86–94. DOI: 10.1016/J.SEMCDB.2017.06.020.
3. *Acetaminophen (paracetamol) poisoning in adults: Treatment*. n.d. Available: https://www.medilib.ir/uptodate/show/318 [2022, August 27].
4. ah Jung, J., Kim, T., lee, hyun, Jeong, B., Yun Park, hye, Jeon, K., Jung Kwon, O., Ko, J.-W., et al. 2015. a proposal for an individualized pharmacogenetic-guided isoniazid dosage regimen for patients with tuberculosis. DOI: 10.2147/DDDT.S87131.
5. Ahn, E.Y. & Park, Y. 2017. Facile fabrication of gold nanoparticles with ethambutol. *Journal of Nanoscience and Nanotechnology*. 17(7):4851–4857. DOI: 10.1166/JNN.2017.13443.
6. Aldini, G., Altomare, A., Baron, G., Vistoli, G., Carini, M., Borsani, L. & Sergio, F. 2018. N-Acetylcysteine as an antioxidant and disulphide breaking agent: the reasons why. DOI: 10.1080/10715762.2018.1468564.
7. Ali, M. & de Perera, G. n.d. *Basic & Clinical Pharmacology Fourteenth Edition a LANGE medical book Related papers Kat zung-Basic and Clinical Pharmacology 14t h Edit ion c2018 t xt bk Tomás Vargas Llibre-Basic and Clinical Pharmacology 12t h Edit ion=Bert ram Kat zung Susan Mast ers Ant hony Trevor=007 … Afrim Ademi Basic and Clinical Pharmacology*.
8. Ali, S., Champagne, D.L. & Richardson, M.K. 2012. Behavioral profiling of zebrafish embryos exposed to a panel of 60 water-soluble compounds. *Behavioural Brain Research*. 228(2):272–283. DOI: 10.1016/J.BBR.2011.11.020.
9. Attril, S., Rana, S. v, Vaiphei2, K., Sodhil, C.P., Katyall, R., Goell, R.C., Nain', C.K. & Singh', K. 2000. *Isoniazid-and rifampicin-induced oxidative hepatic injury-protection by N-acetylcysteine*. Available: www.arnoldpublishers.com/journals.
10. Au, V., Zakaria, M.I., Au, V. & Kong, H. 2014. *A study on the medication errors in the administration of N-acetylcysteine for paracetamol overdose patients in Malaysia*
11. Aycan, I.Ö., Tüfek, A., Tokgöz, O., Evliyaoğlu, O., Firat, U., Kavak, G.Ö., Turgut, H. & Yüksel, M.U. 2014. Thymoquinone treatment against acetaminophen-induced hepatotoxicity in rats. *International Journal of Surgery*. 12(3):213–218. DOI: 10.1016/J.IJSU.2013.12.013.

12. Babu, D., Morgan, A.G., Reiz, B., Whittal, R.M., Almas, S., Lacy, P. & Siraki, A.G. 2019. Eosinophil peroxidase oxidizes isoniazid to form the active metabolite against M. tuberculosis, isoniazid-NAD +. *Chemico-Biological Interactions*. 305:48–53. DOI: 10.1016/J.CBI.2019.03.019.
13. Banerjee, S. & Mazumdar, S. 2012. Electrospray Ionization Mass Spectrometry: A Technique to Access the Information beyond the Molecular Weight of the Analyte. *International Journal of Analytical Chemistry*. 2012:40. DOI: 10.1155/2012/282574.
14. Baniasadi, S., Eftekhari, P., Tabarsi, P., Fahimi, F., Raoufy, M.R., Masjedi, M.R. & Velayati, A.A. 2010. Protective effect of N-acetylcysteine on antituberculosis drug-induced hepatotoxicity. *European Journal of Gastroenterology and Hepatology*. 22(10):1235–1238. DOI: 10.1097/MEG.0B013E32833AA11B.
15. Bastiaan, A.D., Tucker, C.S., Pozo, J. del & Dear, J.W. 2014a. Zebrafish as model organisms for studying drug-induced liver injury. DOI: 10.1111/bcp.12408.
16. Bastiaan, A.D., Tucker, C.S., Pozo, J. del & Dear, J.W. 2014b. Zebrafish as model organisms for studying drug-induced liver injury. DOI: 10.1111/bcp.12408.
17. Bessaire, T., Mujahid, C., Beck, A., Tarres, A., Savoy, M.-C., Woo, P.-M., Mottier, P. & Desmarchelier, A. 2018. Screening of 23 β-lactams in foodstuffs by LC-MS/ MS using an alkaline QuEChERS-like extraction Screening of 23 β-lactams in foodstuffs by LC-MS/MS using an alkaline QuEChERS-like extraction. DOI: 10.1080/19440049.2018.1426891.
18. Bhandari, M. & Bhandari, M. 2021. Bedaquiline nanoparticle-mediated drug therapy against tuberculosis in the zebrafish embryo model. Available: https://www.duo.uio.no/handle/10852/87007 [2022, August 27].
19. Bharati, S., Anjaly, K., Thoidingjam, S. & Tiku, A.B. 2022. Oil Red O based method for exosome labelling and detection. *Biochemical and Biophysical Research Communications*. 611:179–182. DOI: 10.1016/J.BBRC.2022.04.087.
20. Björnsson, E.S. 1901. Global Epidemiology of Drug-Induced Liver Injury (DILI). DOI: 10.1007/s11901-019-00475-z.
21. Bouazzi, O. el, Hammi, S., Bourkadi, J.E., Tebaa, A., Tanani, D.S., Soulaymani-Bencheikh, R., Badrane, N., Bengueddour, R., et al. 2016. First line anti-tuberculosis induced hepatotoxicity: incidence and risk factors Case series Open Access. *Pan African Medical Journal-ISSN*. 25:1937-8688. DOI: 10.11604/pamj.2016.25.167.10060.
22. Bouz, G. & al Hasawi, N. 2018. The zebrafish model of tuberculosis - no lungs needed. *Critical Reviews in Microbiology*. 44(6):779–792. DOI: 10.1080/1040841X.2018.1523132.
23. Braunbeck, T., Görge, G., Storch, V. & Nagel, R. 1990. Hepatic steatosis in zebra fish (Brachydanio rerio) induced by long-term exposure to γ-hexachlorocyclohexane.

Ecotoxicology and Environmental Safety. 19(3):355–374. DOI: 10.1016/0147-6513(90)90036-5.

24. Bruells, C.S., Duschner, P., Marx, G., Gayan-Ramirez, G., Frank, N., Breuer, T., Krenkel, O., Tacke, F., et al. n.d. Acute liver injury following acetaminophen administration does not activate atrophic pathways in the mouse diaphragm. DOI: 10.1038/s41598-021-85859-2.
25. Byran, G., Babu, B. & Nagappan, K. 2019. A NEW VALIDATED STABILITY-INDICATING DIRECT HIGH-PERFORMANCE LIQUID CHROMATOGRAPHY METHOD FOR THE DETERMINATION OF ROSIGLITAZONE ENANTIOMERS IN THE PRESENCE OF ITS. DOI: 10.22159/ajpcr.2019.v12i3.24960.
26. Caballero, M.V. & Candiracci, M. 2018. Zebrafish as screening model for detecting toxicity and drugs efficacy. *Journal of Unexplored Medical Data*. 3(2):4. DOI: 10.20517/2572-8180.2017.15.
27. Caminero, J.A. & Scardigli, A. 2015. Classification of antituberculosis drugs: a new proposal based on the most recent evidence. *European Respiratory Journal*. 46(4):887–893. DOI: 10.1183/13993003.00432-2015.
28. Campbell, E.A., Korzheva, N., Mustaev, A., Murakami, K., Nair, S., Goldfarb, A. & Darst, S.A. 2001. Structural mechanism for rifampicin inhibition of bacterial RNA polymerase. *Cell*. 104(6):901–912. DOI: 10.1016/S0092-8674(01)00286-0.
29. Cao, J., Mi, Y., Shi, C., Bian, Y., Huang, C., Ye, Z., Liu, L. & Miao, L. 2018. First-line anti-tuberculosis drugs induce hepatotoxicity: A novel mechanism based on a urinary metabolomics platform. *Biochemical and Biophysical Research Communications*. 497(2):485–491. DOI: 10.1016/J.BBRC.2018.02.030.
30. Cassar, S., Adatto, I., Freeman, J.L., Gamse, J.T., Iturria, I., Lawrence, C., Muriana, A., Peterson, R.T., et al. 2020. Use of Zebrafish in Drug Discovery Toxicology. *Chemical Research in Toxicology*. 33(1):95–118. DOI: 10.1021/ACS.CHEMRESTOX.9B00335/ASSET/IMAGES/LARGE/TX9B00335_0008.JPEG.
31. Chakaya, J., Khan, M., Ntoumi, F., Aklillu, E., Fatima, R., Mwaba, P., Kapata, N., Mfinanga, S., et al. 2021. Global Tuberculosis Report 2020 – Reflections on the Global TB burden, treatment and prevention efforts. *International Journal of Infectious Diseases*. 113:S7–S12. DOI: 10.1016/J.IJID.2021.02.107.
32. Chalasani, N. & Björnsson, E. 2010. Risk Factors for Idiosyncratic Drug-Induced Liver Injury. *Gastroenterology*. 138(7):2246–2259. DOI: 10.1053/J.GASTRO.2010.04.001.
33. Chalasani, N.P., Maddur, H., Russo, M.W., Wong, R.J. & Reddy, K.R. 2021. ACG Clinical Guideline: Diagnosis and Management of Idiosyncratic Drug-Induced Liver Injury. *American Journal of Gastroenterology*. 116(5):878–898. DOI: 10.14309/ajg.0000000000001259.

34. Chandrasekhar, K. & Manikandan, A. 2020. A New RP-HPLC Method Development and Validation of Paracetamol and Aceclofenac in Tablets by separating Diclofenac. *Research J. Pharm. and Tech*. 13(9). DOI: 10.5958/0974-360X.2020.00766.0.
35. "CHEMOTHERAPY OF PULMONARY TUBERCULOSIS". n.d. DOI: 10.1136/bmj.1.5138.1610.
36. Ciobanu, A.-M., Pop, A.L., Traian, G., Burcea-Dragomiroiu, A. & Daniela, P. n.d. HPLC studies for assessing the stability of carvedilol tablets "Studies on the use of dry extract of Usneae lichen like mucoadhesive patches, in the treatment of oral cancers" View project Food supplements View project. Available: https://www.researchgate.net/publication/319066215 [2022, August 27].
37. Cohen, K., Chughlay, M.F., Kramer, N., Spearman, C.W. & Werfalli, M. 2016. SYSTEMATIC REVIEW N-acetylcysteine for non-paracetamol drug-induced liver injury: a systematic review. DOI: 10.1111/bcp.12880.
38. Combrink, M., Loots, D.T. & du Preez, I. 2020. Metabolomics describes previously unknown toxicity mechanisms of isoniazid and rifampicin. *Toxicology Letters*. 322:104-110. DOI: 10.1016/J.TOXLET.2020.01.018.
39. *Current Trends in Cancer Management - Google Books*. n.d. Available: https://books.google.co.za/books?hl=en&lr=&id=ZTj8DwAAQBAJ&oi=fnd&pg=PA3&dq=84.+Khan,+F.R.+and+Alhewairini,+S.S.,+2018.+Zebrafish+(Danio+rerio)+as+a+model+organism.+Current+Trends+in+Cancer+Management,+pp.3-18.&ots=O54oj23B90&sig=f6JkWJy9uGU_jRK1jNqtcbQF_74&redir_esc=y#v=onepage&q&f=false [2022, August 27].
40. Czaplicki, S. 2013. Chromatography in Bioactivity Analysis of Compounds. *Column Chromatography*. (April, 10). DOI: 10.5772/55620.
41. Dai, W., Wang, K., Zheng, X., Chen, X., Zhang, W., Zhang, Y., Hou, J. & Liu, L. 2012. Chromium picolinate and chromium histidinate protects against renal dysfunction by modulation of NF-κB pathway in high-fat diet fed and Streptozotocin-induced diabetic rats. DOI: 10.1186/s12986-015-0036-z.
42. Dai, W., Wang, K., Zhen, X., Huang, Z. & Liu, L. 2020. Magnesium isoglycyrrhizinate attenuates acute alcohol-induced hepatic steatosis in a zebrafish model by regulating lipid metabolism and ER stress. DOI: 10.1186/s12986-022-00655-7.
43. Dal, N.-J.K. & Dal, N.-J.K. 2018. Nanoparticle-mediated drug therapy against tuberculosis in the zebrafish embryo model. Available: https://www.duo.uio.no/handle/10852/63021 [2022, August 27].
44. Dalton, J.P., Uy, B., Okuda, K.S., Hall, C.J., Denny, W.A., Crosier, P.S., Swift, S. & Wiles, S. n.d. Screening of anti-mycobacterial compounds in a naturally infected zebrafish larvae model. DOI: 10.1093/jac/dkw421.

45. Dalton, J.P., Uy, B., Okuda, K.S., Hall, C.J., Denny, W.A., Crosier, P.S., Swift, S. & Wiles, S. n.d. Screening of anti-mycobacterial compounds in a naturally infected zebrafish larvae model. DOI: 10.1093/jac/dkw421.
46. Darweesh, S.K., Ibrahim, M.F. & El-Tahawy, M.A. 2017. Effect of N-Acetylcysteine on Mortality and Liver Transplantation Rate in Non-Acetaminophen-Induced Acute Liver Failure: A Multicenter Study. 37:473–482. DOI: 10.1007/s40261-017-0505-4.
47. David, S., Hamilton, J.P. & Hopkins, J. 2010. *Drug-induced Liver Injury*.
48. Devaki, S.J. & Raveendran, R.L. 2017. Vitamin C: Sources, Functions, Sensing and Analysis. *Vitamin C*. (August, 2). DOI: 10.5772/INTECHOPEN.70162.
49. Devarbhavi, H. 2011. *Quarterly Review Antituberculous drug-induced liver injury: current perspective*.
50. Diekmann, H. & Hill, A. 2013. ADMETox in zebrafish. *Drug Discovery Today: Disease Models*. 10(1). DOI: 10.1016/J.DDMOD.2012.02.005.
51. Driessen, M., Vitins, A.P., Pennings, J.L.A., Kienhuis, A.S., Water, B. van de & van der Ven, L.T.M. 2015. A transcriptomics-based hepatotoxicity comparison between the zebrafish embryo and established human and rodent in vitro and in vivo models using cyclosporine A, amiodarone and acetaminophen. *Toxicology Letters*. 232(2):403–412. DOI: 10.1016/J.TOXLET.2014.11.020.
52. Dunn, W. & Shah, V.H. 2016. Pathogenesis of Alcoholic Liver Disease. *Clinics in Liver Disease*. 20(3). DOI: 10.1016/j.cld.2016.02.004.
53. Elbashir, A., Ali, R. & Osman, M. 2017. Development and Validation of Stability Indicating HPLC Method for the Simultaneous Analysis of Amlodipine, Hydrochlorothiazide and Valsartan in Pharmaceutical Formulation. DOI: 10.15406/japlr.2017.06.00188.
54. Ellard, G.A. & Fourie, P.B. 1999. *INT J TUBERC LUNG DIS 3(11):S301-S308 Rifampicin bioavailability: a review of its pharmacology and the chemotherapeutic necessity for ensuring optimal absorption*.
55. Ershad, M., Naji, A. & Vearrier, D. 2022. *N Acetylcysteine*.
56. Fang, P., Wei, H.|, Xie, F. & Xie, W.F. 2018. Corticosteroid therapy in drug-induced liver injury: Pros and cons. DOI: 10.1111/1751-2980.12697.
57. *FDA, 2014. New Chemical Entity Exclusivity Determinations for Certain Fixed-Combination Drug Products | FDA*. Retrieved August 28, 2022, from https://www.fda.gov/regulatory-information/search-fda-guidance-documents/new-chemical-entity-exclusivity-determinations-certain-fixed-combination-drug-products.
58. Francis, P. & Navarro, V.J. 2022. Drug Induced Hepatotoxicity. *StatPearls*. (March, 18). Available: https://www.ncbi.nlm.nih.gov/books/NBK557535/ [2022, August 27].

59. Garcia-Cortes, M., Robles-Diaz, M., Stephens, C., Ortega-Alonso, A., Lucena, · M Isabel & Andrade, R.J. 2020. Drug induced liver injury: an update. 94:3381–3407. DOI: 10.1007/s00204-020-02885-1.
60. Gerriets, V., Anderson, J. & Nappe, T.M. 2022. *Acetaminophen*.
61. Ghanem, C.I., Pérez, M.J., Manautou, J.E. & Mottino, A.D. 2016a. Acetaminophen from liver to brain: New insights into drug pharmacological action and toxicity. *Pharmacological Research*. 109:119–131. DOI: 10.1016/J.PHRS.2016.02.020.
62. Ghanem, C.I., Pérez, M.J., Manautou, J.E. & Mottino, A.D. 2016b. Acetaminophen from liver to brain: New insights into drug pharmacological action and toxicity. *Pharmacological Research*. 109:119–131. DOI: 10.1016/J.PHRS.2016.02.020.
63. Gill, M.K., Raman Patyar, R. & Patyar, S. n.d. European Journal of Molecular & Clinical Medicine Antitubercular Drug Induced Hepatotoxicity: A Review.
64. Goessling, W. & Sadler, K.C. 2015. Zebrafish: An Important Tool for Liver Disease Research. *Gastroenterology*. 149(6):1361–1377. DOI: 10.1053/J.GASTRO.2015.08.034.
65. He, J.H., Guo, S.Y., Zhu, F., Zhu, J.J., Chen, Y.X., Huang, C.J., Gao, J.M., Dong, Q.X., et al. 2013. A zebrafish phenotypic assay for assessing drug-induced hepatotoxicity. *Journal of Pharmacological and Toxicological Methods*. 67(1):25–32. DOI: 10.1016/J.VASCN.2012.10.003.
66. Hojjati, H. & Rohani, S. 2006. Measurement and Prediction of Solubility of Paracetamol in Water-Isopropanol Solution. Part 1. Measurement and Data Analysis. DOI: 10.1021/op060073o.
67. Hosen, M.J., Vanakker, O.M., Willaert, A., Huysseune, A., Coucke, P., de Paepe, A., Perkins, T., Zhang, Z., et al. 2013. Zebrafish models for ectopic mineralization disorders: practical issues from morpholino design to post-injection observations. DOI: 10.3389/fgene.2013.00074.
68. Hsiao, C. der, Han, L., He, Q., Chen, W., Sun, C., Wang, X., Chen, X., Wang, R., et al. 2017. A rapid assessment for predicting drug-induced hepatotoxicity using zebrafish. *Journal of Pharmacological and Toxicological Methods*. 84:102–110. DOI: 10.1016/J.VASCN.2016.12.002.
69. Huang, H.-S., Ho, C.-H., Weng, S.-F., Hsu, C.-C., Wang, J.-J., Su, S.-B., Lin, H.-J. & Huang, C.-C. n.d. Long-term mortality of acetaminophen poisoning: a nationwide population-based cohort study with 10-year follow-up in Taiwan. DOI: 10.1186/s13049-017-0468-8.
70. Ignatius, M.S., Hayes, M.N., Moore, F.E., Tang, Q., Garcia, S.P., Blackburn, P.R., Baxi, K., Wang, L., et al. 2018. Tp53 deficiency causes a wide tumor spectrum and increases embryonal rhabdomyosarcoma metastasis in zebrafish. *eLife*. 7. DOI: 10.7554/ELIFE.37202.

71. Imam, F., Sharma, M., Khayyam, K.U., Al-Harbi, N.O., Rashid, M.K., Ali, M.D., Ahmad, A. & Qamar, W. 2020. Adverse drug reaction prevalence and mechanisms of action of first-line anti-tubercular drugs. *Saudi Pharmaceutical Journal*. 28(3):316–324. DOI: 10.1016/J.JSPS.2020.01.011.
72. *Introduction to Clinical Pharmacology - E-Book - Constance G Visovsky, Cheryl H Zambroski, Shirley Hosler - Google Books*. n.d. Available: https://books.google.co.za/books?hl=en&lr=&id=vt8SEAAAQBAJ&oi=fnd&pg=PP1&dq=+Introduction+to+Clinical+Pharmacology-E-Book.+Elsevier+Health+Sciences.&ots=rNQ3Jqtchw&sig=A0cziMtfg9tOX4p-WSyL14ltD3w&redir_esc=y#v=onepage&q=Introduction%20to%20Clinical%20Pharmacology-E-Book.%20Elsevier%20Health%20Sciences.&f=false [2022, August 27].
73. Jaeschke, H., Akakpo, J.Y., Umbaugh, D.S. & Ramachandran, A. n.d. Novel Therapeutic Approaches Against Acetaminophen-induced Liver Injury and Acute Liver Failure. DOI: 10.1093/toxsci/kfaa002.
74. Jia, Z. li, Cen, J., Wang, J. bo, Zhang, F., Xia, Q., Wang, X., Chen, X. qiang, Wang, R. chun, et al. 2019. Mechanism of isoniazid-induced hepatotoxicity in zebrafish larvae: Activation of ROS-mediated ERS, apoptosis and the Nrf2 pathway. *Chemosphere*. 227:541–550. DOI: 10.1016/J.CHEMOSPHERE.2019.04.026.
75. Jiang. n.d. *CPT: Pharmacometrics & Systems Pharmacology Acetaminophen PBPK Model for Application in Children Systemic concentration (CSys) (mg/l) Systemic concentration (CSys) (mg/l)*. Available: www.nature.com/psp.
76. Kanthale, S. 2020. Development of a Rapid Chemometric Reverse Phase HPLC Method for the Simultaneous Estimation of Paracetamol and Ibuprofen in Bulk and Tablet Formulation. *Int J Cur Res Rev* |. 12. DOI: 10.31782/IJCRR.2020.122331.
77. Karumbi, J. & Garner, P. 2015. DOI: 10.1002/14651858.CD003343.pub4.
78. Kaushal, G., Rochani, A.K., Wheatley, M., Oeffinger, B.E., Eisenbrey, J.R. & Kaushal, G. n.d. LC-MS based stability-indicating method for studying the degradation of lonidamine under physical and chemical stress conditions. DOI: 10.4103/1735-5362.293509.
79. Kim, S., Kim, S., Cohen, T., Horsburgh, C.R., Miller, J.W., Hill, A.N., Marks, S.M., Li, R., et al. n.d. Clinical Infectious Diseases Trends, Mechanisms, and Racial/Ethnic Differences of Tuberculosis Incidence in the US-Born Population Aged 50 Years or Older in the United States. DOI: 10.1093/cid/ciab668.
80. Klein, D.J., Boukouvala, S., Mcdonagh, E.M., Shuldiner, S.R., Laurieri, N., Thorn, C.F., Altman, R.B. & Klein, T.E. n.d. PharmGKB Summary: Isoniazid Pathway, Pharmacokinetics (PK). DOI: 10.1097/FPC.0000000000000232.

81. Koblov, P., Sklen, H., Brabcov, I. & Solich, P. n.d. Development and validation of a rapid HPLC method for the determination of ascorbic acid, phenylephrine, paracetamol and caffeine using a monolithic column †. DOI: 10.1039/c2ay05784k.
82. Krell, M. & Schmidt, J. 2020. Biology teachers' views towards using living organisms in biology education. DOI: 10.1080/00219266.2020.1812694.
83. Kumar, A. & Sunil, J. 2013. Recent analytical method developed by RP-HPLC. *Article in Global Journal of Pharmacology*. DOI: 10.5829/idosi.gjp.2013.7.3.7579.
84. Kumar Sahu, R., Singh, K. & Subodh, S. n.d. Adverse Drug Reactions to Anti-TB Drugs: Pharmacogenomics Perspective for Identification of Host Genetic Markers.
85. Labib, R., Abdel-Rahman, M. & Turkall, R. 2003. N-Acetylcysteine Pretreatment Decreases Cocaine and Endotoxin-Induced Hepatotoxicity. *Journal of Toxicology and Environmental Health Part A*. 66(3):223–239. DOI: 10.1080/15287390306370.
86. Lai, Y., Zhou, C., Huang, P., Dong, Z., Mo, C., Xie, L., Lin, H., Zhou, Z., et al. 2018. Polydatin alleviated alcoholic liver injury in zebrafish larvae through ameliorating lipid metabolism and oxidative stress. *Journal of Pharmacological Sciences*. 138(1):46–53. DOI: 10.1016/J.JPHS.2018.08.007.
87. Lai Poon, K., Wang, X., P Lee, S.G., Ng, A.S., Huang Goh, W., Zhao, Z., Al-Haddawi, M., Wang, H., et al. n.d. Transgenic Zebrafish Reporter Lines as Alternative In Vivo Organ Toxicity Models. DOI: 10.1093/toxsci/kfw250.
88. Lee, N. & Nguyen, H. 2021. Ethambutol. *Kucers the Use of Antibiotics: A Clinical Review of Antibacterial, Antifungal, Antiparasitic, and Antiviral Drugs, Seventh Edition*. (November, 10):2346–2360. DOI: 10.1201/9781315152110.
89. Lehmann, J. 1946. Para-Aminosalicylic Acid in the Treatment of Tuberculosis. *Lancet*. 15–16.
90. Lei, S., Gu, R. & Ma, X. 2021. Clinical perspectives of isoniazid-induced liver injury. *Liver Research*. 5(2):45–52. DOI: 10.1016/J.LIVRES.2021.02.001.
91. Lin, H., Zhou, Z., Zhong, W., Huang, P., Ma, N., Zhang, Y., Zhou, C., Lai, Y., et al. 2017. Naringenin inhibits alcoholic injury by improving lipid metabolism and reducing apoptosis in zebrafish larvae. *Oncology Reports*. 38(5):2877–2884. DOI: 10.3892/OR.2017.5965/HTML.
92. Liu, Y. & Chen, Z. 2019. New role of oil red O in detection of double stranded DNA. *Talanta*. 204:337–343. DOI: 10.1016/j.talanta.2019.05.100.
93. Liu, K., Li, F., Lu, J., Liu, S., Dorko, K., Xie, W. & Ma, X. 2014. Bedaquiline Metabolism: Enzymes and Novel Metabolites. *Drug Metabolism and Disposition*. 42(5):863–866. DOI: 10.1124/DMD.113.056119.
94. Liu, Y.S., Yuan, M.H., Zhang, C.Y., Liu, H.M., Liu, J.R., Wei, A.L., Ye, Q., Zeng, B., et al. 2021. Puerariae Lobatae radix flavonoids and puerarin alleviate alcoholic liver injury

in zebrafish by regulating alcohol and lipid metabolism. *Biomedicine and Pharmacotherapy*. 134. DOI: 10.1016/J.BIOPHA.2020.111121.

95. Lohar, S., Aseri, V., Godara, V., Kumari, P., Nagar, V., Pandit, P.P., Chopade, R.L., Singh, A., et al. 2022. Comparative study of development of latent fingerprint by using cost effective waste materials. *Materials Today: Proceedings*. (June). DOI: 10.1016/J.MATPR.2022.06.262.
96. Lokhande, L. & Sachidanandan, C. n.d. *"Developing DILI models in zebrafish for screening of hepatoprotective agents"*.
97. Lu, Y., Zhuge, J., Wang, X., Bai, J., & Cederbaum, A. I. (2008). Cytochrome P450 2E1 contributes to ethanol-induced fatty liver in mice. *Hepatology*, *47*(5), 1483–1494. https://doi.org/10.1002/HEP.22222
98. Maddur, H. & Chalasani, N. n.d. Idiosyncratic Drug-Induced Liver Injury: A Clinical Update. DOI: 10.1007/s11894-010-0154-8.
99. Maksimchik, Y.Z., Lapshina, E.A., Sudnikovich, E.Y., Zabrodskaya, S. v & Zavodnik, I.B. n.d. Protective effects of N-acetyl-L-cysteine against acute carbon tetrachloride hepatotoxicity in rats. DOI: 10.1002/cbf.1382.
100. Makunyane, P. & Mathebula, S. 2016. Update on ocular toxicity of ethambutol. *African Vision and Eye Health*. 75(1):353. DOI: 10.4102/AVEH.V75I1.353.
101. Manjelievskaia, J., Erck, D., Piracha, S. & Schrager, L. n.d. Drug-resistant TB: deadly, costly and in need of a vaccine. DOI: 10.1093/trstmh/trw006.
102. Mazaleuskaya, L.L., Sangkuhl, K., Thorn, C.F., Fitzgerald, G.A., Altman, R.B. & Klein, T.E. n.d. PharmGKB summary: Pathways of acetaminophen metabolism at the therapeutic versus toxic doses. DOI: 10.1097/FPC.0000000000000150.
103. Mccrae, J.C., Mccrae, J.C., Morrison, E.E., Macintyre, I.M., Dear, J.W. & Webb, D.J. 2018. REVIEW Long-term adverse effects of paracetamol-a review Correspondence. DOI: 10.1111/bcp.13656.
104. Melatonin prevents the free radical and MADD metabolic profiles induced by antituberculosis drugs in an animal model". n.d. DOI: 10.1111/j.1600-079X.2004.00176.x.
105. Mesens, N., Crawford, A.D., Menke, A., Duc Hung, P., Goethem, F. van, Nuyts, R., Hansen, E., Wolterbeek, A., et al. 2015. Are zebrafish larvae suitable for assessing the hepatotoxicity potential of drug candidates? DOI: 10.1002/jat.3091.
106. Method for treating patients with OA". n.d. DOI: 10.1093/pm/pnaa274.
107. Mirzayev, F., Viney, K., Linh, N.N., Gonzalez-Angulo, L., Gegia, M., Jaramillo, E., Zignol, M. & Kasaeva, T. 2021. World Health Organization recommendations on the treatment of drug-resistant tuberculosis, 2020 update. *European Respiratory Journal*. 57(6). DOI: 10.1183/13993003.03300-2020.

108. Mohar, I., Stamper, B.D., Rademacher, P.M., White, C.C., Nelson, S.D. & Kavanagh, T.J. 2014. Acetaminophen-induced liver damage in mice is associated with gender-specific adduction of peroxiredoxin-6. *Redox Biology*. 2(1):377–387. DOI: 10.1016/J.REDOX.2014.01.008.

109. Narayanan, V.L. & Austin, A. 2016. Determination of Acetaminophen and Caffeine using reverse phase liquid (RP-LC) chromatographic technique. *Quest Journals Journal of Research in Pharmaceutical Science*. 3:5–10. Available: www.questjournals.org [2022, August 27].

110. North, T.E., Babu, I.R., Vedder, L.M., Lord, A.M., Wishnok, J.S., Tannenbaum, S.R., Zon, L.I. & Goessling, W. 2010. PGE2-regulated wnt signaling and N-acetylcysteine are synergistically hepatoprotective in zebrafish acetaminophen injury. *Proceedings ofthe National Academy of Sciences of the United States of America*. 107(40):17315–17320. DOI: 10.1073/PNAS.1008209107.

111. Ntamo, Y., Ziqubu, K., Chellan, N., Nkambule, B.B., Nyambuya, T.M., Mazibuko-Mbeje, S.E., Gabuza, K.B., Marcheggiani, F., et al. 2021. Drug-Induced Liver Injury: Clinical Evidence of N-Acetyl Cysteine Protective Effects. DOI: 10.1155/2021/3320325.

112. Oren, M., Tarrant, A.M., Alon, S., Simon-Blecher, N., Elbaz, I., Appelbaum, L. & Levy, O. 2015. Profiling molecular and behavioral circadian rhythms in the non-symbiotic sea anemone Nematostella vectensis OPEN. DOI: 10.1038/srep11418.

113. *Pain Relief: From Analgesics to Alternative Therapies - Google Books*. n.d. Available: https://books.google.co.za/books?hl=en&lr=&id=uvSODwAAQBAJ&oi=fnd&pg=PA207&dq=105.%09Mallet,+C.,+Eschalier,+A.+and+Daulhac,+L.,+2017.+Paracetamol:+update+on+its+analgesic+mechanism+of+action.+Pain+relief%E2%80%93From+analgesics+to+alternative+therapies.&ots=BvXsJCoTqo&sig=J6cC8EBn4vrvWSQe47btdZlJcBA&redir_esc=y#v=onepage&q&f=false [2022, August 27].

114. Pandya, M., Patel, D., Rana, J., Patel, M. & Khan, N. 2015. Hepatotoxicity by Acetaminophen and Amiodarone in Zebrafish Embryos. *Journal of Young Pharmacists*. 8(1):50–52. DOI: 10.5530/jyp.2016.1.11.

115. Parmer, J., Macario, E., Tatum, K., Brackett, A., Allen, L., Picard, R., Deluca, N. & Dowling, M. 2021. Global Public Health Latent tuberculosis infection: Misperceptions among non-U.S.-born-populations from countries where tuberculosis is common. *Public Health*. 17(8):1728–1742. DOI: 10.1080/17441692.2021.1947342.

116. Paschalis, V., Theodorou, A.A., Margaritelis, N. v., Kyparos, A. & Nikolaidis, M.G. 2018. N-acetylcysteine supplementation increases exercise performance and reduces oxidative stress only in individuals with low levels of glutathione. *Free Radical Biology and Medicine*. 115:288–297. DOI: 10.1016/J.FREERADBIOMED.2017.12.007.

117. Passeri, M.J., Cinaroglu, A., Gao, C. & Sadler, K.C. 2008. Hepatic Steatosis in Response to Acute Alcohol Exposure in Zebrafish Requires Sterol Regulatory Element Binding Protein Activation. DOI: 10.1002/hep.22667.

118. Patel, S.J., Milwid, J.M., King, K.R., Bohr, S., Iracheta-Vellve, A., Li, M., Vitalo, A., Parekkadan, B., et al. 2012. nature biotechnology VOLUME. 30. DOI: 10.1038/nbt.2089.

119. Pedre, B., Barayeu, U., Ezeriņa, D. & Dick, T.P. 2021. The mechanism of action of N-acetylcysteine (NAC): The emerging role of H2S and sulfane sulfur species. *Pharmacology and Therapeutics*. 228. DOI: 10.1016/J.PHARMTHERA.2021.107916.

120. Pettie, J.M., Caparrotta, T.M., Hunter, R.W., Morrison, E.E., Wood, D.M., Dargan, P.I., Thanacoody, R.H., Thomas, S.H.L., et al. 2019. Safety and Efficacy of the SNAP 12-hour Acetylcysteine Regimen for the Treatment of Paracetamol Overdose. *EClinicalMedicine*. 11:11–17. DOI: 10.1016/J.ECLINM.2019.04.005.

121. *Pharmacology and Pharmacotherapeutics - RS Satoskar, SD Bhandarkar - Google Books*. n.d. Available: https://books.google.co.za/books?hl=en&lr=&id=FR4OEAAAQBAJ&oi=fnd&pg=PP1&dq=144.%09Satoskar,+R.S.+and+Bhandarkar,+S.D.,+2020.+Pharmacology+and+pharmacotherapeutics.+Elsevier+India&ots=DlQ2BGNXz8&sig=8VTfqT0L0Jzn4oJT_Xd961h0zf4&redir_esc=y#v=onepage&q&f=false [2022, August 27].

122. Rahal, A., Kumar, A., Singh, V., Yadav, B., Tiwari, R., Chakraborty, S. & Dhama, K. 2014. Oxidative Stress, Prooxidants, and Antioxidants: The Interplay. DOI: 10.1155/2014/761264.

123. Rajaram, S., Vemuri, V.D. & Natham, R. 2014. Ascorbic acid improves stability and pharmacokinetics of rifampicin in the presence of isoniazid. *Journal of Pharmaceutical and Biomedical Analysis*. 100:103–108. DOI: 10.1016/J.JPBA.2014.07.027.

124. Ramachandran, A. & Jaeschke, H. 2018. Acetaminophen. *Liver Pathophysiology: Therapies and Antioxidants*. (March, 2):101–112. DOI: 10.1016/B978-0-12-804274-8.00006-0.

125. Ramappa, V. & Aithal, G.P. 2013. Hepatotoxicity Related to Anti-tuberculosis Drugs: Mechanisms and Management. *Journal of Clinical and Experimental Hepatology*. 3(1):37–49. DOI: 10.1016/J.JCEH.2012.12.001.

126. Reuter, I., Knaup, S., Romanos, • Marcel, Lesch, K.-P., Drepper, • Carsten & Lillesaar, C. n.d. Developmental exposure to acetaminophen does not induce hyperactivity in zebrafish larvae. DOI: 10.1007/s00702-016-1556-z.

127. Rothstein, D.M. 2016. Rifamycins, Alone and in Combination. *Cold Spring Harbor Perspectives in Medicine*. 6(7):a027011. DOI: 10.1101/CSHPERSPECT.A027011.

128. Rotundo, L. & Pyrsopoulos, N. 2020. Liver injury induced by paracetamol and challenges associated with intentional and unintentional use ORCID number. *World J Hepatol*. 12(4):125–136. DOI: 10.4254/wjh.v12.i4.125.

129. Russmann, S., Kullak-Ublick, G.A. & Grattagliano, I. 2009. *Current Concepts of Mechanisms in Drug-Induced Hepatotoxicity*.

130. Sachar, M., Li, F., Liu, K., Wang, P., Lu, J. & Ma, X. 2016. Chronic Treatment with Isoniazid Causes Protoporphyrin IX Accumulation in Mouse Liver. DOI: 10.1021/acs.chemrestox.6b00121.

131. Sahu, P.K., Ramisetti, N.R., Cecchi, T., Swain, S., Patro, C.S. & Panda, J. 2018. An overview of experimental designs in HPLC method development and validation. *Journal of Pharmaceutical and Biomedical Analysis*. 147:590–611. DOI: 10.1016/J.JPBA.2017.05.006.

132. Saito, C., Zwingmann, C. & Jaeschke, H. 2009. Novel Mechanisms of Protection Against Acetaminophen Hepatotoxicity in Mice by Glutathione and N-Acetylcysteine. DOI: 10.1002/hep.23267.

133. Sandmann, L., Schulte, B., Manns, M.P. & Maasoumy, B. 2019. Treatment of Chronic Hepatitis C: Efficacy, Side Effects and Complications. *Visceral Medicine*. 35(3):161–170. DOI: 10.1159/000500963.

134. Santus, P., Corsico, A., Solidoro, P., Braido, F., di Marco, F. & Scichilone, N. 2014. COPD: Journal of Chronic Obstructive Pulmonary Disease Oxidative Stress and Respiratory System: Pharmacological and Clinical Reappraisal of N-Acetylcysteine. DOI: 10.3109/15412555.2014.898040.

135. Sarkar, S., Ganguly, A. & Sunwoo, H.H. 2017. Current Overview of Anti-Tuberculosis Drugs: Metabolism and Toxicities. DOI: 10.4172/2161-1068.1000209.

136. Saukkonen, J.J., Cohn, D.L., Jasmer, R.M., Schenker, S., Jereb, J.A., Nolan, C.M., Peloquin, C.A., Gordin, F.M., et al. 2012. An Official ATS Statement: Hepatotoxicity of Antituberculosis Therapy. *https://doi.org/10.1164/rccm.200510-1666ST*. 174(8):935–952. DOI: 10.1164/RCCM.200510-1666ST.

137. Schechter, M., Zajdenverg, R., Falco, G., Barnes, G.L., Faulhaber, J.C., Coberly, J.S., Moore, R.D. & Chaisson, R.E. 2012a. Weekly Rifapentine/Isoniazid or Daily Rifampin/Pyrazinamide for Latent Tuberculosis in Household Contacts. *https://doi.org/10.1164/rccm.200512-1953OC*. 173(8):922–926. DOI: 10.1164/RCCM.200512-1953OC.

138. Schechter, M., Zajdenverg, R., Falco, G., Barnes, G.L., Faulhaber, J.C., Coberly, J.S., Moore, R.D. & Chaisson, R.E. 2012b. Weekly Rifapentine/Isoniazid or Daily Rifampin/Pyrazinamide for Latent Tuberculosis in Household Contacts. *https://doi.org/10.1164/rccm.200512-1953OC*. 173(8):922–926. DOI: 10.1164/RCCM.200512-1953OC.

139. Schwalfenberg, G.K. 2021. N-Acetylcysteine: A Review of Clinical Usefulness (an Old Drug with New Tricks). DOI: 10.1155/2021/9949453.

140. Shehu, A.I., Ma, X. & Venkataramanan, R. 2017. Mechanisms of Drug-Induced Hepatotoxicity. *Clinics in Liver Disease*. 21(1). DOI: 10.1016/j.cld.2016.08.002.

141. Shih, T.Y., Pai, C.Y., Yang, P., Chang, W.L., Wang, N.C. & Hu, O.Y.P. 2013. A novel mechanism underlies the hepatotoxicity of pyrazinamide. *Antimicrobial Agents and Chemotherapy*. 57(4):1685–1690. DOI: 10.1128/AAC.01866-12/ASSET/93443D3E-1500-4420-9FE8-CC53033C2A0A/ASSETS/GRAPHIC/ZAC0051317200003.JPEG.

142. So, J., Kim, A., Lee, S.-H. & Shin, D. 2020. Liver progenitor cell-driven liver regeneration. *Experimental & Molecular Medicine*. 52:1230–1238. DOI: 10.1038/s12276-020-0483-0.

143. Sotgiu, G., Centis, R., D'Ambrosio, L., Alffenaar, J.W.C., Anger, H.A., Caminero, J.A., Castiglia, P., de Lorenzo, S., et al. 2012. Efficacy, safety and tolerability of linezolid containing regimens in treating MDR-TB and XDR-TB: systematic review and meta-analysis. *European Respiratory Journal*. 40(6):1430–1442. DOI: 10.1183/09031936.00022912.

144. Stosic, M., Vukovic, D., Babic, D., Antonijevic, G., Foley, K.L., Vujcic, I. & Grujicic, S.S. 2018. Risk factors for multidrug-resistant tuberculosis among tuberculosis patients in Serbia: A case-control study. *BMC Public Health*. 18(1):1–8. DOI: 10.1186/S12889-018-6021-5/TABLES/5.

145. Su, Q., Liu, Q., Liu, J., Fu, L., Liu, T., Liang, J., Peng, H. & Pan, X. 2021. Study on the associations between liver damage and antituberculosis drug rifampicin and relative metabolic enzyme gene polymorphisms. DOI: 10.1080/21655979.2021.2003930.

146. Suresh, A.B., Rosani, A. & Wadhwa, R. 2022. Rifampin. *Encyclopedia of Toxicology: Third Edition*. (April, 13):134–136. DOI: 10.1016/B978-0-12-386454-3.00781-8.

147. Tardiolo, G., Bramanti, P. & Mazzon, E. 2018. molecules Overview on the Effects of N-Acetylcysteine in Neurodegenerative Diseases. DOI: 10.3390/molecules23123305.

148. "Therapeutic Advances in Respiratory Disease Review Sputum production in chronic". n.d. DOI: 10.1177/1753465812437563.

149. "The Selection and Use of Essential Medicines The Selection and Use of Essential Medicines WHO Technical Report Series". n.d. Available: http://www.who.int/ [2022, August 27].

150. Tiberi, S., Pontali, E., Tadolini, M., D'Ambrosio, L. & Migliori, G.B. 2019. Challenging MDR-TB clinical problems – The case for a new Global TB Consilium supporting the compassionate use of new anti-TB drugs. *International Journal of Infectious Diseases*. 80:S68–S72. DOI: 10.1016/J.IJID.2019.01.040.

151. Treweeke, A.T., Winterburn, T.J., Mackenzie, I., Barrett, F., Barr, C., Rushworth, G.F., Dransfield, I., Megson, I.L., et al. 2012. N-Acetylcysteine inhibits platelet-monocyte conjugation in patients with type 2 diabetes with depleted intraplatelet glutathione: a randomised controlled trial. DOI: 10.1007/s00125-012-2685-z.

152. Verstraelen, S., Peers, B., Maho, W., Hollanders, K., Remy, S., Berckmans, P., Covaci, A. & Witters, H. 2016. Phenotypic and biomarker evaluation of zebrafish larvae as an alternative model to predict mammalian hepatotoxicity. DOI: 10.1002/jat.3288.

153. Vilchèze, C. n.d. Mycobacterial Cell Wall: A Source of Successful Targets for Old and New Drugs. DOI: 10.3390/app10072278.

154. Vilchèze, C. & Jacobs JR., W.R. 2014. Resistance to Isoniazid and Ethionamide in Mycobacterium tuberculosis : Genes, Mutations, and Causalities . *Microbiology Spectrum*. 2(4). DOI: 10.1128/MICROBIOLSPEC.MGM2-0014-2013/ASSET/564F6046-E9B7-4989-AB98-AC22C6B805F1/ASSETS/GRAPHIC/MGM2-0014-2013-FIG3.GIF.

155. Wai YEW, W. & Chiu LEUNG, C. 2006. Antituberculosis drugs and hepatotoxicity. *Respirology*. 11:699–707. DOI: 10.1111/j.1400-1843.2006.00941.x.

156. Webb, J.G., Pate, G.E., Humphries, K.H., Buller, C.E., Shalansky, S., al Shamari, A., Sutander, A., Williams, T., et al. 2004. A randomized controlled trial of intravenous N-acetylcysteine for the prevention of contrast-induced nephropathy after cardiac catheterization: Lack of effect. *American Heart Journal*. 148(3):422–429. DOI: 10.1016/J.AHJ.2004.03.041.

157. Wong, A., Isbister, G., McNulty, R., Isoardi, K., Harris, K., Chiew, A., Greene, S., Gunja, N., et al. 2020. Efficacy of a two bag acetylcysteine regimen to treat paracetamol overdose (2NAC study). *EClinicalMedicine*. 20. DOI: 10.1016/J.ECLINM.2020.100288.

158. Wu, C.-Y., Lee, H.-J., Liu, C.-F., Korivi, M., Chen, H.-H. & Chan, M.-H. 2014.Protective role of L-ascorbic acid, N-acetylcysteine and apocynin on neomycin-inducedhair cell loss in Zebrafish. DOI: 10.1002/jat.3043.

159. Ying, H. 2021. *In vitro 3D Liver Model Utilizing iPSC-Induced Hepatocytes for Drug Testing*.

160. Yoganantharajah, P. 2018. *Zebrafish: Drug discovery, toxicity testing and chemical modulators of lipids*.

161. Yoon, E., Babar, A., Choudhary, M., Kutner, M. & Pyrsopoulos, N. 2016. Acetaminophen-Induced Hepatotoxicity: a Comprehensive Update. DOI: 10.14218/JCTH.2015.00052.

162. Younossian, A.B., Rochat, T., Ketterer, J.P., Wacker, J. & Janssens, J.P. 2005. High hepatotoxicity of pyrazinamide and ethambutol for treatment of latent tuberculosis. *European Respiratory Journal*. 26(3):462–464. DOI: 10.1183/09031936.05.00006205.

163. Yuan, L. & Kaplowitz, N. 2013. Mechanisms of Drug-induced Liver Injury. *Clinics in Liver Disease*. 17(4). DOI: 10.1016/j.cld.2013.07.002.

164. Zhang, N., Savic, R.M., Boeree, M.J., Peloquin, C.A., Weiner, M., Heinrich, N., Bliven-Sizemore, E., Phillips, P.P.J., et al. 2021. Optimising pyrazinamide for the treatment of tuberculosis. *European Respiratory Journal*. 58(1). DOI: 10.1183/13993003.02013-2020.

165. Zhang, X., Li, C. & Gong, Z. 2014. Development of a convenient in vivo hepatotoxin assay using a transgenic zebrafish line with liver-specific dsred expression. *PLoS ONE*. 9(3). DOI: 10.1371/journal.pone.0091874.

166. Zhang, Y., Liu, K., Hassan, H.M., Guo, H., Ding, P., Han, L., He, Q., Chen, W., et al. 2016a. Liver fatty acid binding protein deficiency provokes oxidative stress, inflammation, and apoptosis-mediated hepatotoxicity induced by pyrazinamide in zebrafish larvae. *Antimicrobial Agents and Chemotherapy*. 60(12):7347–7356. DOI: 10.1128/AAC.01693-16.

167. Zhang, Y., Liu, K., Hassan, H.M., Guo, H., Ding, P., Han, L., He, Q., Chen, W., et al. 2016b. Liver fatty acid binding protein deficiency provokes oxidative stress, inflammation, and apoptosis-mediated hepatotoxicity induced by pyrazinamide in zebrafish larvae. *Antimicrobial Agents and Chemotherapy*. 60(12):7347–7356. DOI: 10.1128/AAC.01693-16/FORMAT/EPUB.

168. Zheng, X., Dai, W., Chen, X., Wang, K., Zhang, W., Liu, L. & Hou, J. 2015. Caffeine reduces hepatic lipid accumulation through regulation of lipogenesis and ER stress in zebrafish larvae. *Journal of Biomedical Science*. 22(1):1–12. DOI: 10.1186/S12929-015-0206-3/FIGURES/5.

169. Zloh, M., Gupta, M., Parish, T. & Brucoli, F. 2021. Novel C-3-(N-alkyl-aryl)-aminomethyl rifamycin SV derivatives exhibit activity against rifampicin-resistant Mycobacterium tuberculosis RpoBS522L strain and display a different binding mode at the RNAP β-subunit site compared to rifampicin. *European Journal of Medicinal Chemistry*. 225. DOI: 10.1016/J.EJMECH.2021.113734.

170. Zou, Y., Zhang, Y., Han, L., He, Q., Hou, H., Han, J., Wang, X., Li, C., et al. 2017. Oxidative stress-mediated developmental toxicity induced by isoniazide in zebrafish embryos and larvae. DOI: 10.1002/jat.3432.